SOME ASPECTS OF RADIATION INDUCED NUCLEATION IN WATER

by

Chih-Ping Tso

B.Tech., Loughborough University of Technology, United Kingdom

(1968)

Submitted in Partial Fulfillment of

the Requirements for the Degree of

Master of Science

at the

Massachusetts Institute of Technology

August 1970

Signature of Author_____
                                    Department of Nuclear Engineering

Certified by_____
                                    Thesis Supervisor, Date

Accepted by_____
                                    Chairman, Departmental Committee
                                    on Graduate Students

Dedicated to my

parents and sisters

SOME ASPECTS OF RADIATION INDUCED NUCLEATION OF WATER

by

Chih-Ping Tso

Submitted to the Department of Nuclear Engineering on August 11, 1970 in partial fulfillment of the requirements for the degree of Master of Science.

ABSTRACT

Experimental data for the determination of superheats of separately, fission fragments and fast neutrons in water were taken with an experimentally modified set up of Bell.[2] Attempts to correlate both data from present work and from Bell with theory led to apparent inadequacies with the theory. The theory is based on an "Energy Balance Method" developed by Bell. This method was also used to compute threshold superheat for benzene, for later comparison with data from another investigator[5] when this reference becomes available.

Application of this Energy Balance Method to predict fission neutrons induced nucleation and alpha particles induced nucleation (alpha particles from (n, α) reaction on Boron) at Pressurised Water Reactor conditions indicated that radiation induced nucleation for monoenergetic neutrons and alphas present in reactor may be effective in causing initiation of nucleate boiling. However, detailed consideration of all neutron energies present (spectrum) was not accomplished to arrived at a definite conclusion for this reactor case.

Thesis Supervisor   Neil E. Todreas
Title   Assistant Professor

Acknowledgements

I wish to thank foremostly Dr. C.R. Bell who first introduced me to this interesting topic and gave me invaluable guidance before he graduated earlier on this year.

Professor N.C. Rasmussen was my thesis supervisor from January to late February 1970, after which the capacity was continued by Professor N.E. Todreas with Professor N.C. Rasmussen being kind enough to be my thesis reader. I am much indebted to their helpfulness and friendliness which shall form permanently as part of my educational experience at M.I.T. I would like to thank all members of the M.I.T. Reactor Machine Shop, Mr. D. Lynch and Mr. J. de Padova of the Reactor Electronics Shop, members of the Reactor R.P.O., many members of the M.I.T. Information Processing Center, and other friends who had in one way or another assisted me in the present work. Last but not least, full credit for typing must go to Doris who had so generously donated her time for this purpose.

Table of Contents

List of Figures

List of Tables

Chapter 1

Introduction

1.1 Objectives

The present project will study primarily the effect of radiation in inducing nucleation in water. The main goal of the project is to confirm or modify as necessary some of the conclusions of C.R. Bell's Doctorate Thesis[2]. Basically, the experimental work consists of determination of threshold superheat of an oil-suspended water bubble at various pressure, when subjected separately to fission fragments and fast neutrons radiation.

The objectives of this thesis are enunciated as follows:--

(i) To repeat some of the data points in Bell's work in order to make the following corrections to Bell's data and to compare with the validity of Bell's analytical corrections.

a) Correction on the apparatus in order to create an isothermal field around the water bubble.

b) Correction on the apparatus in order to reduce a thermocouple thermal error present in Bell's work.

c) Correction on a pressure gauge reading error.

(ii) To apply Bell's theory, modified as necessary by the results of (i) above, to the high pressure range of the Pressurised Water Reactor (PWR) conditions.

(iii) To compare the prediction of Bell's theory, modified as necessary to the results of (i) above, to some organic liquid data obtained by other investigators[13][5].

1.2 Background information on theory

The amount of superheat a liquid could attain when heated beyond its saturation point depends on the substance properties as well as the environmental conditions of the system. The presence of radiation is likely to affect superheat owing to deposition of energy into the liquid with consequent increase in instability in the system.

There are primarily two approaches to predict radiation induced nucleation. The Energy Balance Method requires that the energy of formation of a nucleus in water, E_f, be equal to the energy available from radiation for the formation of the nucleus, E_a. That is

$$E_f = E_a \qquad (1.1)$$

The Statistical Method which regards the situation from a micro-scopic viewpoint predicts that an additional energy term E_s is involved, due to the extra energy given from the surrounding vapor to the nucleus. E_s is dependent on the production rate of the number of energy transfer events to the nucleus. Equation (1.1) becomes

$$E_f = E_a + E_s \qquad (1.2)$$

For a given pressure in the system, E_f decreases when the amount of superheat attainable in the system increases. Under idealized conditions, E_f decreases to a threshold minimum, with the corresponding superheat temperature being the Foam limit for the particular system pressure. Thus from equations (1.1) and (1.2), it is clear that for the same E_a, the Energy Balance Method predicts a higher superheat than the Statistical Method. The differences, however, is small, and in this work the

simpler Energy Balance Method will be used and E_s neglected.

1.3 Experimental background

A water bubble of about $\frac{1}{2}$ in. diameter is suspended in oil to avoid cavities, and heated up by the oil to the point of boiling.

The source of radiation used is a combination of five sealed one-Curie Pu-Be sources with neutron spectrum as given by Karaian[9]. The total flux at the water bubble is about 0.53×10^4 neutron-sec^{-1}.

In the case of fission fragments in water, the same neutron source is used, except that a minute quantity of uranium nitrate is introduced in the water bubble. The concentration used is 0.0087 gm of $UO_2(NO_3)_2 \cdot 6H_2O$ in one gm. of water, giving rise to a fission rate of about 2 events per minute in the water bubble.

Chapter 2

Experimental Considerations

The reader is urged to consult Bell[2] for a fuller discussion of the experimental program. Here, the basic set-up is recapitulated with a description of apparatus modification, and the experimental results presented.

2.1 Experimental set-up

Fig. 2.1 gives a diagrammatic representation of the apparatus. The water bubble X is suspended between the suspending oil H, a heavy mineral oil, and a layer of covering oil I, a "Dow Corning 550 Fluid" silicon oil. These fluids are contained in the cylindrical (10" x 3" dia) boiling chamber A which has tube fittings both at the covered flanged top, and at the closed bottom. Sticking out from A at the same level as the bubble is the observation window B through which nucleation of the bubble can be observed. Visibility is maintained by a flood lamp above the light window C. To compensate for heat loss from B to the surrounding, there is a dummy window from the chamber situated diametrically opposite the observation window (not shown).

Two main cooling devices exist in the boiling chamber. One is the condenser F which serves to condense residual water vapor in the air space left by previous boiling of the bubble. The condensate is collected in a container and is dischargeable via a line to the waste tank R.

The other cooling device is the important convection generator G,
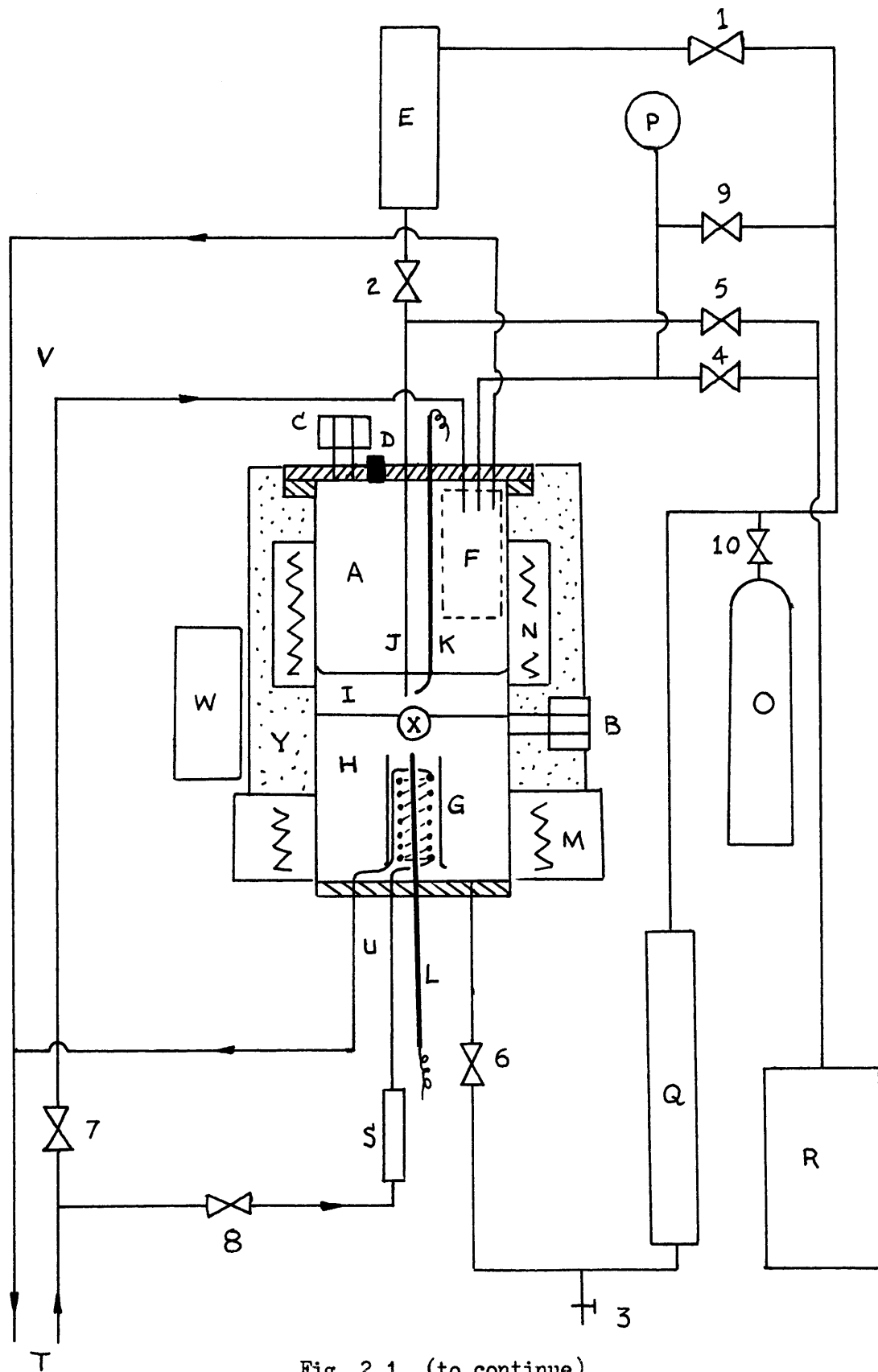
Fig. 2.1 (to continue)

Fig. 2.1 Legend. Diagram of experimental setup.

Number 1 to 10	valves
A	boiling chamber
B	observation window
C	light window
D	bubble entrance
E	cover oil reservoir
F	condenser
G	convection generator
H	supporting oil
I	cover oil
J	cover oil outlet
K	top thermocouple
L	bottom thermocouple
M	bottom heater
N	top heater
O	air pressurizer
P	pressure gauge
Q	supporting oil reservoir
R	waste tank
S	flow indicator
T	supply water line
U	convection generator cooling lines
V	condenser cooling lines
W	neutron source
X	water bubble
Y	fibre glass insulation

which is a hollow open-ended tube with a cooling coil, sitting at the bottom of the chamber as shown. In a heated chamber, a free convection current is generated which circulates the supporting oil such that the flow is radially towards the top of the generator, down through the tube, and radially out at the bottom. In this fashion, the bubble is kept in place radially in the boiling chambers. Vertically the bubble can be located by adjusting the oil levels.

Both these cooling devices are fed by a supply water line T. The condenser cooling lines V are led in from the top while the convection generator cooling lines U from the the bottom of the chamber.

The cover oil reservoir E stores oil to be introduced into the test region through the inlet J. Supporting mineral oil is introduced from the bottom of the chamber from the reservoir Q. O is an air cylinder for pressurizing the system. The pressure gauge P indicates the pressure in the chamber.

2.2 Apparatus modification

In Bell's experiment, the position of the water bubble was kept about 1/8" above a thermocouple L projecting up through the convection generator G as shown in Fig. 2.1. The bubble temperature based on this singular thermocouple measurement was later found by Bell to be incorrect as there existed a temperature gradient in the field of the bubble confirmed by a temperature plot in this region with the aid of a movable thermocouple. Bell corrected the temperature measurements by subtracting $7\frac{1}{2}°F$ from his data. This $7\frac{1}{2}°F$ is based on an analysis in Bell's theses.

Bell used only a circumferential heater M to heat the system. Since heat was lost from the chamber above the cover oil a temperature gradient existed in the cover oil and hence the water drops. To set up an

isothermal region at the bubble a second circumferential heater N was added in this thesis to the upper part of the chamber. At the same time, a second thermocouple probe K(top) was installed to read the temperature at the top of the bubble. Both thermocouples were visible through the observation window. The Chromel-Alumel type thermocouple had been calibrated with reference to boiling water at atmospheric pressure. The readings were recorded to $\pm\frac{1}{4}°$F by a Minneapolis-Honeywell strip chart recorder. By switching connections to and fro, temperatures measured by top and bottom thermocouples were registered alternately on the strip chart to confirm isothermal bubble conditions. The latter was also checked periodically for accuracy with reference to a Leed and Northrup Type K-3 Universal potentiometer. With both heaters being adjustable in power, this arrangement led to good indication of an isothermal field when K and L were in close agreement.

Another modification made was the material of the sheath of lower thermocouple L. This was formerly a 1/8" O/D, 1/16" I/D aluminum tubing with the thermocouple bead pushed against the closed upper end. In the course of preliminary investigation on the isothermal field around the bubble with a third thermocouple, it was found that at about $200°$F atmospheric pressure the third thermocouple while in the vicinity of the tip of L gave a reading of about $4°$F higher than L. This was attributable to heat conduction down the sheath from the chamber to the exterior, producing a temperature difference between the thermocouple bead and the oil. Thermocouple thermal error is inevitable in such temperature measurement, but this case is particularly pronounced since the aluminum sheath with a high thermal conductivity of about 120 BTU-hr^{-1}-ft^{-1}-$°$F^{-1} is embedded in oil of conductivity about 0.07
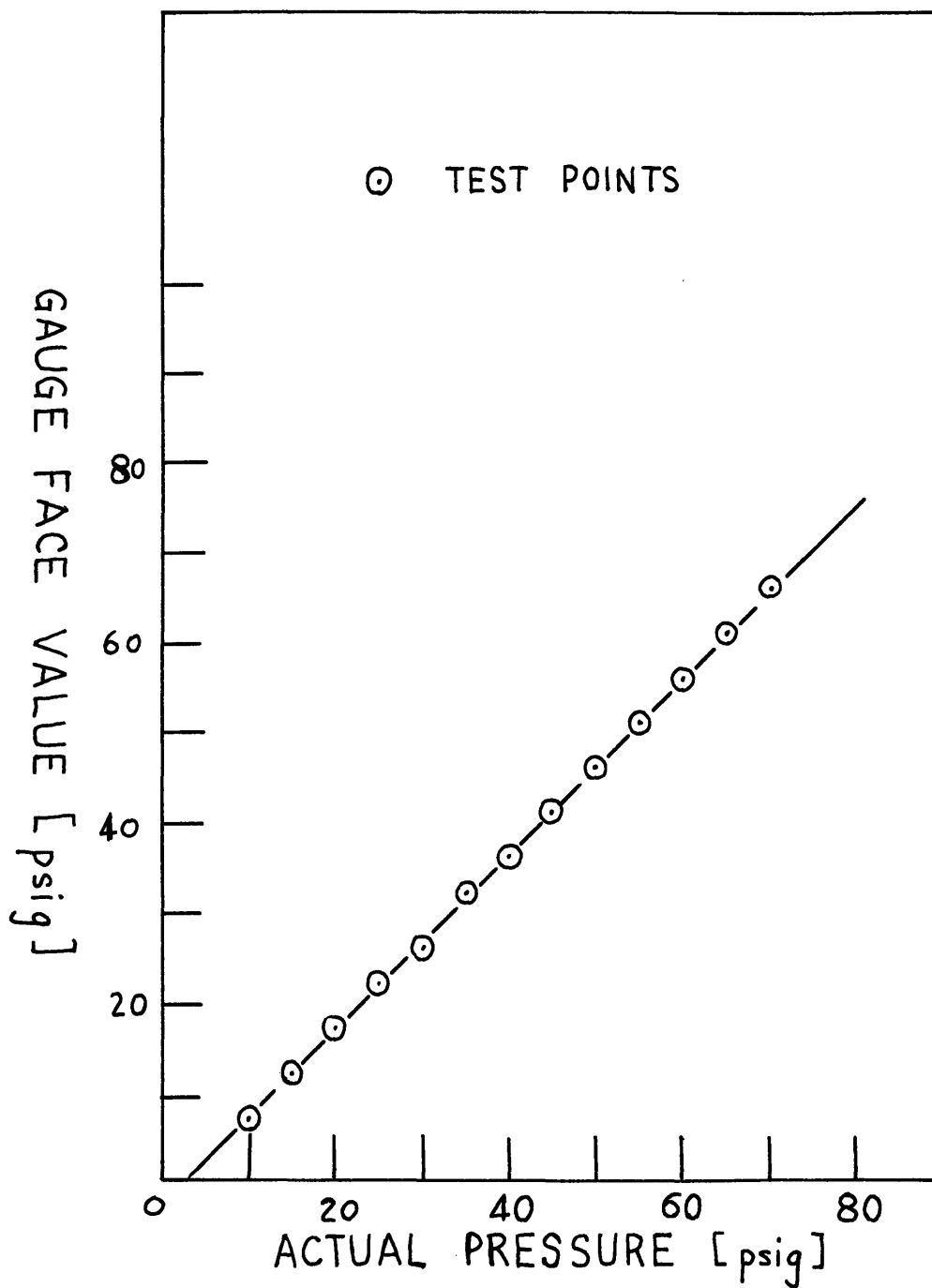
Fig. 2.2 Pressure gauge calibration.

[BTU-hr^{-1}-ft^{-1}-$^{\circ}$F^{-1}] only. An attempt will be made to estimate the

the error in Bell's data taken with the aluminum sheath in Chapter 4.

The aluminum sheath was replaced by a stainless steel sheath which has

a conductivity of about 10 [BTU-hr^{-1}-ft^{-1}-$^{\circ}$F^{-1}] and the thermal error

at the same conditions was then down to with $\frac{1}{2}^{\circ}$F. It is noteworthy that

the error is also sensitive to the convection generator flow rate, as

the convective current encourages heat transfer through L. For the top

thermocouple K, no appreciable error was detected though an aluminum

sheath was used.

Another modification was the way the water bubble was introduced

to the chamber. Instead of an arrangement similar to the path E,2,J

of Figure 2.1, the bubble was put in by a thin glass syringe through an

entrance D. This eliminate unwanted water drops which often drained

down into the oil chamber from the old arrangements in the course of the

experiment.

The 0 to 100 psig Bourdon pressure gauge P had been tested by a

Refinery Supply Company Dead Weight Tester. The calibration graph,

Fig. 2.2, shows that the gauge reads 3-4 psi too low. Bell found that

the same gauge read 1-2 psi too high and corrected accordingly in his

work. The implication of this will be discussed later on.

2.3 <u>Experimental procedure</u>

A typical pressurized run will be described. After the apparatus

was checked to be in running conditions, oil was filled in the chamber.

With reference to Fig. 2.1 again, by closing valves 1 and 9 and opening

valves 10 and 6 supporting oil was forced up the chamber. Covering oil

flowed in by opening valve 2. After the water bubble was carefully

put in at the oil interface, the chamber was pressurized to the required
pressure by opening valves 9 and 10 and closing all other valves.
Heaters M and N were then switched on and adjusted to maintain isother-
mal spatial temperature field as the overall temperature rose on a
reasonable temperature ramp as sensed by K and L. With valve 7 kept
closed and valve 8 crack opened, a convection was generated, stabilizing
the bubble. The system was then left to attain its superheat, attention
being given to the heater adjustment and bubble position all the time.
At a pre-determined temperature level close to but below the incipient
boiling point (either by reference to Bell's results or by a trial run)
the neutron source W was introduced and set close to the face of the
chamber outter container. Henceforth, watchful work determined the
superheat threshold of the bubble; a sudden burst or jump of the bubble
being indicative of boiling.

2.4 Experimental difficulties

A number of snags were encountered in the course of experimental
work. Apart from the mechanical failures in the hardware, work was
often delayed due to one of the following frustrating events.

(i) The bubble boiled well before the expected temperature range
because of foreign particles present inadvertently in the bubble.

(ii) On occasions, it was necessary to change the supporting oil in
the chamber as its density had been decreased through repeated heating,
resulting in the bubble to submerge out of view.

(iii) Owing to reasons still unknown, at high temperatures of about
$400°F$ and pressures above 50 psia, the bubble tended to drift out of
sight to the side chamber wall, in spite of a strong convection generator

(iv) Also at conditions of (iii), there is a tendancy for evaporation to take place from the bubble in the form of a stream of tiny steam bubbles rising upwards. A result is that the bubble is set into slight motion by the principle of momentum conservation. This may upset the super-heat threshold and may also make the threshold less distinguishable since at these higher temperatures and pressures the first indication of boiling is a weak quiver without the bubble breaking up.

While (i) and (ii) are difficulties present for all experimental work, (iii) and (iv) are dominant only in the fast neutron runs.

2.5 Experimental Results of Present Work.

Table 2.1 shows data obtained for the fission fragment induced boiling at four system pressures. T_{sat} is the saturation temperature of water at that pressure. T_t and T_b are the electromotive forces recorded at nucleation by the top and bottom thermocouples respectively, in millivolts. For chromel-alumel thermocouples, and with reference junction at $32^\circ F$, these electromotive forces are easily converted to $^\circ F$ from standard tables.

The average superheat temperature is T, and the amount of superheat attained is ΔT. The mean values of each set of data are T_{mean} and ΔT_{mean}, with the standard deviation for T_{mean} being σ. The values in parentheses are those from Bell's work on which more will be said in section 2.6.

'No. of trials' is the actual total number of experimental attempts made. Not all these attempts gave results because of experimental diffi-culties mentioned in section 2.4. And out of the 'no. of results' as tabulated in the table, some data represent cases where nucleation took place too early due to such factor as foreign bodies present. These

cases are underlined in the table. The number of data not underlined is denoted by the item 'usuable results,' and these are used to compute ΔT_{mean} and T_{mean}.

Table 2.2 shows data for the fast neutron case at two system pressures. They are much more difficult to obtain as stated in the previous section because of higher experimental superheats at the same pressure. TR_t is the temperature ramp in $^\circ F$/min as recorded by the top thermocouple, and TR_b by the bottom thermocouple, giving an average value of TR.

For a system pressure of 55 psia, the TR had been obtained by taking the temperature trace on the strip chart recorder for the last one minute history before boiling occurred. This criteria, even though is now believed incorrect (compared to the one that will be mentioned in the next paragraph) is used here because the traces obtained in the experiment for 55 psia could not be interpreted in the other way. Only the last minute ramps were fairly constant.

For a system pressure of 75 psia, Fig. VI.6 of Bell[2,p.168] showed that for 'a' at and below 12, there is a threshold superheat of about 77°F below which there is not likely to be any boiling event at any finite TR. Bell[2,p.151] showed that above about 77°F, the boiling event is a function of the TR from that superheat (of 77°F) up to boiling. The plots in Bell's Fig. VI.6 were actually obtained based on a constant TR for each boiling event (for a particular 'a'). Thus if experimental results were to be compared with theory (Bell's Fig. VI.6), the experimental results should best have a constant TR from Δ T around 77°F. This corresponds to an electromotive force of about 8.00 mv on the chart. In table 2.2 for 75 psia pressure, only the runs with TR 1.70 and 5.50 $^\circ$F/min have fairly constant ramps as well as being constant from 8.00 mv onwards. The run

of TR 0.41 °F/min has a constant ramp about 10°F too late or at about 88°F.
The experimental charts are kept with N.E. Todreas[22].

Table 2.1 Fission fragment data of
Tso and that reported by Bell (in parentheses)

Pressure	14.7 psia				32.7 psia			
T_{sat}	212.4 °F				255.8 °F			
No. of trials	12				9			
No. of results	12				6			
Usable results	11				5			
Temperatures	T_t mv	T_b mv	T °F	ΔT °F	T_t mv	T_b mv	T °F	ΔT °F
Results	5.08	5.09	255.0	42.6	6.27	6.20	306.5	50.7
	5.46	5.48	272.5	60.1	6.20	6.18	304.5	48.7
	5.41	5.54	273.5	61.1	6.28	6.30	309.0	53.2
	5.55	5.60	277.0	64.6	6.16	6.22	304.5	48.7
	5.65	5.53	278.0	65.6	6.14	6.08	301.0	45.2
	5.44	5.50	272.5	60.1	5.80	5.80	287.0	31.0
	5.60	5.60	280.0	65.6				
	5.53	5.52	275.4	63.0				
	5.49	5.62	276.4	64.0				
	5.52	5.54	274.4	63.0				
	5.55	5.59	278.4	66.0				
	5.47	5.57	275.4	63.0				
ΔT_{mean}	63.5 °F (55.1)				49.3°F (39.0)			
T_{mean}	275.9°F (267.5)				305.1°F(294.8)			
$\sigma (T_{mean})$	± 2.0°F (0.3)				± 3.0°F (0.5)			

Table 2.1 (Continued)

Pressure	53.7 psia				74.2 psia			
T_{sat}	285.5 °F				306.9 °F			
No. of trials	8				10			
No. of results	7				8			
Usable results	5				6			
Temperatures	T_t mv	T_b mv	T °F	Δ T °F	T_t mv	T_b mv	T °F	Δ T °F
Results	6.50	6.54	319.5	34.0	6.94	6.98	339.0	32.1
	6.67	6.62	325.0	39.5	6.83	6.88	334.5	27.6
	6.43	6.35	313.5	28.0	6.96	6.91	340.0	33.1
	6.70	6.57	324.6	39.1	7.02	6.98	341.0	34.1
	6.61	6.56	322.5	37.0	7.07	6.99	342.5	35.6
	6.66	6.60	324.5	39.0	7.08	7.00	343.0	36.1
	6.75	6.70	329.0	23.5	6.86	6.84	334.0	27.1
					7.03	6.97	341.0	34.1
Δ T_{mean}	38.7°F (29.5)				34.2°F (24.6)			
T_{mean}	324.2°F(315.0)				341.1°F (331.5)			
σ (T_{mean})	± 2.5°F(0.7)				±2.4°F (0.6)			

Table 2.2 Fast neutron data of Tso

Pressure	55 psia
T_{sat}	287.1 °F
No. of trials	11
No. of results	4
Usable results	2

	T_t mv	T_b mv	T °F	T °F	TR_t °F/min	TR_b °F/min	TR °F/min
Results	7.15	7.15	348	51	--	--	--
	8.09	8.06	389.5	102.4	1.30	1.90	1.60
	6.80	6.80	332	45	--	--	--
	8.32	8.00	393.0	105.9	0.80	1.90	1.35

ΔT_{mean}	1.04.2 °F (106.5)
T_{mean}	391.3 °F (393.6)

Table 2.2 (Continued)

Pressure	75 psia
T_{sat}	308.0 °F
No. of trials	24
No. of results	9
Usable results	3

	T_t mv	T_b mv	T °F	ΔT °F	TR_t °F/min	TR_b °F/min	TR °F/min
Results	7.03	7.01	342	34	--	--	--
	7.00	7.40	350	42	--	--	--
	7.20	7.40	354	46	--	--	--
	7.50	7.30	404	51	--	--	--
	7.60	7.60	368	60	--	--	--
	8.27	8.24	397.5	89.5	0.42	0.40	0.41
	8.20	8.20	395	87	2.10	1.30	1.70
	7.35	7.35	357	49	--	--	--
	8.35	8.15	397	89.0	5.50	5.50	5.50

ΔT_{mean}	88.8°F (89.4)
T_{mean}	396.8°F (397.5)

2.6 Re-interpretation of Bell's Data

The one condition Bell made on his own data is that due to non-isothermal field and this he did by an analysis which resulted in subtracting 7.5°F from the superheat threshold temperatures he obtained.

In this thesis, this effect was corrected by addition of heaters to create an isothermal field. However, since several changes were simultaneously made in the apparatus and data, it appears prudent to to re-interpret Bell's data by identifying each correction independently. Thus, we have three corrections on ΔT and one correction on TR (temperature ramp) as follows:--

ΔT - correction(i). Bubble in Bell's runs was not in an isothermal field

ΔT - correction(ii). Thermocouple sheath error. Bell's data was recorded by a thermocouple reading lower than 'true.'

ΔT - correction(iii). Pressure gauge reading difference of 5 psia as mentioned earlier.

TR - correction(i). In the case of fast neutrons in water, the temperature ramps reported by Bell are based on varying lengths of time and temperature intervals before boiling. As mentioned in section 2.5, it is now thought more accurate to base the TR on an average basis (provided TR variation is not too drastic) from the temperature recording of about 8.00 mv or ΔT of 77°F (see section 2.5) onwards. (This 8.00 mv is only applicable for 75psia system pressure). Hence the TR should be re-interpreted, if necessary, from Bell's experimental charts.[22]

2.6.1 Fast neutrons. Table 2.3 presents a re-interpretation of Bell's data for fast neutrons in water at 75 psia system pressure. Similar tables could be compiled from Bell's temperature charts for 55 psia and 95 psia,

the other system pressures Bell worked on.

Table 2.3 Re-interpretation of Bell's fast neutron data

Pressure = 75 psia; $T_{sat} = 307.6°F$

A run no.	B TR°F/min reported by Bell(2)	C TR °F/min interpreted by Tso TR-correction(i)	D Status	E ΔT °F reported by Bell Uncorrected	F ΔT °F reported by Bell (-7.5°F)	G ΔT °F column E corrected by Tso ΔT-correction(iii)
27	0.09	0.09	**	98.4	90.9	94.0
5	0.30	0.30	*	94.4	86.9	90.0
2	0.38	0.38	**	98.4	90.9	94.0
26	0.41	0.41	**	94.9	87.4	90.5
4	0.50	0.50	*	98.4	90.9	94.0
6	0.33	0.58	***	97.4	89.9	93.0
7	0.60	0.60	**	98.4	90.9	94.0
25	0.95	0.95	**	102.9	95.4	98.5
19	0.95	0.95	**	102.9	95.4	98.5
23	1.10	1.10	**	104.9	97.4	100.5
22	1.10	1.10	*	104.9	97.4	100.5
1	1.20	1.20	***	100.4	92.9	96.0
21	1.30	1.30	**	103.4	95.9	99.0
7	0.40	1.30	***	97.4	89.9	93.0
10	1.50	1.50	***	107.9	100.4	103.5
20	1.30	1.70	***	101.4	93.9	97.0
11	1.90	1.90	**	107.9	100.4	103.5
24	1.90	1.90	***	103.9	96.4	99.5
8	2.10	1.90	***	114.9	107.4	110.5
16	1.70	2.00	***	104.4	96.9	100.0
21	2.00	2.00	***	105.9	98.4	101.5
9	1.60	2.30	***	115.4	107.9	111.0
14	2.30	2.30	***	101.4	93.9	97.0
13	2.40	2.40	**	102.4	94.9	98.0
18	2.50	2.50	**	110.4	102.9	108.0
17	2.00	2.70	**	102.4	102.4	98.0
12	2.80	2.80	***	106.4	98.9	102.0

* Ramp not constant
** Fairly constant ramp--but not extending from $\Delta T = 77°F$
***Fairly constant ramp and extending from $\Delta T = 77°F$

Column A gives the run number as marked on Bell's charts[22]. Column

B shows the TR as reported by Bell, while column C lists the TR as interpreted by TR-correction(i). The status as marked in column D indicates how good the data in column C are, as explained at the end of the table.

The entry *** indicates the best data. Data with the entry * will be discarded for comparison with theory on TR. The data are arranged in ascending order of the TR magnitude in column C.

The amount of superheat above the saturation temperature (T_{sat}) are given in columns E,F, and G as ΔT. Column E indicates values reported by Bell uncorrected. Column F are values reported by Bell but with his $7.5^{\circ}F$ correction made. In column G, ΔT-correction(iii) of above is made, which is simply column E minus $4.4^{\circ}F$ $(T_{sat}$ at 80 psia minus T_{sat} at 75 psia).

In figure 2.3, the data marked are for a TR of 1.7 $^{\circ}F/min$, the only ramp which is common between Bell's data from Table 2.3 amd data from the present work, Table 2.2. On Table 2.3, this is shown in run number 20. As a comparison, Fig. 2.3 shows that there is a $10^{\circ}F$ difference in superheats attributable to ΔT-corrections(i) and (ii). For a different TR, this difference would be different so that this $10^{\circ}F$ difference cannot be applied confidently to each of the other data collected by Bell.

2.6.2 Fission Fragments. For fission fragments in water data, only the three ΔT-corrections are applicable, as no TR is involved. Table 2.4 with associated notes shows a re-interpretation of Bell's fission fragment data for the same four system pressures as Table 2.1.

Fig. 2.4 shows results from Table 2.1 and Table 2.4 plotted as ΔT versus system pressure.

Table 2.4 Re-interpretation of Bell's fission fragment data

	X	Y	Z
Pressure = 14.7 psia			
ΔT_{mean}	62.6	55.1	62.6*
T_{mean}	275.0	267.5	275.0*
$\sigma (T_{mean})$		0.3	
Pressure = 32.7 psia			
ΔT_{mean}	46.5	39.0	38.3
T_{mean}	302.3	294.8	302.3
$\sigma (T_{mean})$		0.5	
Pressure = 53.7 psia			
ΔT_{mean}	37.0	29.5	31.0
T_{mean}	322.5	315.0	322.5
$\sigma (T_{mean})$		0.7	
Pressure = 74.2 psia			
ΔT_{mean}	32.1	24.6	27.8
T_{mean}	339.0	331.5	339.0
$\sigma (T_{mean})$		0.6	

All data in °F
Column X = Raw data reported by Bell (Δ)
Column Y = X corrected by -7.5 °F only (▲)
Column Z = X corrected by pressure gauge error (ΔT-correction(iii)) only
      values are for pressures 5 psia higher than stated pressures($\widetilde{\Delta}$)
   * = No gauge error here since chamber opened and gauge not used
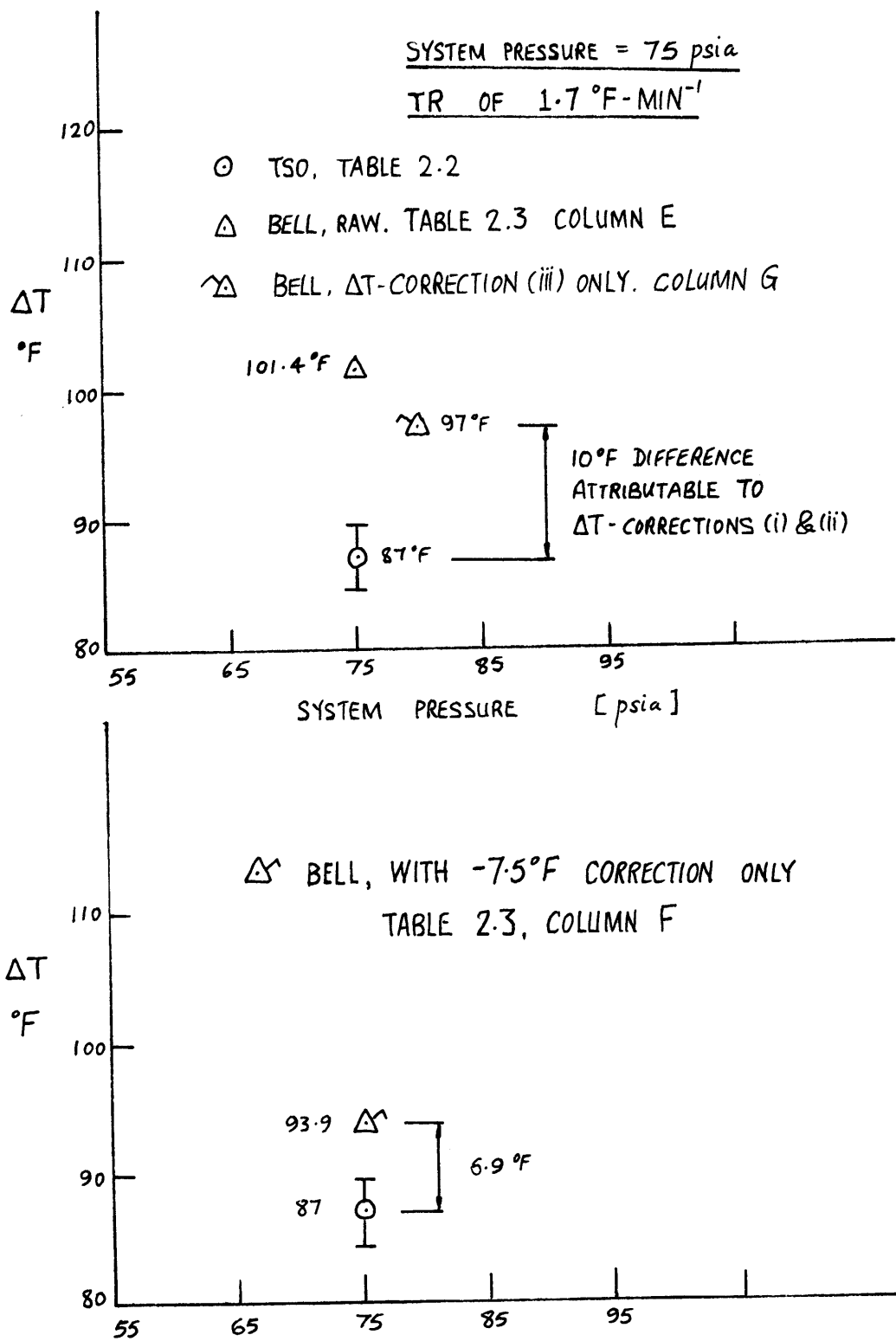
Fig. 2.3 Experimental results for fast neutrons in water.

LEGEND
△ BELL, RAW. TABLE 2·4 COLUMN X
△ BELL, ΔT-CORRECTION (iii) ONLY. COLUMN Z
⊙ TSO, TABLE 2·1

ΔT
°F

0.9°F

11.0 °F

7.7°F

6.4 °F

DIFFERENCES
ATTRIBUTABLE
TO
ΔT-CORRECTION
(i) & (ii)

SYSTEM PRESSURE [psia]

▲ BELL WITH -7·5°F CORRECTIONS ONLY
COLUMN Y (REPORTED IN BELL THESIS)

ΔT
°F

8·4°F

10·3°F

9·2°F

9·6°F
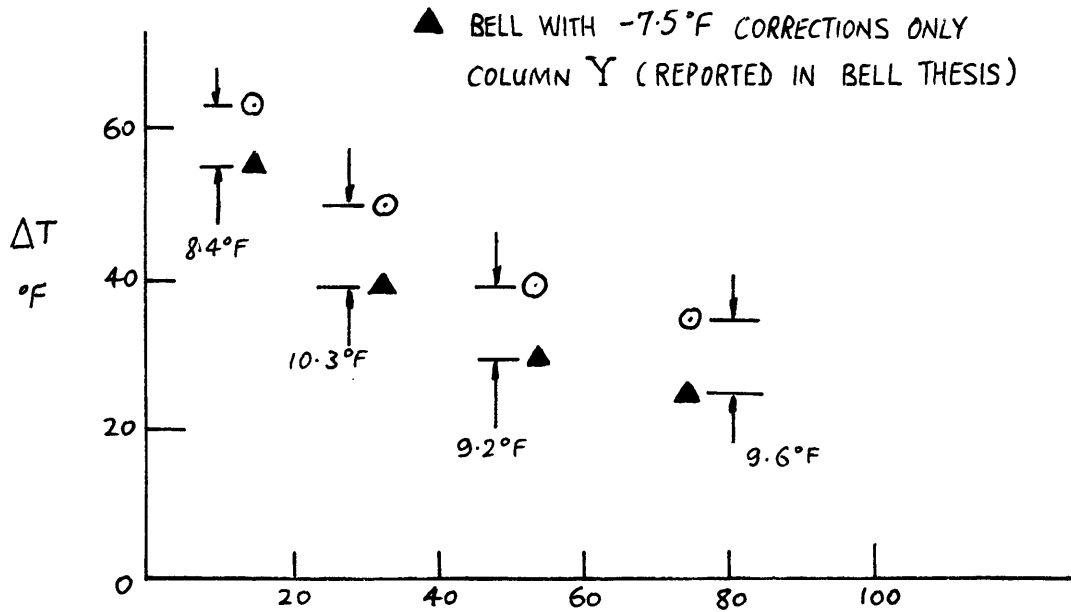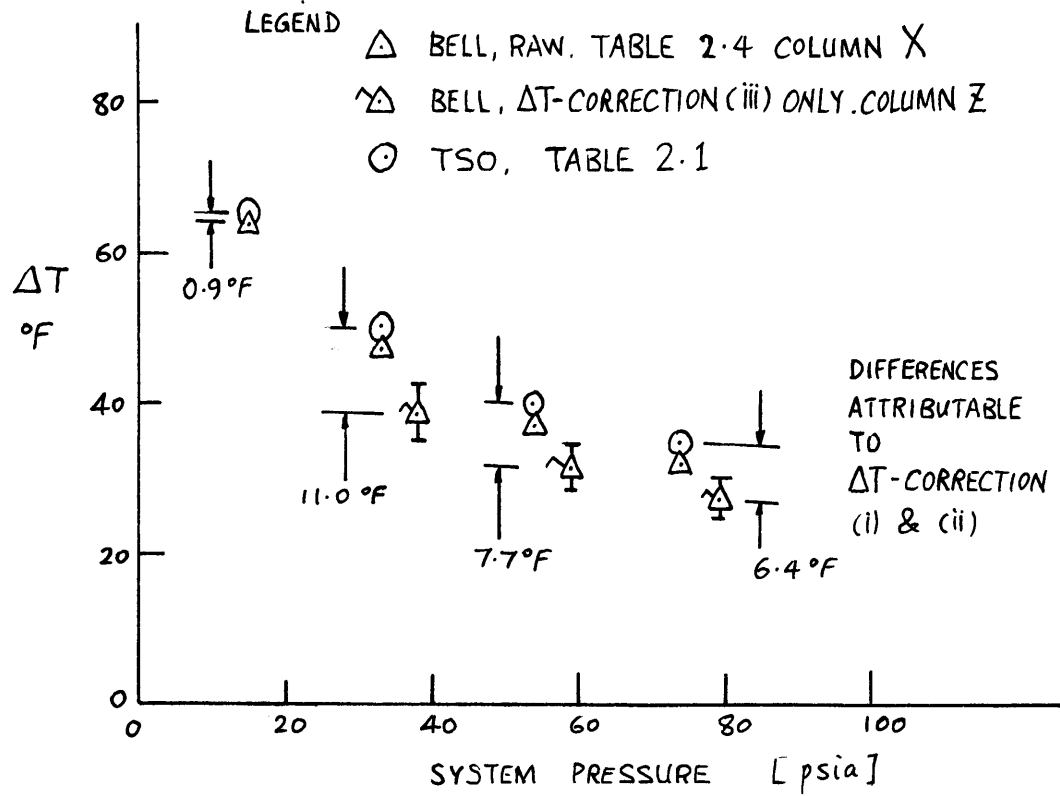
Fig. 2.4   Experimental results for fission fragments in water.

Chapter 3

Theoretical Considerations

3.1 The Energy Balance equation

Bell[2, p.62] postulated that a roughly cylindrical length of vapor would be formed along the radiation path in water due to energy deposition to the water. Fig. 3.1 shows a typical situation. The cylinder radius is less than $50\overset{\circ}{A}$, and it is assumed that the cylinder
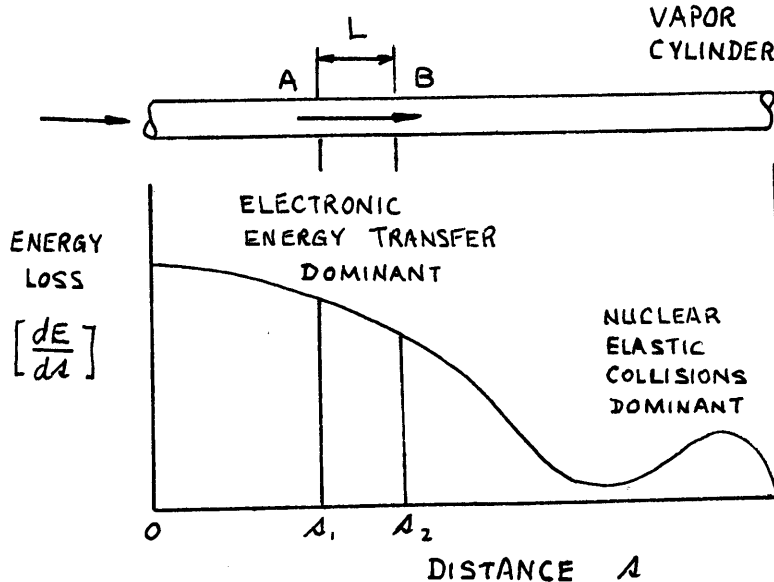
Fig. 3.1 Typical energy loss for a heavy charged
particle interacting with matter (From Bell).

would break up into small lengths L before forming the more stable spherical embryos of radius r. If radiation induced nucleation equation (1.1) is satisfied, then $r = r^*$, the critical radius. Bell theorised that $(\frac{L}{r}*) \equiv a$, a constant of 6.07 based on a certain criteria for spherical nucleation[2,p.198].

The energy of formation of an embryo is made up of several components.

The enthalpy change from liquid to vapor form is $\frac{4}{3}\pi(r^*)^3 \rho_v h_{fg}$, where ρ_v is the density of the vapor state in $[\text{lb-ft}^{-3}]$ and h_{fg} is the specific enthalpy change by evaporation in $[\text{BTU-lb}^{-1}]$. The change in free energy can be represented[2, p.69] by the term $\frac{4}{3}\pi(r^*)^3 \cdot \frac{(P_v^*)b}{2}$, where (P_v^*) is the vapor pressure at critical conditions, and b the ratio of the pressure difference across the embryo interface to the vapor pressure. With reference to Fig. 3.2,

$$b = \frac{(P_v^*) + P_g - P_\ell}{(P_v^*)} \qquad (3.1)$$

where P_ℓ and P_g are the liquid and gas pressure respectively, and in units of $[\text{lbf-ft}^{-2}]$.

The energy losses by way of dissociation of water due to radiation can be approximated[2, p.124] by the expression

Fig. 3.2 Equilibrium of a critical embryo
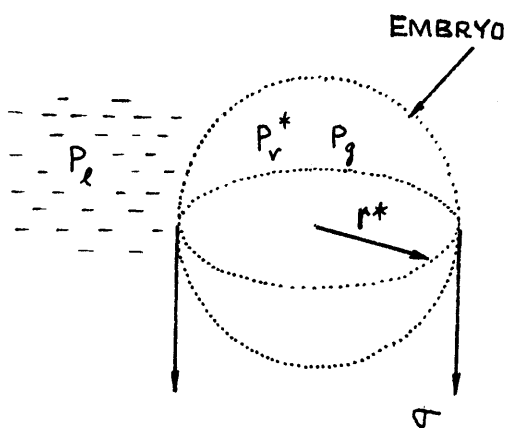
$$\underline{\frac{Q \Delta E \; G(H_2) \; 10^6}{\mathcal{N}}}$$

where $Q = 90.3 \; (\text{Kcal})(\text{mole } H_2)^{-1}$

ΔE = Energy available from radiation

$G(H_2)$ = yield = 1.8 $(\text{molecules})(100\text{ev}^{-1})$

$\mathcal{N}$ = Avogadro's number

If we now neglect the energy of expansion losses from the hot cylinder by way of heat conduction and viscous flow[19], equation (1.1) may be written

as

$$\frac{4}{3}\pi r^{*3} \frac{P_v^* b}{2} + \frac{4}{3}\pi r^{*3} \rho_v h_{fg} + \frac{Q \Delta E \, G(H_2) \, 10^6}{\mathcal{N}} = \Delta E \tag{3.2}$$

Now, from Fig. 3.1,

$$s_2 = s_1 + L = s_1 + a(r^*) \tag{3.3}$$

also
$$E = E(s_2) - E(s_1) \tag{3.4}$$

Combining equations (3.2), (3.3) and (3.4),

$$\frac{4}{3}\pi r^{*3}\left[\frac{P_v^* b}{2} + \rho_v h_{fg}\right] = \left[E(A_1 + ar^*) - E(A_1)\right]\left[1 - \frac{Q\,G(H_2)\,10^6}{\mathcal{N}}\right] \tag{3.5}$$

Now apart from the endothermic production of hydrogen gas, the presence of the hydrogen gas also reduces the vapor pressure (and therefore superheat) requirements in the critical embryo. Thus from Fig. 3.2 the equilibrium condition for a critical embryo is

$$((P_v^*) + P_g - P_\ell)\pi (r^*)^2 = \sigma \, 2\pi (r^*)$$

or
$$(P_v^*) + P_g - P_\ell = \frac{2\sigma}{(r^*)} \tag{3.6}$$

Here, σ is the surface tension in $[\text{lbf-ft}^{-1}]$.

Using equations (3.1) and (3.6), equation (3.5) becomes

$$\frac{4}{3} \pi r^{*3} \left[\frac{\sigma}{r} + \rho_v \, h_{fg} \right] = \left[E(A_1 + ar^*) - E(A_1) \right] \left[1 - \frac{Q \, G(H_2) \, 10^6}{N} \right]$$

$$(3.7)$$

This is the basic Energy Balance Criterion to be applied to radiation induced nucleation.

3.2 Energy Deposition Rate in Water

It is next required to find the energy deposition rate of the radiation in water. The average energy deposition rate over the energy range $E(s_1)$ to $E(s_2)$ is

$$\left(\frac{dE}{dA} \right)_{AV} = \frac{1}{E(A_2) - E(A_1)} \int_{E(A_1)}^{E(A_2)} \left(\frac{dE}{dA} \right) dE$$

$$\doteq \frac{E(A_2) - E(A_1)}{A_2 - A_1} = \frac{E(A_2) - E(A_1)}{ar^*}$$

$$\therefore \quad \frac{\left[E(A_2) - E(A_1) \right]^2}{ar^*} = \int_{E(A_1)}^{E(A_2)} \left(\frac{dE}{dA} \right) dE \qquad (3.8)$$

For radiation particles such as fission fragments, primary knock-on oxygen atoms, and alpha particles, and over the energy range considered in this work, it is justifiable to apply the usual classical theory of heavy charged particle interaction with matter. The following expression is modified from Segre[18].

$$\frac{1}{N}\frac{dE}{dx} = \frac{4\pi e^4}{m_o V^2}(Z_1)_{eff}^2 \sum_{i=H,O} \nu_i Z_i \, \ln\left[\frac{1.123 \, m_o V^3}{(I_i/\hbar)e^2(Z_1)_{eff}}\right]$$

$$+ \frac{4\pi e^4}{V^2}(Z_1)_{eff}^2 \sum_{i=H,O} \nu_i \frac{Z_i^2}{M_i} \, \ln\left[\frac{M_1 M_i V^2 (a_{1i}^{scr})_i}{(M_1+M_i) Z_1 Z_i e^2}\right] \tag{3.9}$$

where e = charge on an electron

m_o = electron mass

V = velocity of the incident particle

$(Z_1)_{eff}$ = effective charge on the incident particle = $(Z_1)^{1/3} \left(\frac{\hbar V}{e^2}\right)$

Z_1 = atomic number of the incident particle

Z_i = atomic number of the ith atom in the stopping medium

$(Z_H = 1; \ Z_O = 8)$

ν_i = number of ith atom per molecule $(\nu_H = 2; \ \nu_O = 1)$

I_i = mean ionization potential of the ith component

$(I_H = 15.5; \ I_O = 100, \text{ from Evans}^{(6)})$

M_1 = mass of incident particle in amu

M_i = mass of ith atom $(M_H = 1 \text{ amu}; \ M_O = 16 \text{ amu})$

a_{1i}^{scr} = impact parameter = $a_B/[(Z_1)^{2/3} + (Z_i)^{2/3}]^{1/2}$

a_B = radius of first Bohr orbit for hydrogen atom = 0.5291×10^{-8}cm

$\hbar$ = Planck's constant divided by 2π $(\hbar c = 1.9732 \times 10^{-11} \text{Mev-cm})$

N = number of molecules of stopping medium per unit volume

= $(\mathcal{N}\rho_1)/M$, M = molecular weight of water

= $0.3347 \times 10^{23} \, \rho_1$ $[\#-cm^{-3}]$

Equation (3.9) will be evaluated for particular cases and inserted into equation (3.8).

3.3 Fission Fragments in Water at Low Pressure Range

For fission fragments in water, equation (3.9) becomes, to a good approximation,

$$\frac{dE}{ds} = \rho_1 \, 3.620 \times 10^4 \, \ln(0.0549 \, E) \tag{3.10}$$

where the light fragment only need be considered [2, p.118] and has characteristics of $Z_1 = 38$, $A = 97$, and initial energy of 95 Mev have been used. The energy deposition to water through nuclear elastic collisions has also been neglected. [2, p.117]

The corresponding equation (3.8) after integrating and inserting the appropriate unit conversion factors, is

$$\frac{\left[E(A_2) - 95 \, Mev \right]^2}{61.75 - E(A_2) \, \ln E(A_2) - 3.900 \, E(A_2)} = \frac{a \, \sigma \, \rho_\ell}{P_v^* + P_g - P_\ell} \, (3.440 \times 10^4) \tag{3.11}$$

Note that in equation (3.11), use is made of equation (3.6), and that σ is in $[\text{lbf-ft}^{-1}]$, ρ_1 in $[\text{lb-ft}^{-3}]$, and pressures in $[\text{lbf-ft}^{-2}]$.

Bell has developed a computer program to calculate the superheat threshold in the pressure range of atmospheric to 100 psia, the details of which are found in his work. [2, p.122] Basically it is an iterative process to find a system temperature that satisfies equation (3.10) and (3.6). The final results involve three variable, viz., the system pressure P_1, the system temperature T_1 and the parameter a, with a and

P_1 considered independent variables. The theoretical results are plotted and compared with experimental data in Chapter 5.

It is noteworthy that the above iterative process requires the physical properties (vapor pressure, liquid and vapor densities, surface tension, and enthalpy change by evaporation) of water to be known over the pressure (and hence temperature) range considered. These have been obtained conveniently through empirical relations as given in Appendix C.

A typical computer program for the above calculations is included in Appendix F. The program is for fission neutrons in water at PWR conditions, but the fission fragment programs are very similar to it.

3.4 Fast Neutrons in Water at Low Pressure Range

In the case of the Pu-Be neutrons in water, the main mechanism of energy loss to the water is by way of primary knock-on oxygen atom (PKOA) in water. The energy of a PKOA, J , can be expressed by the usual elastic scattering theory[7] as

$$ J = \tfrac{1}{2}En \left[1 - (\tfrac{A-1}{A+1})^2 \right] (1 - \cos\theta) \qquad (3.12) $$

where En is the neutron energy, A the atomic weight of oxygen, and the angle the neutron is scattered in the Center of Mass frame of reference. For a maximum J,

$$ J_{max} = 0.22En \qquad (3.13) $$

The energy loss in this case is, from equation (3.9) with $Z_1 = 8$, $M_1 = 16$,

$$\frac{dE}{ds} = \rho_1 \, 1.282 \times 10^4 \ln 0.5591E \qquad (3.14)$$

Equation (3.8) reduces to

$$\frac{[E(A_2) - J]^2}{J \ln J - E(A_2)\ln E(A_2) - 1.581[J - E(A_2)]} = \frac{a\sigma\rho_\ell}{P_v^* + P_g - P_\ell}(1.2516 \times 10^4) \qquad (3.15)$$

where $B(s_1)$ has been retained as J . The primary knock-on energy of
protons in water has been shown by Bell[2, p.252] to be of less importance
because of the relatively low energy deposition rate. Calculations
leading to equations (3.14) and (3.15) are given in Appendix E.

It might be thought that J in equation (3.15) is simply J_{max} of
equation (3.13), with E_n being the maximum energy of the Pu-Be neutron
spectrum. But, because of the low number of neutrons at the high energy
tail, whether the highest energy neutrons are effective in causing nuclea-
tion would depend on the experimental conditions. The production rate of
highest energy PKOA depends on the intensity of the neutron source as
well as on the temperature ramp of the system.

For the present experimental conditions, Bell has developed a theore-
tical relationship between the minimum participating primary knock-on
energy (that primary knock-on energy at and above which will contribute
to nucleation) and the temperature ramp of the system. For a temperature
ramp of $\frac{1}{2}$°F/min, as is aimed for in the experimental work, this minimum
participating primary knock-on energy is 2.12 Mev. Thus J = 2.12 Mev
in equation (3.14).

As in the fission fragment case, Bell has calculated the superheat threshold over the range of atmospheric pressure to 100 psia, for various values of a. The same empirical formulae for physical properties of water are used. The theoretical results are plotted and compared with experimental data in Chapter 5.

3.5 Application of Theory to Radiation Induced Nucleation in PWR's

3.5.1 Fission Neutrons in Water under PWR Conditions. In an attempt to study radiation induced nucleation in the PWR, radiation induced by the fission neutrons is first considered. The same energy depostion rate expression and energy balance equation as used in section 3.4 is applicable here. However, two of the empirical formulae for physical properties of water (enthalpy change by evaporation and surface tension) must be altered to accommodate pressure in the region of 2235 psia. This is done in Appendix ₵.

The fission spectrum, as given in Glasstone and Sesonske[7] or Kaplan[10] has an energy distribution between 0.025 Mev and 17 Mev with a maximum in number at around 1 Mev. This distribution is assumed to prevail in the coolant in contact with the fuel elements in the PWR by neglecting any effects the thin cladding material may have on the fission spectrum.

An immediate difficulty in applying the theory developed so far to predict radiation induced nucleation is to decide what value of J to use in equation (3.15). The minimum primary knock-on energy cannot be determined as mentioned in section 3.4 because there is essentially zero temperature ramp in the steady-state PWR, and the theory would argue nucleation at the saturation temperature in all cases. This difficulty

Table 3.1 Theoretical Results for Fission Neutrons in Water

	System Pressure $lbf\text{-}ft^{-2}$	Sat. Temp. $^{\circ}F$	$\Delta_o T$ F	Superheat Temp. $^{\circ}F$
a = 6.07	302400.0	642.920	1.080	644.000
17 Mev neutrons	309600.0	646.330	0.890	647.220
	316800.0	649.640	0.750	650.390
	324000.0	652.900	0.610	653.510
	331200.0	656.090	0.500	656.590
	338400.0	659.230	0.390	659.620
	345600.0	662.310	0.300	662.610
a = 6.07	302400.0	642.920	3.260	646.180
9.55 Mev neutrons	309600.0	646.330	2.870	649.200
	316800.0	649.640	2.540	652.180
	324000.0	652.900	2.200	655.100
	331200.0	656.090	1.900	657.990
	338400.0	659.230	1.610	660.840
	345600.0	662.310	1.350	663.660
a = 3.70	302400.0	642.920	1.750	644.670
17 Mev neutrons	309600.0	646.330	1.480	647.810
	316800.0	649.640	1.270	650.910
	324000.0	652.900	1.070	653.970
	331200.0	656.090	0.900	656.990
	338400.0	659.230	0.730	659.960
	345600.0	662.310	0.590	662.900

has not been resolved in the present work.

Nonetheless, to have some idea of how the energy of the neutrons would affect nucleation in the PWR, Bell's program is again used. A typical program run is given on Appendix F. Table 3.1 tabulates results for three cases—threshold superheat for 17 Mev neutrons with a = 3.70 and a = 6.07, and for 9.55 Mev neutrons with a = 6.07. These results will be plotted and discussed in Chapter 5.

3.5.2 Neutron Induced Alpha Particles in Water under PWR Conditions.

Another possible source of radiation which induces nucleation in the PWR coolant is the (n, α) reaction on Boron, the latter being added in the form of boric acid for chemical shim control in the PWR. The reaction is exothermic.

$$_5B^{10} + {}_0n^1 \rightarrow [\, _5B^{11}\,] \rightarrow {}_3Li^7 + {}_2He^4 + 2.793 \text{ Mev}$$
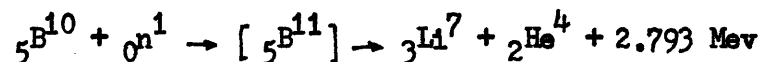
The energy deposition to water is here considered to be due to the alpha particles emitting from the (n, α) reaction. Hence equation (3.9) is again applicable, and is calculated (with $Z_1 = 2$, $M_1 = 4$) to be

$$\frac{dE}{d\lambda} = \rho_1 \, 5.090 \times 10^3 \ln 3.5495E \qquad (3.16)$$

where again the energy deposition to protons has been neglected. Equation (3.7) becomes

$$\frac{[E(\lambda_1) - E(\lambda_2)]^2}{E(\lambda_1)\ln(\lambda_1) - E(\lambda_2)\ln E(\lambda_2) + 0.267[E(\lambda_1) - E(\lambda_2)]} = \frac{a\sigma \rho_\ell (4.97 \times 10^3)}{P_v^* + P_g - P_\ell}$$

$$(3.17)$$

With equation (3.16) and (3.17), a computer program very similar to that used in section 3.5.1 and given in Appendix F may be used to find the threshold superheats, provided suitable values for $E(s_1)$ are taken. Here one is confronted with exactly the same difficulty as mentioned in section 3.5.1.

From Evans[6] the kinetic energy of the alpha particle, E_3, may be expressed as

$$\sqrt{E_3} = \frac{\sqrt{M_1 M_3 E_1}}{M_3 + M_4} \cos \theta \pm \sqrt{\frac{M_1 M_3 E_1 \cos^2 \theta}{(M_3 + M_4)^2} + \frac{M_4 Q + E_1 (M_4 - M_1)}{(M_3 + M_4)}}$$

$$(3.18)$$

where M_1, E_1 = rest mass and kinetic energy of incident neutron

M_3 = rest mass of alpha particle

M_4 = rest mass of $_3\text{Li}^7$

Q = "Q" value of the reaction = +2.793 Mev

θ = exit angle made by alpha particle with direction of incident neutron measured in the Laboratory frame of reference.

The relationship between E_3 and E_1 is plotted on Fig. 3.3, showing the two extremes of $\theta = \pi/2$ and $\theta = 0$, corresponding to minimum and maximum energy transfers respectively. To have some idea of how this (n, α) phenomenon could affect nucleation in the PWR, three specific cases are considered--nucleation due to the action of 17 Mev, 1 Mev, and 0.025 Mev neutrons. From Fig. 3.3, the alpha particles energies corresponding to the maximum energy transfer of $\theta = 0$ are 17.3 Mev, 2.95 Mev
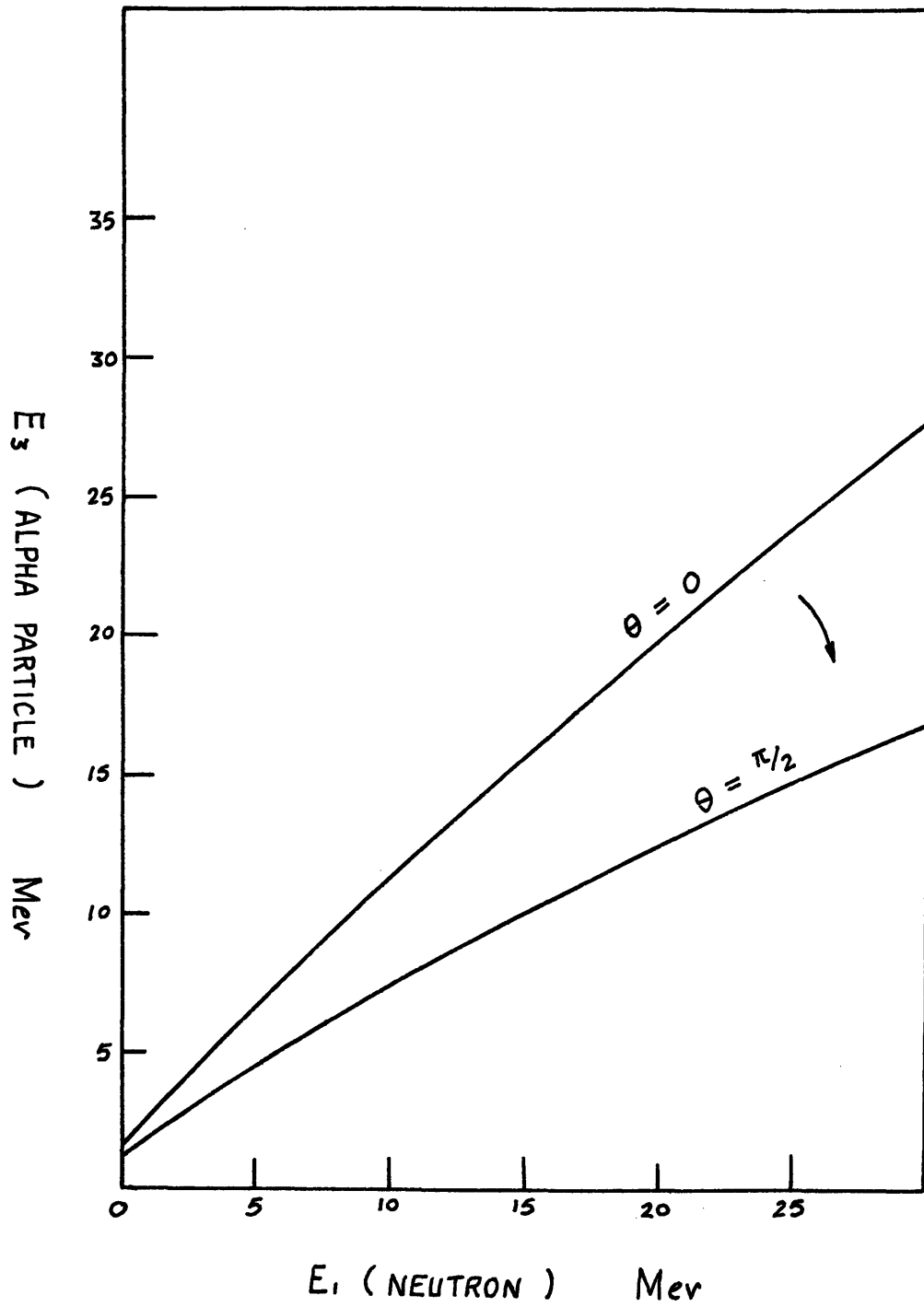
Fig. 3.3 Relationship between incident neutron energy and emitting alpha
particle energy.

Table 3.2 Theoretical results for neutron induced
alpha particles in water

	System Pressure lbf-ft^{-2}	Sat.Temp. ^{o}F	Δ T ^{o}F	Superheat temp. ^{o}F
a = 6.07	302400.0	642.920	0.380	643.300
17 Mev neutrons	309600.0	646.330	0.280	646.610
	316800.0	649.640	0.210	649.850
	324000.0	652.900	0.150	653.050
	331200.0	656.090	0.100	656.190
	338400.0	659.230	0.050	659.280
	345600.0	662.310	0.010	662.320
a = 6.07	302400.0	642.920	0.830	643.750
1 Mev neutrons	309600.0	646.330	0.670	647.000
	316800.0	649.640	0.560	650.200
	324000.0	652.900	0.450	653.350
	331200.0	656.090	0.360	656.450
	338400.0	659.230	0.270	659.500
	345600.0	662.310	0.190	662.500
a = 6.07	302400.0	642.920	4.390	647.310
0.025 Mev neutrons	309600.0	646.330	3.970	650.300
	316800.0	649.640	3.610	653.250
	324000.0	652.900	3.260	656.160
	331200.0	656.090	2.940	659.030
	338400.0	659.230	2.630	661.860
	345600.0	662.310	2.340	664.650

and 1.87 Mev respectively. Hence $E(s_1)$ is put equal to these values in the program. The results are tabulated in Table 3.2. 'a' has been taken as 6.07 throughout. These results will be plotted and discussed in Chapter 5.

It is noteworthy that for values of a > 6.07, the corresponding superheat would be decreased. And conversely a higher superheat for a < 6.07.

3.6 Mononergetic Neutrons in Benzene at Low Pressure Range.

In the course of a literature survey, it was found that other investigators had worked on radiation induced nucleation in some organic liquids. Becker[1] worked on diethyl ether, and El-Nagdy[5] considered neutron-induced nucleation for 2.45 and 14.1 Mev in acetone and in benzene. It was decided then to apply Bell's theory to such liquids and compare the results with these investigators. However, within the limited time for the present thesis work, only the physical properties of benzene were completely obtained for use in calculating threshold superheats.

This section will consider neutron induced nucleation in pure benzene in the pressure region of 0 to 100 psia. The benzene ring structure, being composed of covalently bonded C_6H_6, may for the present purpose considered free carbon and hydrogen atoms. The bond energy of each member atom is of the order below an ev.

The main mechanism of energy loss by neutrons in benzene is by primary knock-on carbon atoms (PKCA) in benzene. The energy of a PKCA J_c, can be evaluated with equation (3.12) to be $J_c = 0.142 E_n (1-\cos \theta)$ Maximised with respect to θ ,

$$J_c = 0.284 E_n \qquad (3.19)$$

En is again the neutron energy used.

The energy loss of the PKCA in benzene can again be found by equation (3.9) by taking $Z_1 = 6$, $M_1 = 12$, and summing over i = 6C and 6H. The final result is

$$\frac{dE}{ds} = \rho_1 \; (1.025 \times 10^4 \; \ln 0.9450E) + \frac{10.5}{E} \; \ln 1230E$$

Again to a good approximation, the energy loss to protons may be neglected (i.e. i = 6C only). Then,

$$\frac{dE}{d\mathcal{A}} = \rho_1 \; 1.025 \times 10^4 \; \ln 0.9450E \qquad (3.20)$$

Equation (3.8) becomes

$$\frac{[\,E(\mathcal{A}_2) - J_c\,]^2}{J_c \ell_n J_c - E(\mathcal{A}_2)\ell_n E(\mathcal{A}_2) - 1.0565[\,J_c - E(\mathcal{A}_2)\,]} = \frac{a\sigma \rho_\ell \;(1.000 \times 10^4)}{P_v^* + P_g - P_\ell} \qquad (3.21)$$

Mononergetic neutrons of energies 2.45 Mev and 14.1 Mev are separately considered here (as per Becker[1]) so that J_c from equation (3.19) are simply 0.695 Mev and 4.00 Mev respectively.

Using a modified Bell's program, the threshold superheats for benzene for the above two neutrons energies were obtained, as a function of the 'a'. A typical program run is found in Appendix F. Physical properties of benzene over the required pressure range is given in Appendix D. Fig. 3.4 and Fig. 3.5 show the results.

The spread in the curves for 2.45 Mev neutrons as in Fig. 3.4 seems to be very narrow, with respect to values of a. In contrast, in Fig. 3.5,

the results for 14.1 Mev neutrons has a fairly good spread, like the results for water considered in this chapter. However, in Fig. 3.5 there is an upper limit of a in the vicinity of a = 4.62. Higher values of a did not yield any result from the computer program. These behaviors are not understood at present and further investigation is necessary.

THRESHOLD SUPERHEAT ΔT [°F]

SYSTEM PRESSURE [psia]

$a = 0.01$

$a = 100$
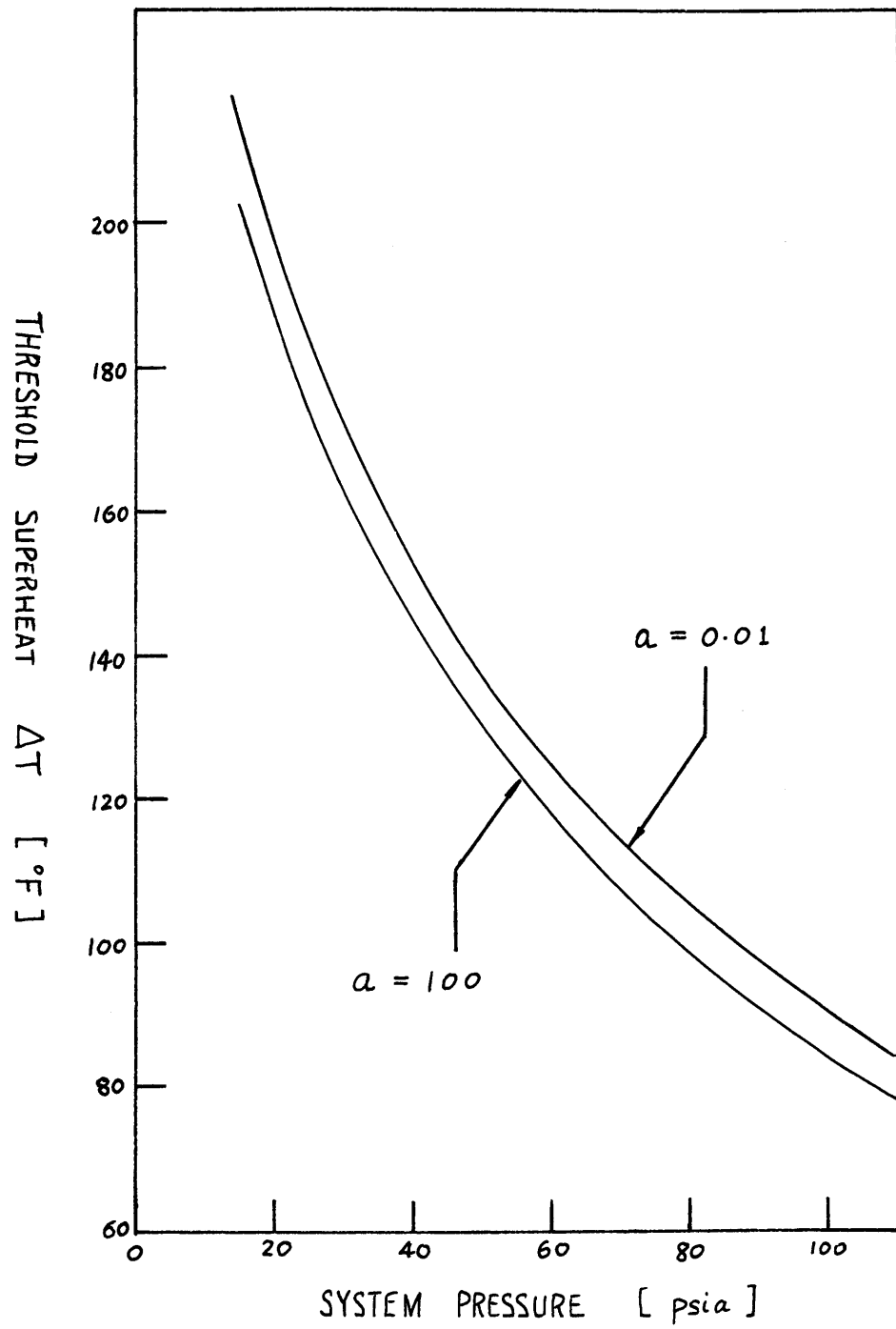
Fig. 3.4 Theoretical results for 2.45 Mev neutrons in benzene.
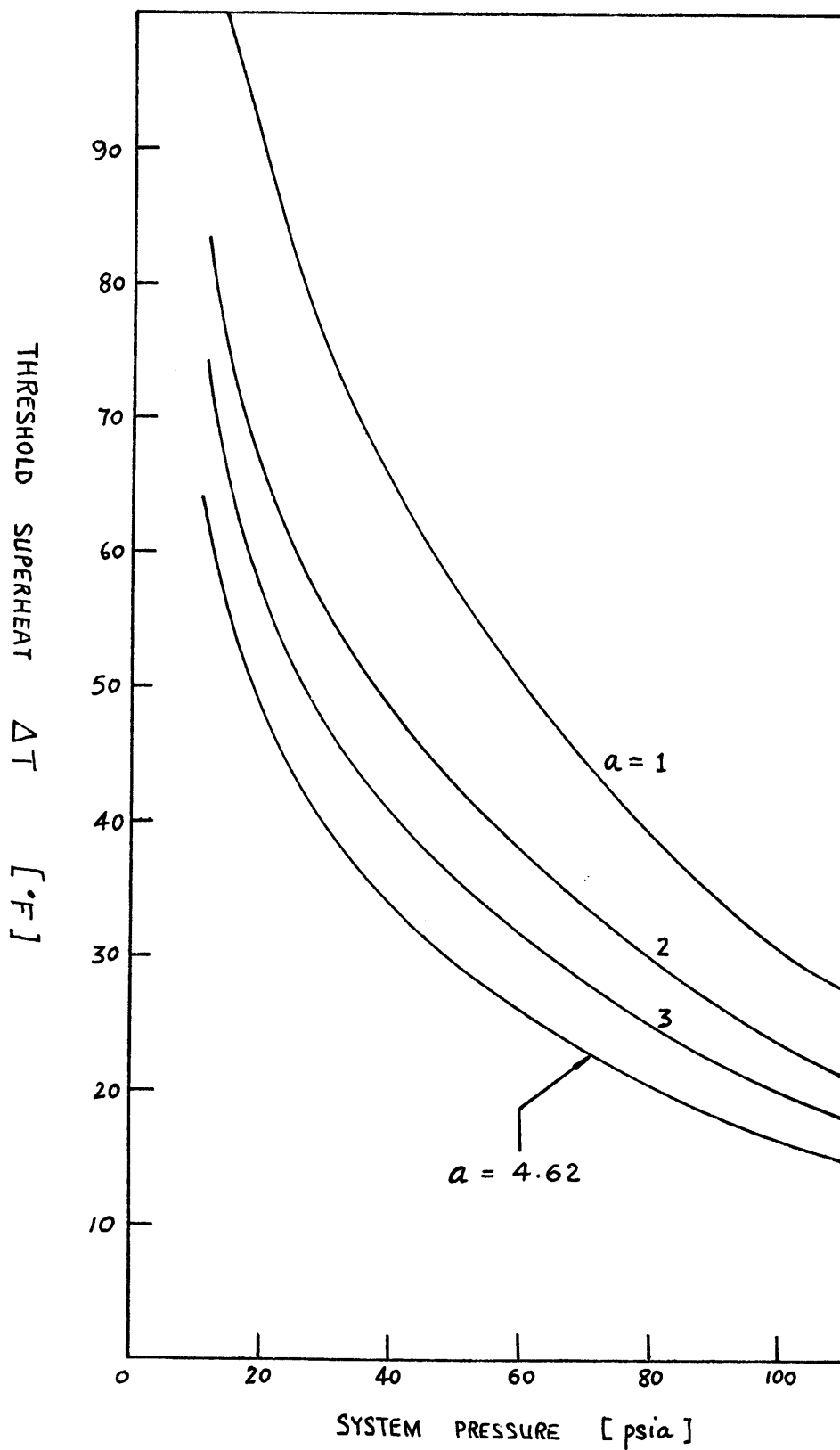
Fig. 3.5   Theoretical results for 14.1 Mev neutrons in benzene.

Chapter 4

Thermocouple Correction

An attempt will be made here to assess the temperature error present when the bottom thermocouple sheath is of aluminum and of stainless steel material. The analysis is based on an article by Rizika and Rohsenow[16] The assumption made are that the system is in steady state, the thermal conductivity k and the film coefficient of heat transfer h of the sheath are uniform and constant, and the end effects of the sheath are negligible, and the oil in the chamber has uniform temperature (see Fig. 4.3). These are valid since a more uniform thermal field is created in the oil by the addition of the top circumferential heater.

4.1 Analysis of Problem

Fig. 4.1 shows the thermocouple sheath of length l, submerged in supporting oil in length l_i. Considering the heat balance on an elementary length dx with outside surface area dA,

$$q(dA) = q(x + dx) - q(x) \qquad (4.1)$$

Now, $q(x) = -kS \frac{dT}{dx}$, Fourier conduction law with S being the cross-sectional area of the sheath. Therefore, $q(x + dx) = -kS \frac{d}{dx}(T + \frac{dT}{dx}dx)$. And in air, $q(dA) = h_o(T_a-T)Pdx$, while in oil, $q(dA) = h_i(T_f-T)Pdx$, where h_o is the film coefficient of heat transfer between the air and the sheath, h_i the total coefficient of heat transfer between the oil and the sheath, P is the perimeter of the sheath, and T_a, T_f are the temperatures of the ambient air and oil respectively. These equations may be
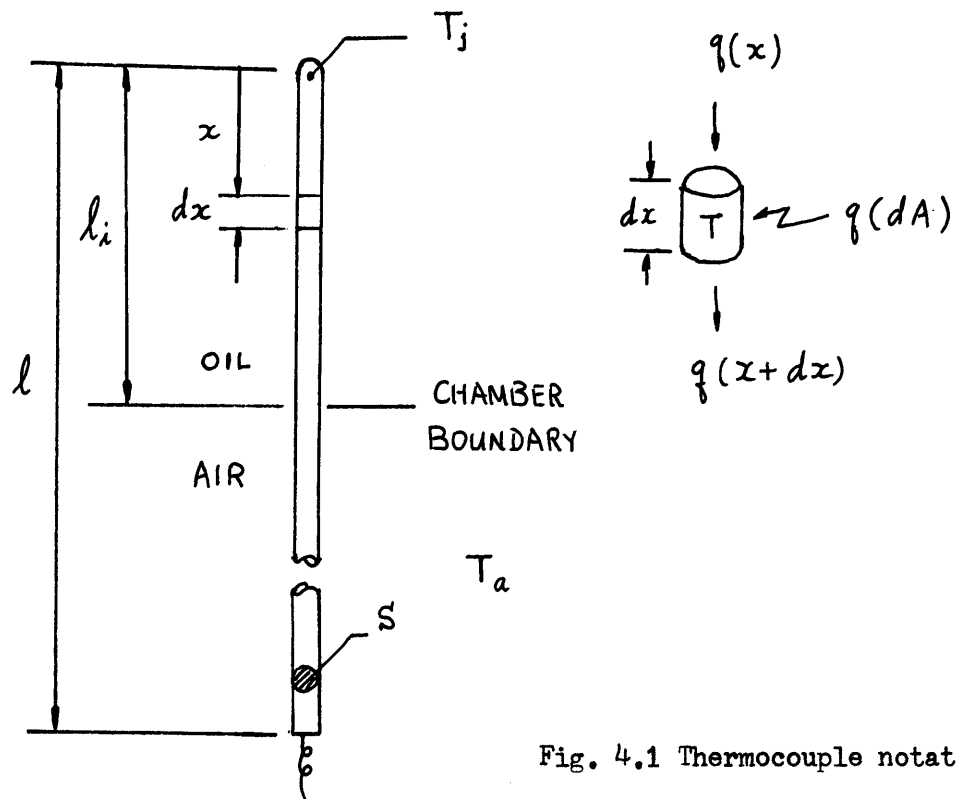
Fig. 4.1 Thermocouple notations

substituted into equation (4.1) to yield the following two linear equations.

In air,
$$\frac{d^2}{dx^2}(T - T_a) - (\frac{h_o P}{k\,S})(T - T_a) = 0 \qquad (4.2)$$

In oil,
$$\frac{d^2}{dx^2}(T - T_f) - (\frac{h_o P}{k\,S})(T - T_f) = 0 \qquad (4.3)$$

The solutions of equations (4.2) and (4.3) are

$$(T - T_a) = C_1 \exp(B_o x) + C_2 \exp(-B_o x) \qquad (4.4)$$

$$(T - T_f) = C_3 \exp(B_1 x) + C_4 \exp(-B_1 x) \qquad (4.5)$$
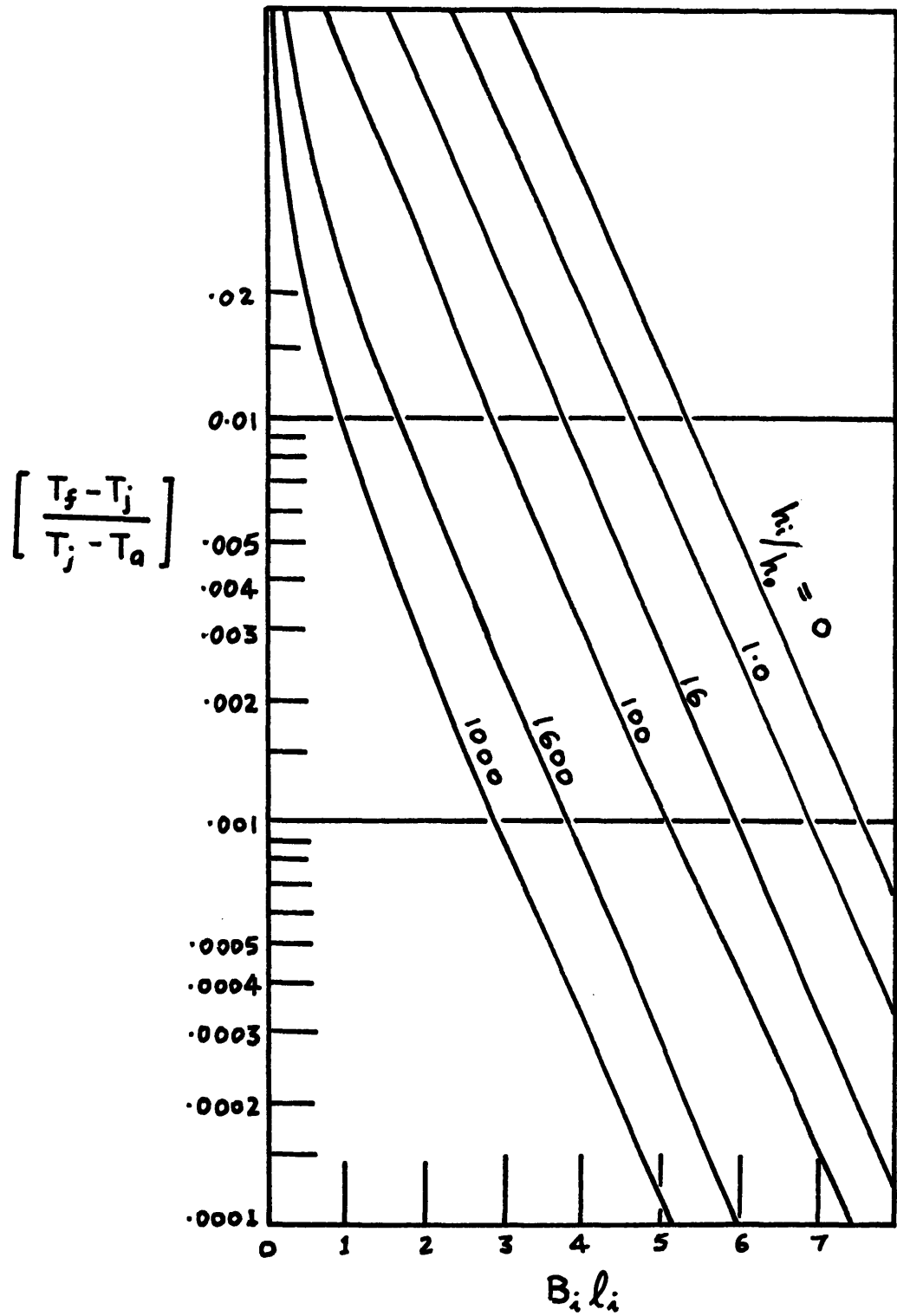
Fig. 4.2 Parameters plot in thermocouple error analysis[16].

with
$$B_o = \left[h_o P/(kS) \right]^{\frac{1}{2}}$$

$$B_i = \left[h_i P/(kS) \right]^{\frac{1}{2}}$$

Applying the boundary conditions,

$$x = 0, \quad \frac{d}{dx}(T - T_f) = 0$$

$$x = L, \quad \frac{d}{dx}(T - T_a) = 0$$

$$x = l_i, \quad T = T \text{ for equations (4.4) and (4.5)}$$

$$\frac{d}{dx}(T - T_f) = \frac{d}{dx}(T - T_a),$$

and then substituting $x = 0$ (whence $T = T_j$, the thermocouple junction temperature) and $l \to \infty$, the following final expression is obtained.

$$\frac{T_f - T_j}{T_j - T_a} = \left[\frac{B_i}{B_o} \sinh(B_i l_i) + \cosh(B_i l_i) - 1 \right]^{-1} \qquad (4.6)$$

A plot of equation (4.6) is given on Fig. 4.2 with the dimensionless variables $\left[(T_f - T_j)/(T_j - T_a) \right]$, $B_i l_i$, and (h_i/h_o).

4.2 Heat Transfer Coefficients

Before the temperature difference $(T_f - T_j)$ or ΔT can be evaluated, the various heat transfer coefficients must be determined. The evaluation of these coefficients involves property values of the oil which are functions of temperature, as well as ΔT, so that a trial and error method is imperative.

Two levels of temperature will be considered, namely 300°F and 400°F

corresponding respectively to the temperature ranges of the fission

fragment and the fast neutron cases considered in Chapter 2.

(i) h_c. The film coefficient of heat transfer between the oil and the

sheath.

According to p.172 equation (7-4b) of McAdam[12] the expression for

free convection over vertical cylinderw in laminar regime is given by

$$Nu = 0.59(GrPr)^{\frac{1}{4}} \qquad (4.7)$$

where Nu is the Nusselt number, Gr the Grashof number and Pr the Prandtl

number. Equation (4.7) may be written as

$$h_c = 0.59 \frac{k_f}{\ell_i} \left[\frac{\ell_i^3 \rho_f^2 g \beta_f \Delta T}{\mu_f^2} P_r \right]^{1/4} \qquad (4.8)$$

where l_i is again the length of sheath in oil, k the thermal conductivity

of oil, ρ_f the oil density, g the acceleration due to gravity, β_f the

coefficient of volumetric expansion and μ_f the oil viscosity. Table

4.1 tabulates these values for oil.[15]

In the 300°F region, equation (4.8) reduces to

$$h_c = 11.2(\Delta T)^{\frac{1}{4}} \qquad (4.9)$$

and in the 400°F region,

$$h_c = 13.8(\Delta T)^{\frac{1}{4}} \qquad (4.10)$$

Table 4.1 Quantities for equation (4.8)

Quantity	Units	300°F	400°F
k_f	BTU-hr^{-1}-ft^{-1}-$^\circ$F^{-1}	0.073	0.0725
ρ_f	lb-ft^{-3}	52.8	49.5
β_f	$^\circ$R^{-1}	0.45×10^{-3}	0.46×10^{-3}
μ_f	lb-hr^{-1}-ft^{-1}	3.0	1.2
Pr	dimensionless	22	9
l_i	ft	0.271	
g	ft-hr^{-2}	4.17×10^8	

(ii) h_r. The radiation coefficient of heat transfer between the oil and the sheath.

This may be approximated by the relation

$$h_r = \sigma \frac{(T_f^4 - T_j^4)}{(T_f - T_j)} = \sigma (T_f^2 + T_j^2)(T_f + T_j) \qquad (4.11)$$

where $\sigma = 0.1723 \times 10^{-8}$ $\left[\text{BTU-ft}^{-2}\text{-hr-}^{-1}\text{°R}^{-4} \right]$, the stefan constant.

(iii) h_o. The film coefficient of heat transfer between air and the sheath.

A procedure given in McAdams, pp.173-174 is used to find h_o. First, the film temperature T_{fm}^{air}, as indicated in Fig. 4.3, is calculated to be 126°F and 151°F, based on $T_a = 68^\circ$F and $T_j = 300^\circ$F and 400°F respectively. Then from p.174, Fig. 7-8 of McAdam, the values for the quantity

$$\left[\frac{\rho_f^2 g \beta_f c_p}{\mu_f k_f} \right]$$

TEMPERATURE

T_a T_j T_f

DISTANCE

ΔT

T_j

T_m

$\Delta T = T_j - T_f$

$T_m = \frac{1}{2}(T_j + T_a)$

$\Delta t = T_m - T_a$

$T_{fm}^{oil} = \frac{1}{2}(T_j + T_f)$

$T_a = 68°F$

$T_{fm}^{air} = \frac{1}{2}(T_m + T_a)$
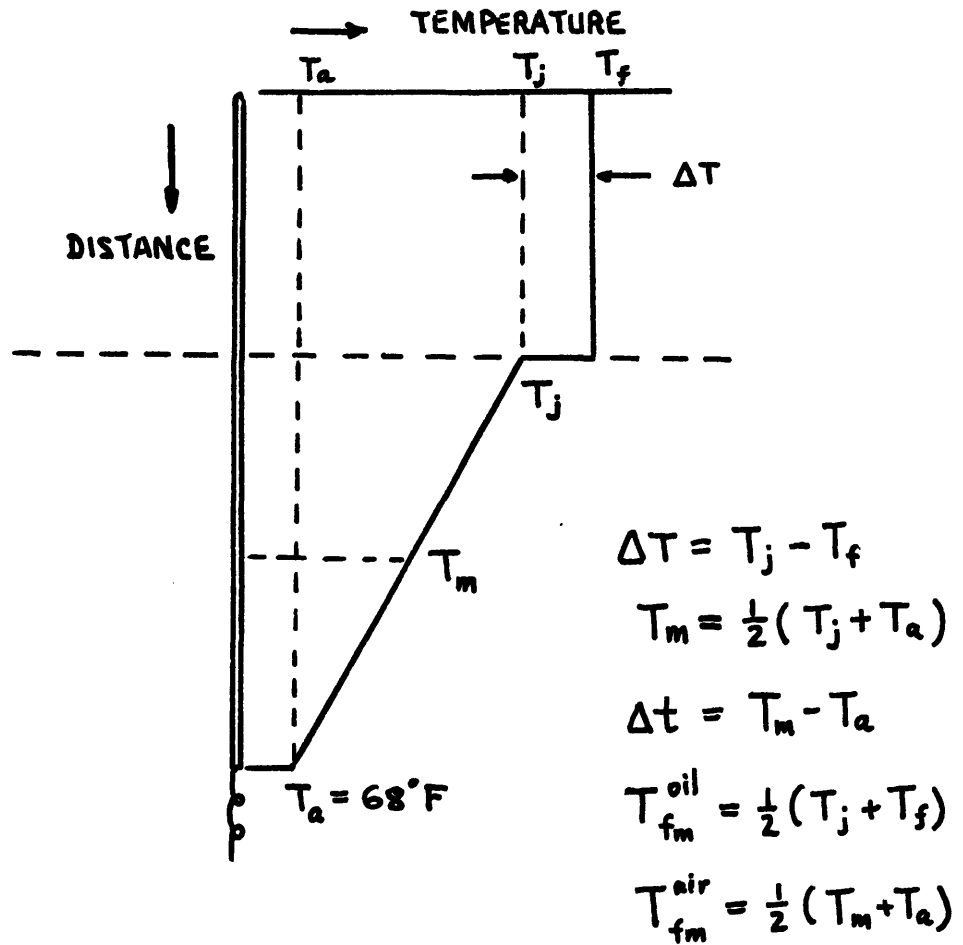
Fig. 4.3 Thermocouple temperature profile—idealized.

are found to be 1×10^6 and 0.9×10^6 $[ft^{-3}-°F^{-1}]$. Next, (GrPr) is evaluated for both cases and found to lie within the range of 10^4-10^9, so that equation (7-5b) from the same reference is used for h_o. Namely,

$$h_o = 0.29(\frac{\Delta t}{1 - 1i})$$ (4.12)

with T_a as 68°F, h_o is found to be 1.32 and 1.44 $[BTU-hr^{-1}-ft^{-2}-°F^{-1}]$ for $T_j = 300$ F and 400 F respectively.

4.3 Evaluation of error.

An assumed value for ΔT is taken as 1, 5, 10 and $20°F$ for each of the two temperature regions. h_c is thus evaluated with results shown in Table 4.2, using equations (4.9) and (4.10). In calculating h_r from equation (4.11), equal intervals of temperatures are taken above and below $300°F$ (or $400°F$) for T_f and T_j. From Table 4.2, it is seen that h_r is a weak function of ΔT.

h_i, the total coefficient of heat transfer between the oil and the sheath, equals the sum of h_c and h_r. $B_i l_i$, as defined in equation (4.4) and (4.5) is also tabulated under separate columns for aluminum (Al) and stainless steel (S.S.). The last column give the ΔT as predicted by equation (4.6). T_a has been taken as $68°F$.

Assumed ΔT $°F$	T_f $°R$	T_j $°R$	h_c	h_r	h_i	h_o [BTU-hr^{-1}-ft^{-2}-$°F^{-1}$]	$\left(\dfrac{h_i}{h_o}\right)$	$\left(\dfrac{B_i}{B_o}\right)$	$B_i l_i$ Al	$B_i l_i$ S.S.	Predicted ΔT $°F$ Al	Predicted ΔT $°F$ S.S.
Region of $300°F$												
1	$300\frac{1}{2}$	$299\frac{1}{2}$	11.2	3.04	14.2	1.32	10.8	3.28	1.69	5.86	22.4	0.31
5	$302\frac{1}{2}$	$297\frac{1}{2}$	16.7	3.04	19.7	1.32	15.0	3.87	1.99	6.90	14.0	0.10
10	305	295	19.9	3.03	21.9	1.32	17.4	4.17	2.14	7.45	11.0	0.05
20	310	290	23.8	3.02	26.8	1.32	20.4	4.51	2.32	8.04	8.7	0.03
Region of $400°F$												
1	$300\frac{1}{2}$	$299\frac{1}{2}$	13.8	4.4	18.2	1.44	12.6	3.55	1.91	6.62	21.6	0.20
5	$302\frac{1}{2}$	$297\frac{1}{2}$	20.6	4.4	25.0	1.44	17.4	4.17	2.24	7.77	14.4	0.05
10	305	295	24.4	4.4	28.8	1.44	20.0	4.47	2.41	8.31	11.3	0.03
20	310	290	29.3	4.4	33.7	1.44	23.4	4.84	2.60	9.02	8.7	0.014

Table 4.2 Tabulation for equation (4.6) solution.

Fig. 4.4 and Fig. 4.5 show plots of the assumed ΔT against the predicted ΔT. The intersections of these curves with the 45° lines indicate that for the aluminum sheath, there is an inherent error of about 11°F to be added to the experimental thermocouple readings. Based on the above model, the error seems to be fairly insensitive to the system temperature over the temperature region considered. For the stainless steel case, the errors are well below 1°F and hence are not of any concern.
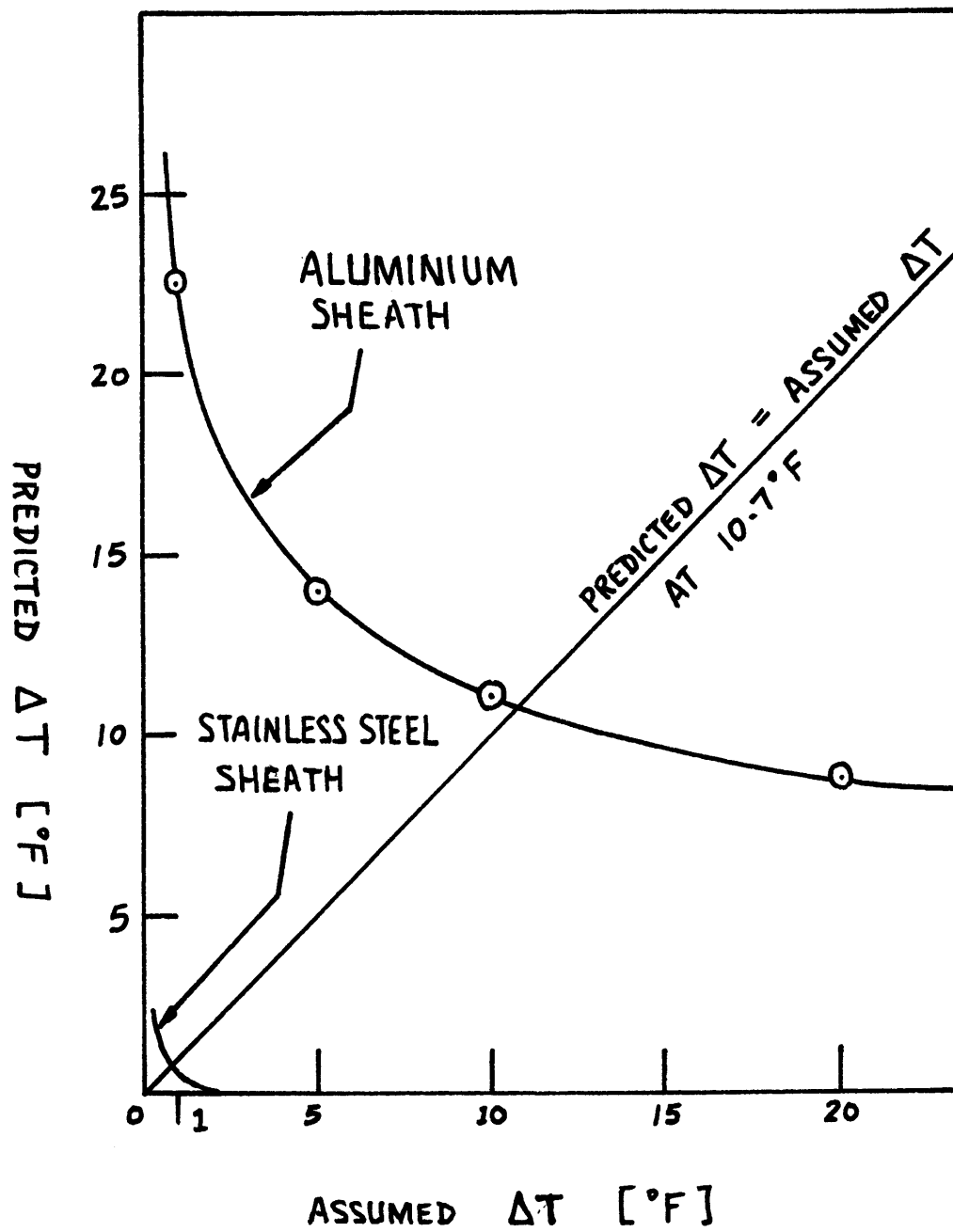
Fig. 4.4 Temperature correction for 300°F region.
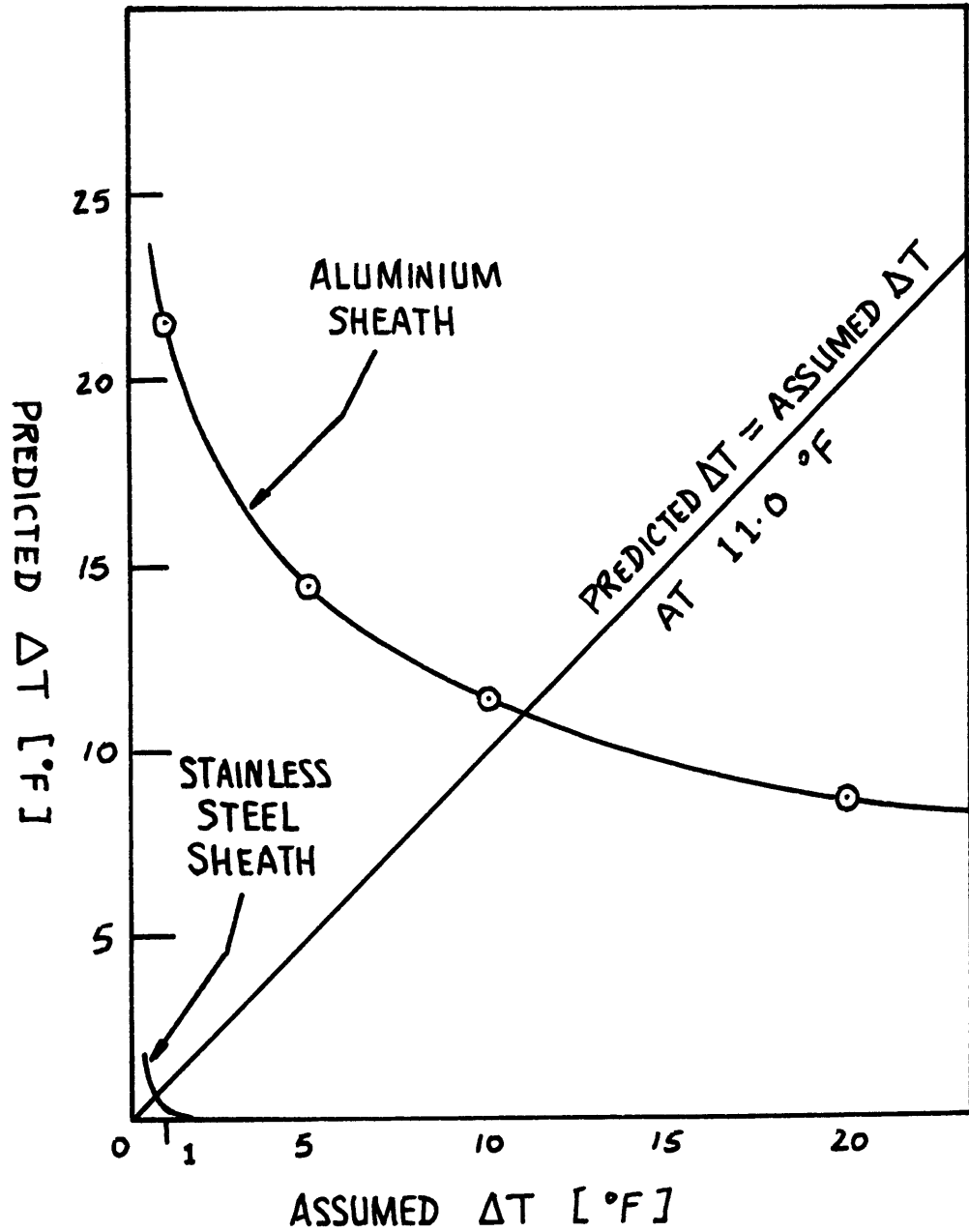
Fig. 4.5 Temperature correction for 400°F region.

Chapter 5

Conclusions and Recommendations

5.1 Conclusions

5.1.1 Fission Fragments in Water. Fig. 5.1 shows a comparison of theoretical and experimental superheat thresholds for fission fragments in water, with data taken from Tables 2.1 and 2.4. Data from present work indicate a value of a = 3.5 to 4.5. This data from the present work is most reliable since

a) All the known errors in the experimental set up were corrected, and

b) There were no special difficulties in performing this experiment (see section 2.4) so that sufficient data were collected at each system pressure.

Therefore, if "a" were to be accepted as constant, a value of a = 3.7 seems appropriate.

In considering the atmospheric pressure run, the closeness of present work data, $\odot$, and Bell raw, $\triangle$, may be an indication that the $\triangle$ T-corrections(i) and (ii) (isothermal and thermocouple sheath) cancel off each other very nearly. This supports the thermocouple error analysis result of plus $\approx 11^{\circ}F$ and Bell's isothermal correction of minus $\approx 7.5^{\circ}F$. However, in the other three runs where a pressure gauge was used, the $\triangle$ T-correction(iii) (gauge) do not seem to support the above. Perhaps the basis of the 5 psia gauge correction to Bell's raw data is questionable.

Fig. 5.1 Comparison of theoretical and experimental superheats thresholds for fission fragments in water.

LEGEND

ORDINATE : SUPERHEAT ΔT °F
ABSCISSA : SYSTEM PRESSURE psia
△ BELL, RAW
⊙ TSO.

△ BELL, CORRECTED BY 5 psia GAUGE DIFFERENCE.

▲ BELL, CORRECTED BY MINUS $7\frac{1}{2}$°F (REPORTED IN BELL THESIS)

$a = 3$
3.7
4
4.5
6.07
7

14.7 psia   32.7   53.7   74.2
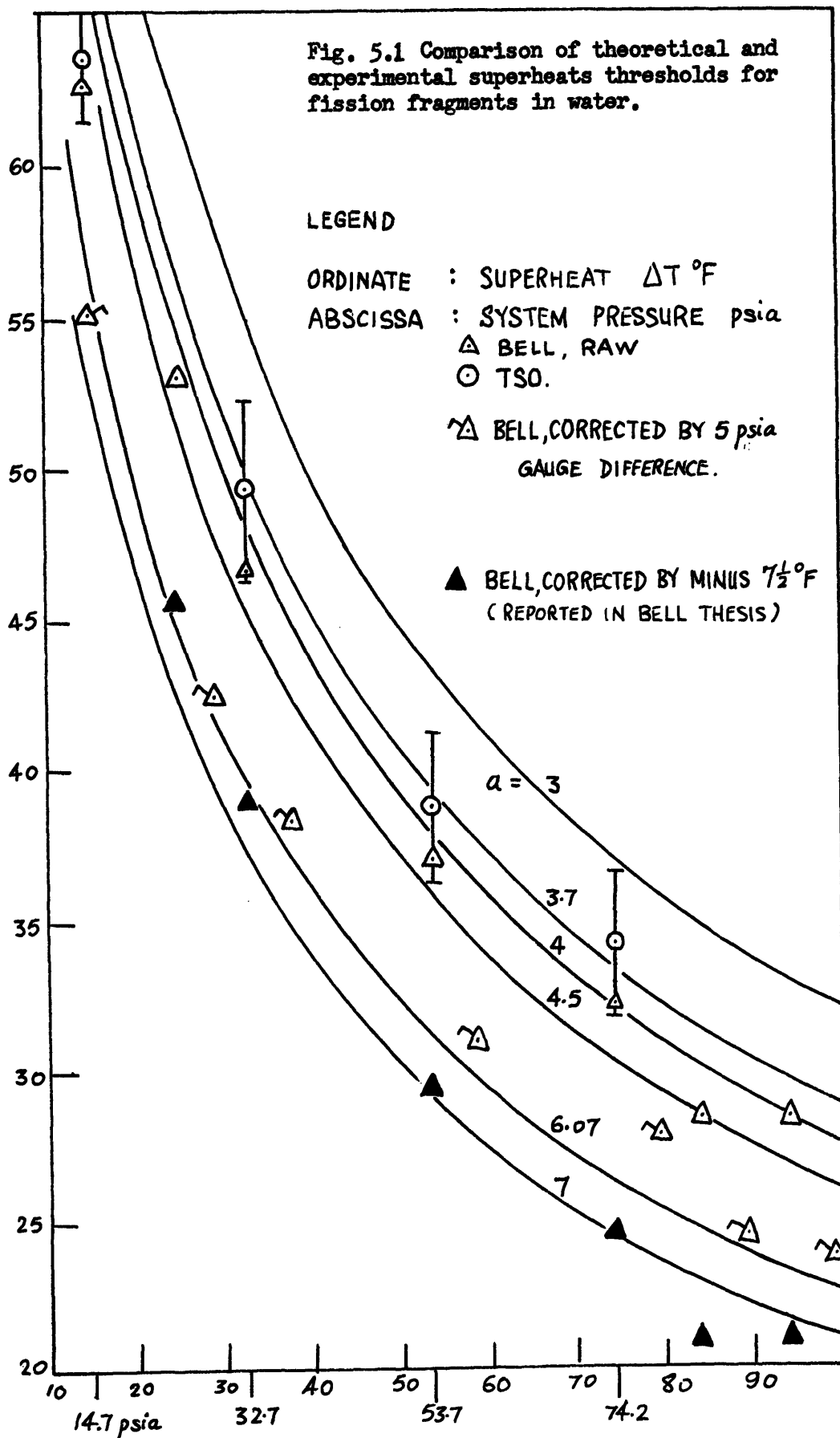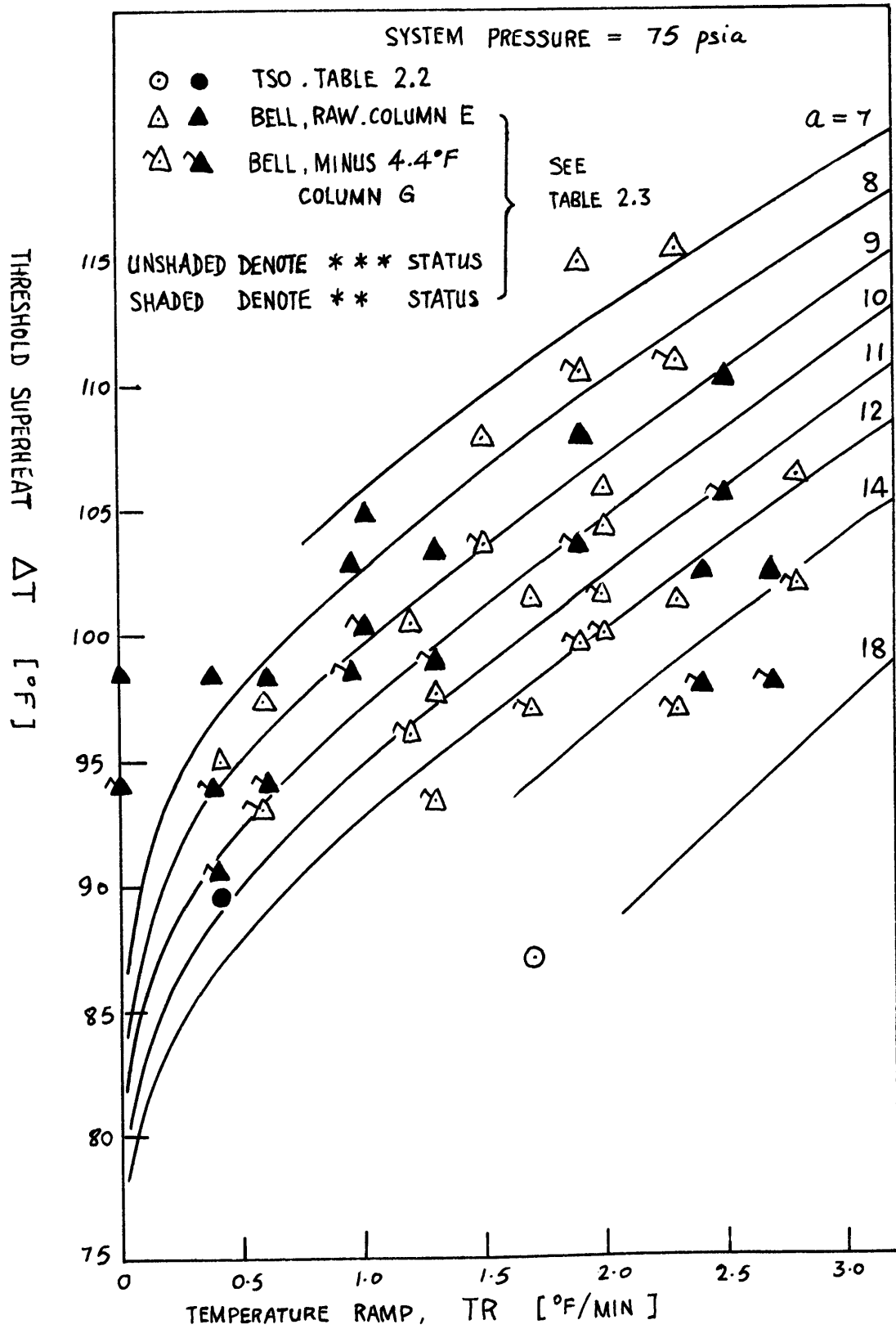
Fig. 5.2   Comparison of Theoretical and Experimental Superheat Thresholds
for Fast Neutrons in Water—I
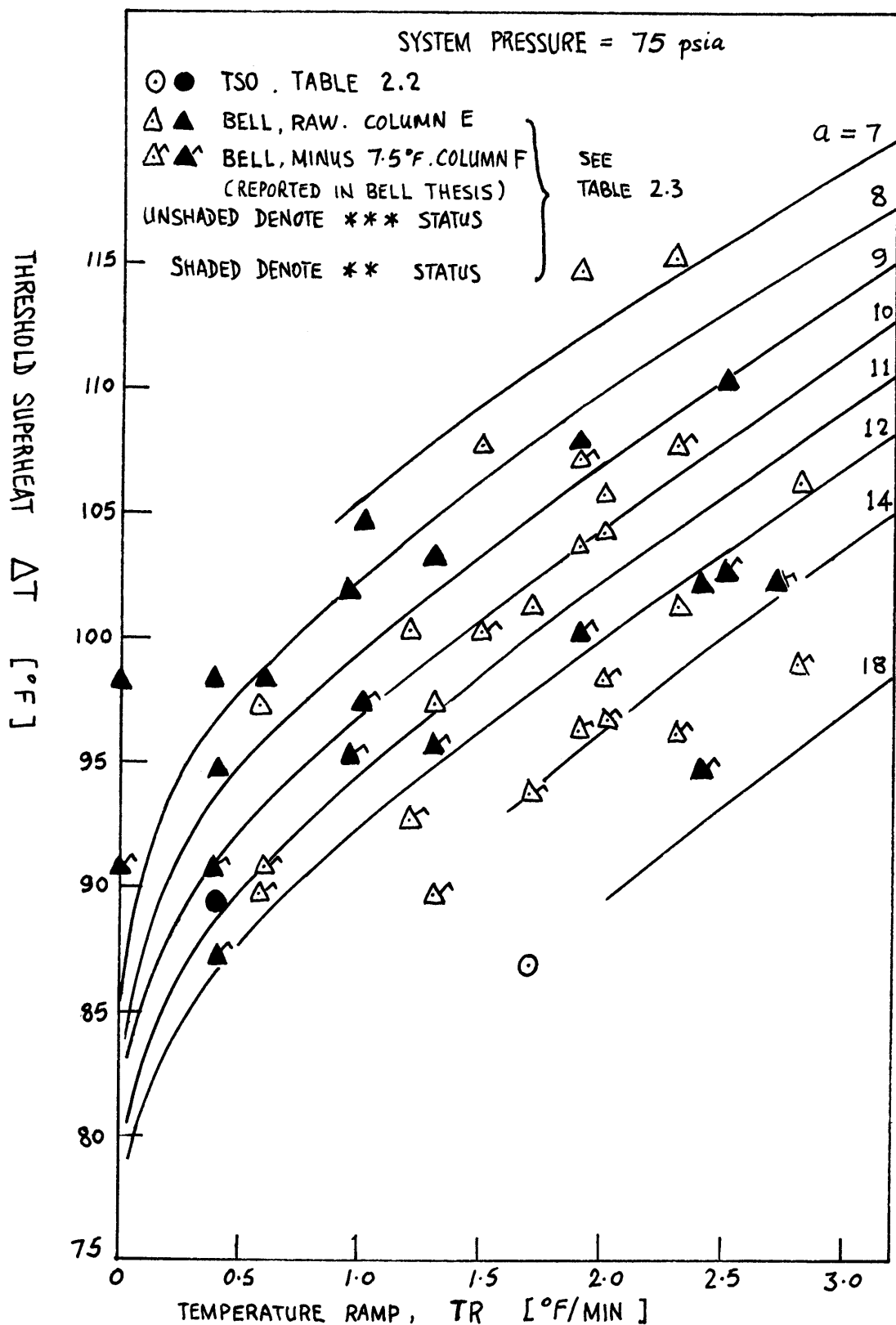
Fig. 5.3 Comparison of theoretical and experimental superheat thresholds
for fast neutrons in water—II
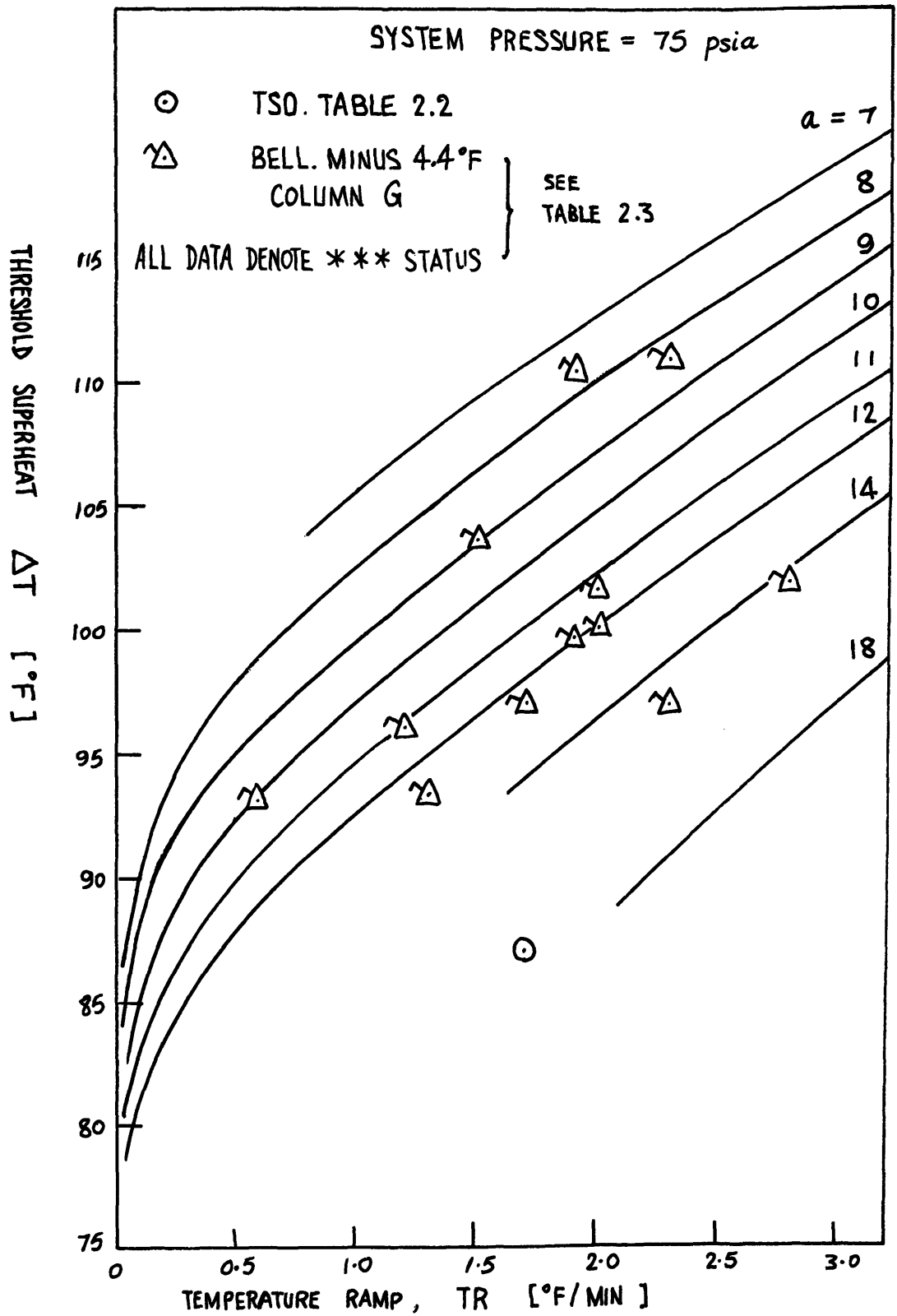
Fig. 5.4 Comparison of theoretical and experimental superheat thresholds for fast neutrons in water--III

5.1.2 <u>Fast Neutrons in Water.</u> As there are many uncertainties in

the fast neutron data of Bell, and there is insufficient good data

from the present work, an attempt is made to correct for each forementioned

error in Bell's data. Fig. 5.2 and Fig. 5.3 show all the corrections made

on data with status ** and *** (see table 2.3). They are plotted on

Fig. VI.6 of Bell's thesis[2, p.168] which shows (based on his theory) the

variation of Δ T against TR for various a. The conclusion in this thesis

is that no combinations of logical corrections on TR selections gives

consistent value of "a."

Fig. 5.4 shows only the data with *** status and for the assumption

that only the correction of minus 4.4°F (Δ, gauge correction) is necessary.

The data as shown have a spread of "a" between a = 8 to 14. If we were

to refer to Fig. 2.3, it would seem that the data shown on Fig.5.4 are

higher than the "true" data in the order of $10^{\circ}F$ (attributable to ΔT-

corrections(i) and (ii)). With this approximate subtraction of $10^{\circ}F$,

"a" has a spread between 12 and 20.

Based on the above evidence it appears that "a" is not a constant

for fast neutrons of one energy spectrum. Also "a" seems to have

different values for fission fragments and for fast neutrons.

5.1.3 <u>PWR Applications.</u> Fig. 5.5 to 5.8 show the plotting of

various cases considered in this work. The line labeled "Bergles-Rohsenow

Criteria for Incipient Boiling" is based on equation (B.1) and the criteria

explained in Appendix B. This line marks the appearance of the first

bubble on the cladding surface of the PWR and boiling progressively

becomes vigorous in the region above this line. In the event of a

temperature excursion in the PWR, the superheat temperature increases,

and if the line denoting RIN (radiation induced nucleation) lies below

Fig.5.5 Theoretical results for fission neutrons in water (a = 6.07).

BERGLES - ROHSENOW
CRITERIA FOR
INCIPIENT BOILING.

MAX. CLADDING ⊙
TEMP. IN PWR

17 Mev
NEUTRONS
$a = 3.7$

17 Mev NEUTRONS
$a = 6.07$

17 Mev NEUTRONS
$a = 12$

SATURATION LINE

655

650

645

2235

2100   2150   2200   2250   2300   2350

SUPERHEAT   TEMPERATURE   [°F]

SYSTEM   PRESSURE   [psia]
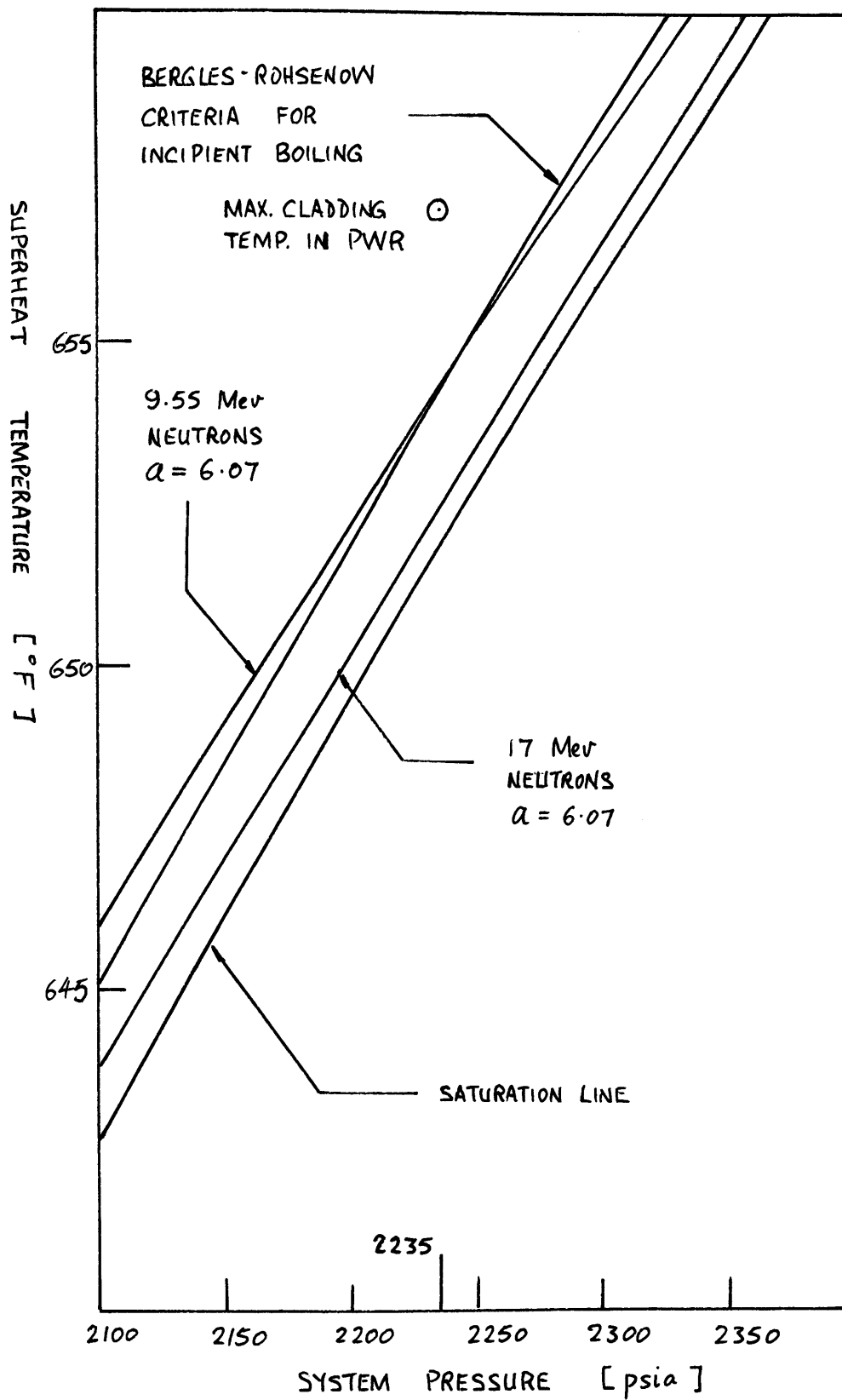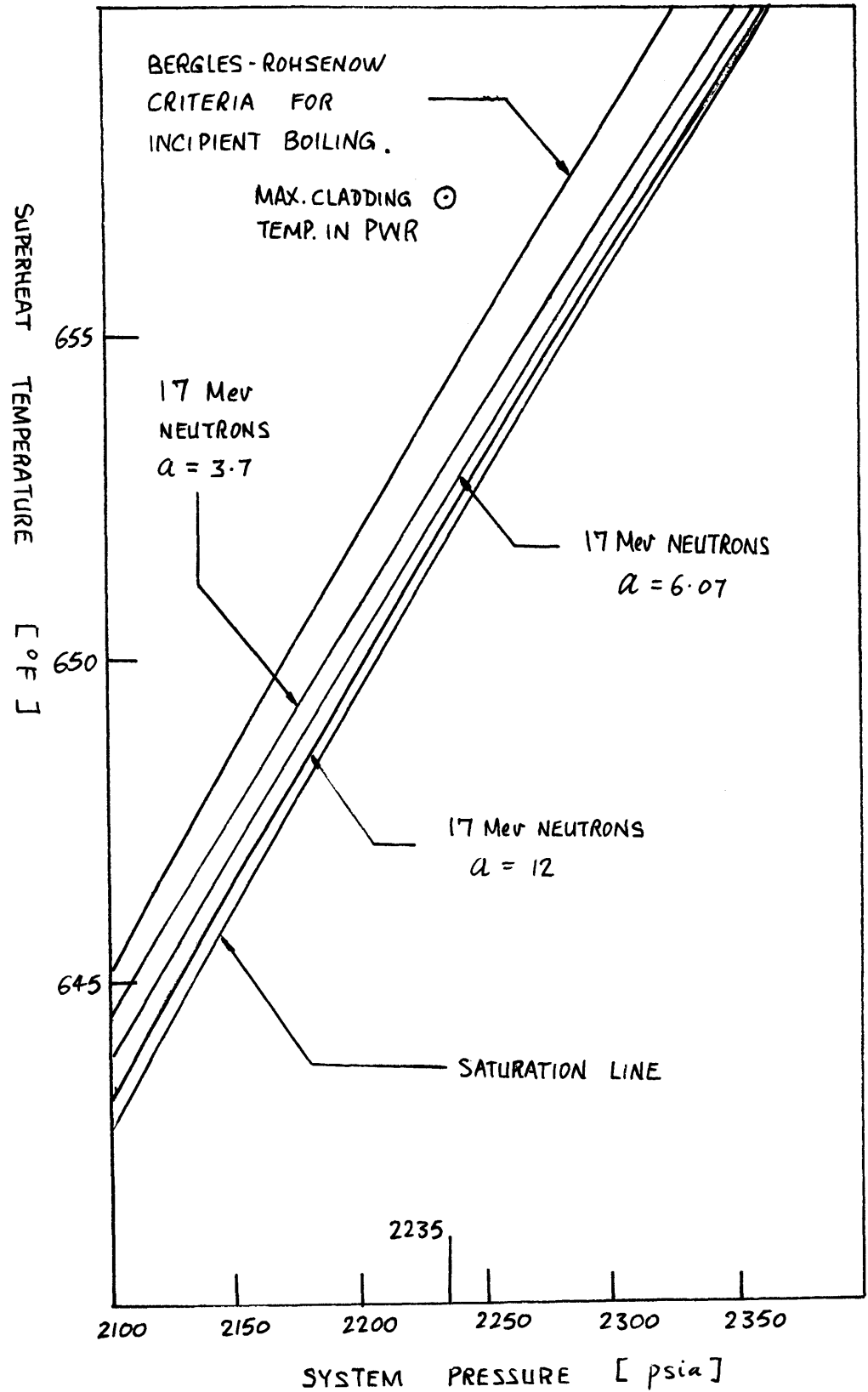
Fig. 5.6   Theoretical results for fission neutrons in water
(17 Mev neutrons)
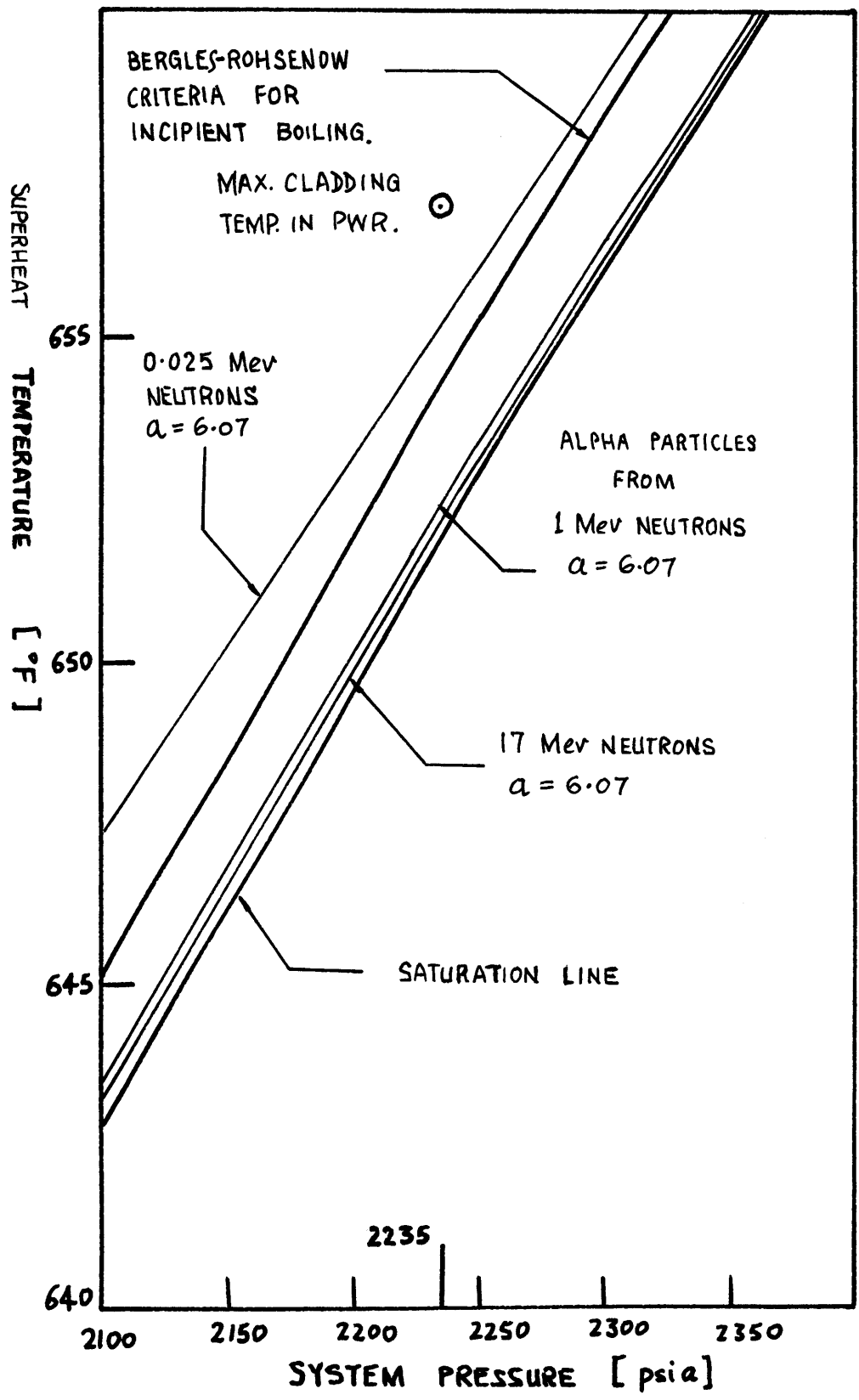
Fig. 5.7   Theoretical results for neutron induced
alpha particles in water (a = 6.07)
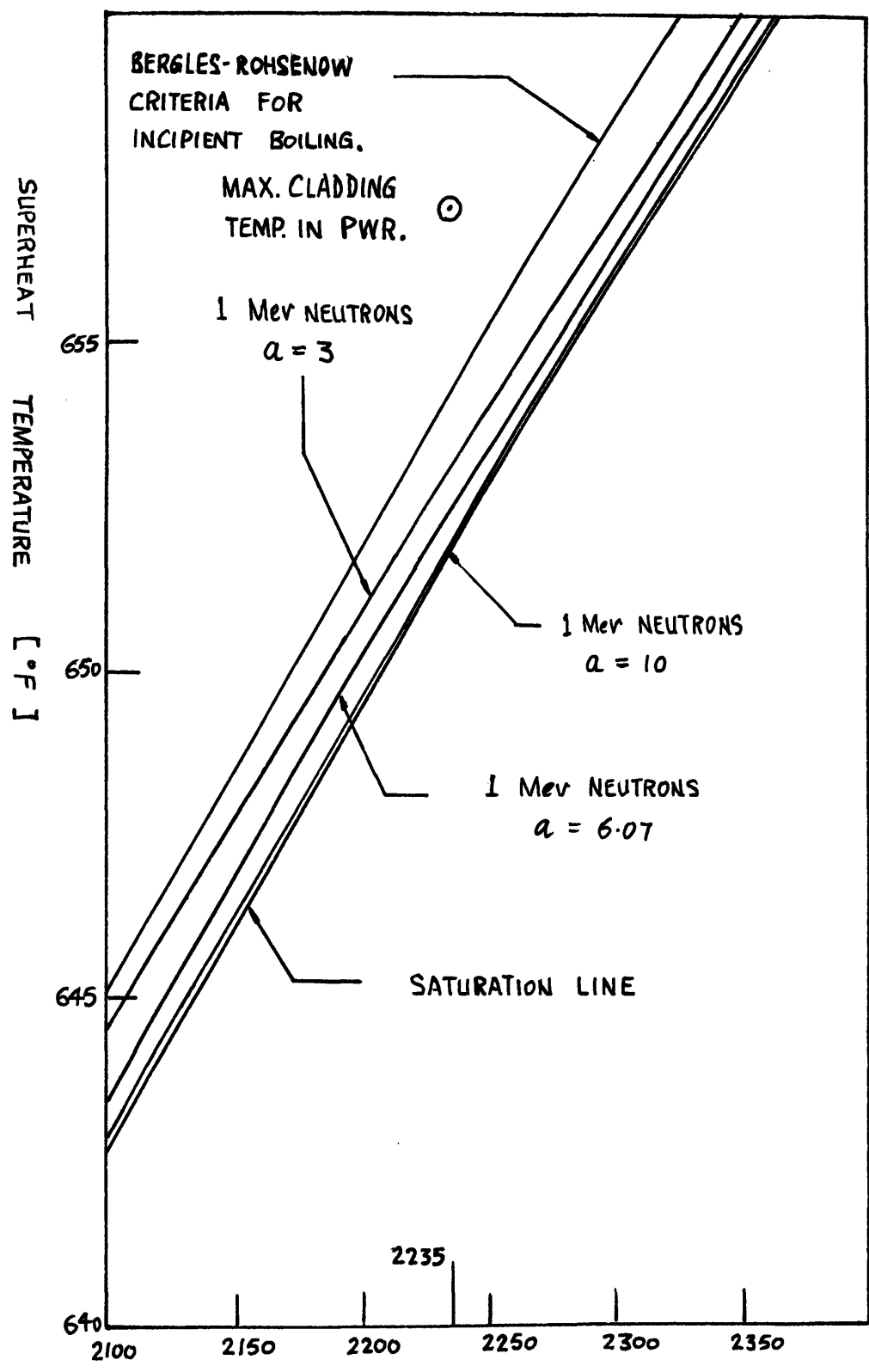
Fig.5.8 Theoretical results for neutron induced alpha
particles in water (from 1 Mev neutrons)

EMPIRICAL FORMULA FOR ENERGY DISTRIBUTION
BETWEEN 0.075 Mev AND 17 Mev

$$N(E) = 4.75 \times 10^6 \, e^{-E} \sinh \sqrt{2E}$$

RELATIVE NUMBER OF NEUTRONS PER UNIT ENERGY RANGE N(E)

ENERGIES OF FISSION NEUTRONS E [Mev]
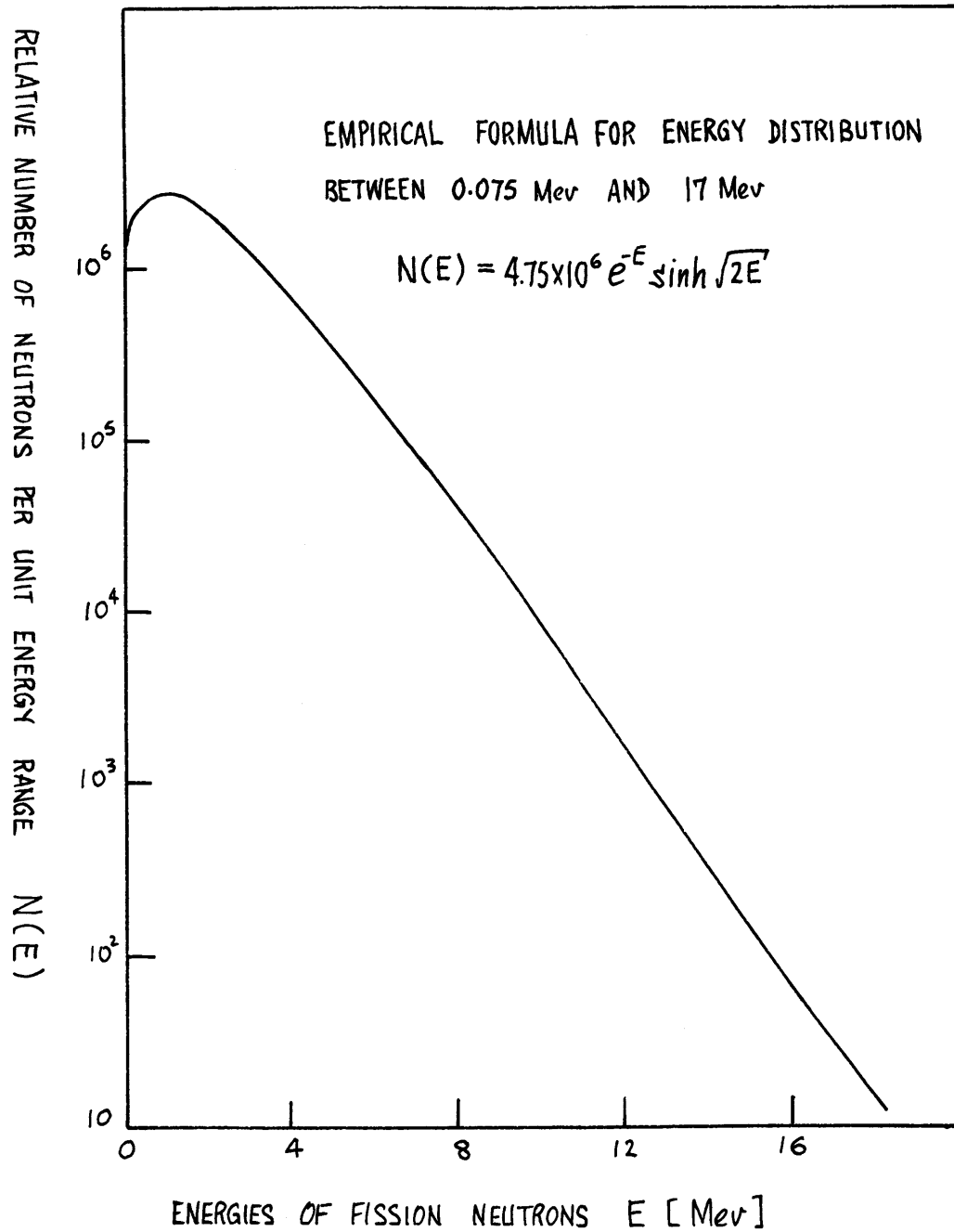
Fig. 5.9 Energies of fission neutrons[10]

the Bergles-Rohsenow line for that particular system pressure, then RIN

may well be the dominant phenomenon in initiating nucleate boiling.

With reference to Fig. 5.5 to 5.8 again, the maximum cladding temperature

of 657°F and the marked pressure of 2235 psia are values from WASH-1082.[24]

Consider the case of fission neutrons. Fig. 5.5 shows the effects

of 9.55 Mev and 17 Mev neutrons in water with a = 6.07 as per Bell

prediction. It is seen that a RIN line is closer to the saturation line

as the energy increases. RIN and incipient boiling are equally likely

at about 655°F for 9.55 Mev neutrons with a = 6.07. Fig.5.6 shows that

for a fixed neutron energy of 17 Mev, a RIN line is closer to the

saturation line as "a" increases.

For neutrons induced alpha particles, exactly the same qualitative

features are present, as displayed on Fig. 5.7 and 5.8 show ing effects

of energy and "a" respectively.

Fig. 5.9 shows a plot of the fission neutron spectrum.[10] It is

seen that there is an abundance of fission neutrons with sufficient

energy to make RIN important. However, the justification of interpreting

the effects of the fission spectrum in the manner we have done is still

open to discussion. Furthermore, the "a" value uncertainty for fission

neutrons and alphas should be borne in mind.

5.2 Recommendations.

Experimentally the following further work could be considered.

(i) Fast neutron data.

(a) Obtaining better fast neutron data by taking the following

experimental precautions with the existing set up.

1) Holding the temperature ramp rates constant above the

particular temperature threshold (with reference to plots of threshold superheat versus temperature ramp).

2) Keeping the upper and lower thermocouples at the same temperature thereby assuring that the bubble is at constant temperature.

3) Recalibrating the pressure gauge over the experimental period.

(b) Modifications of the existing set up to ease experiment and to enable higher temperature range data to be taken. Three suggestions are noteworthy here.

1) Two separate temperature recorders may be used to register the upper and lower thermocouple temperatures.

2) Some form of thermostatic arrangement may be incorporated into the present heating system to ease the heater control.

3) A more reliable way to hold the bubble in place should be seriously considered. One way may be to increase the convection generating power in the chamber.

(c) Testing of temperature ramp effect based on Bell's theory may be done by balancing various ramp rates with varying radiation intensity. No new radiation source is needed as intensity can be conveniently varied by varying the distance of the source from the bubble.

(ii) The present experimental set up may be used for work on some organic liquids in exactly the same manner. Suitable experimental parameters (source energy, source intensity, bubble size) must be decided beforehand so that a suitable spread with "a" exists in a plot of superheat threshold versus system pressure. Suitable supporting and covering oil have to be

found to suspend the organic liquid bubble.

In the area of theory, the following are noteworthy.

(i) The other Bell's data on fast neutrons in water for 55 psia and 95 psia may, together with any future data, be compared to Bell's theory by similar plots as in Fig. 5.2 to Fig. 5.4.

(ii) The experimental and theoretical results for neutron-induced nucleation by El-Nagdy[5] may be compared to the theoretical results of section 3.6 based on Bell's Energy Balance Method. Theoretical results for acetone can be obtained in the same manner as benzene. The properties of organic liquids can be found from suitable references.[20][13][14] (The enthalpy change of evaporation of acetone could not be found in the present survey).

(iii) Based on the present results, the constant "a" theory seems to be unacceptable and the theory needs to be reformulated. Indeed, the basic Energy Balance Method should be re-examined, especially in light of the work of Becker[1] which the author consulted only at the end of his thesis work. A few words on Becker's theory is in place.

Becker worked on neutron induced nucleation in di-ethyl ether and compared his experimental results with theoretical results which were obtained separately by an "Electrostatic Theory" and a "Thermal Thoery." According to Becker, neither theory agreed with his experimental results. His Thermal Theory corresponds to Bell's Energy Balance Method. In comparing with Bell's equation (3.2) of section 3.1, Becker has

$$\frac{4}{3}\pi(r^*)^3 \, P_v^* \, b_{/2} + 4\pi(r^*)^2 \sigma - 4\pi(r^*)^2 T \frac{d\sigma}{dT} + \frac{4}{3}\pi(r^*)^3 \rho_v \, h_{fg} = \Delta E$$

$$(5.1)$$

Becker has neglected dissociation effects in the bubble. but has two extra energy terms—the second and third term. $[4\pi(r^*)^2\sigma]$ arises (together with the first term) from a consideration of the difference in thermodynamic potentials between the states at $r = 0$ and $r = r^*$.

$[-4\pi(r^*)^2 T\frac{d\sigma}{dT}]$ is an entropy term associated with the heat which must be supplied in the production of the surface of the bubble which is non-recoverable.

Becker also questioned the validity of some of the basic properties used in the analysis. He suspected that h_{fg}, the enthalpy change by evaporation, may not be used for metastable equilibrium states (superheat), since h_{fg} is defined for stable equilibrium only.

(iv) In the application of Bell's theory to the PWR, further investigation on the effects of the fission spectrum on causing radiation induced nucleation in water under PWR conditions is necessary.

Appendix A

Nomenclature

B_o, B_i Parameters

E Kinetic energy

E_n Kinetic energy of a neutron

E_f Energy of formation of a nucleus in water

E_a Energy available from radiation for formation of nucleus

E_s Additional energy term in Statistical Theory

Gr Grashof number

$G(H_2)$ Yield of hydrogen gas molecules in radiolysis

I_i Mean ionization potential of the ith component in the stopping medium

L Effective length of the radiation track involved in the formation of a single embryo

M Molecular weight

M_1 Mass of the energetic particle

M_i Mass of the ith atom species

N Molecule density

Nu Nusselt number

$\mathcal{N}$ Avogadro's number

P Perimeter

P Pressure

Pr Prandlt number

Q Heat of reaction

S Cross-section area

T	Temperature
T_a	Temperature of ambient air
T_{fm}	Film temperature
T_j	Temperature at thermocouple junction
$\mathcal{J}$	Energy of the primary knock-on oxygen atom
$\mathcal{J}_C$	Energy of the primary knock-on carbon atom
TR	Experimental temperature ramp
ΔT	Temperature difference
ΔT	Superheat
V	Volume
v	Velocity of the energetic particle passing through the stopping medium
Z_1	Atomic number of the energetic particle
Z_i	Atomic number of the ith atom species in the stopping medium
$(Z)_{eff}$	Effective mean charge of the energetic particle
a	Dimensionless effective track length $= 1/r^*$
a_H	Radius of the first Bohr electron orbit for the hydrogen atom
a_{1i}^{scr}	Maximum impact parameter for the ith atom species in the stopping medium
b	Ratio of the pressure difference across the embryo interface to the vapor pressure
c	Velocity of light
e	Magnitude of the charge on an electron
g	Acceleration due to gravity
h	Film coefficient of heat transfer

h_o	Film coefficient of heat transfer between air and sheath
h_i	Total coefficient of heat transfer between oil and sheath
h_c	Film coefficient of heat transfer between oil and sheath
h_r	Radiation coefficient of heat transfer between oil and sheath
$\hbar$	Plank's constant divided by 2π
h_{fg}	Enthalpy change by vaporization per unit mass
k	Thermal conductivity
l	Length
m	Mass
m_o	Mass of an electron
q	Rate of heat transfer
r	Radius of a spherical cylinder
s	Distance along the radiation track from the starting point of the track
t	Time
Δt	Temperature difference
x	Distance
β_f	Coefficient of volumetric expansion
θ	Scattering angle in the Center of Mass frame of reference
μ_f	oil viscosity
ν_i	Number of atoms of the ith species per molecule
ρ	Density
σ	Surface tension
σ	Stefan constant
σ	Standard deviation

Subscripts

Subscripts

l	Liquid
v	Vapor
g	Gas
f	Fluid/Liquid
AV	Average

Superscripts

*	Critical conditions, i.e. nucleation conditions
air	In air
oil	In oil

Appendix B

Criterion for Incipient Boiling

Bergles and Rohsenow[3] have developed a criterion semi-empirically for incipient boiling of water over a pressure range of 15 to 2000 psia which is

$$(q/A)_i = 15.60 \, P^{1.156} (t_w - t_{sat})^{\frac{2.30}{P^{0.0234}}} \qquad (B.1)$$

where $(q/A)_i$ is the heat flux required for incipient boiling in $[\text{BTU-hr}^{-1}\text{-ft}^{-2}]$, P is the system pressure in psia, and the wall and saturation temperatures are in $^\circ F$.

The qualification for this criterion is that the water is in contact with a heating surface (wall) which has a full range of cavities present for bubble growth. This forced-convection surface boiling condition is assumed to be met in the flow of water over the cladding surface of fuel elements in the Pressurised Water Reactor. So also is it assumed that the criterion is valid in the region of 2235 psia, as is justified by the small variation of the criterion curves with high pressure shown on p.207, Figure 27 of Todreas and Rohsenow[23].

For the purpose of the PWR condition calculation, the heat flux was taken as 5.5×10^5 $\text{BTU-hr}^{-1}\text{-ft}^{-2}$, a value for the maximum heat flux in a PWR as typified in WASH-1082[24]. Table B.1 tabulates pressure and superheat temperatures obtained through equation (B.1) over the range of interest here.

Table B.1 Bergles-Rohsenow criterion in PWR conditions.

P psia	T_{sat} °F	$(T_w - T_{sat})$ °F	T_w °F
2000	636.00	2.40	638.40
2100	642.92	2.33	645.25
2200	649.64	2.27	651.91
2235	651.92	2.24	654.16
2300	656.09	2.22	658.31
2400	662.31	2.15	664.46
2500	668.31	2.11	670.42

Appendix C

Related Properties of Water

C.1 Vapor Pressure Relationship

The following equation is from Keenan and Keyes[11] and is valid for $50°C \leqslant T \leqslant 347°C$.

$$P_v = P_c \exp\left[-2.3 \frac{x}{T}\left\{\frac{a + bx + cx^3 + ex^4}{1 + dx}\right\}\right]$$

where P_v = vapor pressure in atmospheres

P_c = critical pressure = 218.167 atmospheres

T = temperature $[°K]$

x = $T_c - T$

T_c = critical temperature = 647.27°K

a = 3.3463130

b = 4.14113×10^{-2}

c = 7.515484×10^{-9}

d = 1.379448×10^{-2}

e = 6.56444×10^{-11}

C.2 Liquid Density Relationship

From Keenan and Keyes and valid for $32°F \leq T \leq 680°F$,

$$\rho_\ell = \frac{1 + d x^{1/3} + e x}{v_c + a x^{1/3} + b x + c x^4}$$

where ρ_1 = liquid density $[\text{lb-ft}^{-3}]$

x = Tc -T

Tc = critical temperature $374.11°C$

T = temperature $[°C]$

v_c = 3.1975 $[\text{cm}^3 - \text{gm}^{-1}]$

a = -0.3151548

b = -1203374×10^{-3}

c = 7.48908×10^{-13}

d = 0.1342489

e = -3946263×10^{-3}

C.3 Vapor Density Relationship

From Keenan and Keyes

$$\rho_v = \left[\frac{4.55504\,T}{P} + B_o + B_o^2 \jmath_1(\tfrac{1}{T})\frac{P}{T} + B_o^4 \jmath_2(\tfrac{1}{T})\frac{P^3}{T^3} - B_o^{13}\jmath_3(\tfrac{1}{T})\frac{P^{12}}{T^{12}} \right]$$

where ρ_v = vapor density $[\text{gm} - \text{cm}^{-3}]$

T = temperature $[°K]$

P = pressure in atmospheres

$$Bo = 1.89 - \frac{2641.62}{T} \times 10^{80870/T^2}$$

$$g_1\left(\frac{1}{T}\right) = \frac{82.546}{T} - \frac{1.6246 \times 10^5}{T^2}$$

$$g_2\left(\frac{1}{T}\right) = 0.21828 - \frac{1.2697 \times 10^5}{T^2}$$

$$g_3\left(\frac{1}{T}\right) = 3.635 \times 10^{-4} - \frac{6.768 \times 10^{64}}{T^{24}}$$

C.4 Surface Tension Relationship

These relationships are obtained by a least square fit of a straight line through data given in handbooks.

Data from Tipton[21] gives the surface tension of water as

$$\sigma \quad [\text{lbf} - \text{ft}^{-1}] = -8.198 \times 10^{-6} \, T(^\circ F) + 0.005738$$

and valid $200^\circ F \leq T \leq 450^\circ F$. The fit is plotted in Bell's work.

Data from Schmidt[17] for the temperature range of $640^\circ F \leq T \leq 670^\circ F$ yields

$$\sigma \quad [\text{lbf} - \text{ft}^{-1}] = -7.275 \times 10^{-6} \, T(^\circ F) + 0.005081$$

The fit is plotted in Fig. (C.1).

C.5 Enthalpy Change by Evaporation Relationship

These relationships are obtained by fitting a curve through data from Keenan and Keyes. A polynomial regression computer program[8] is used in which powers of an independent variables are generated to

calculate polynomials of successively increasing degrees. (See Appendix D).

For $200^\circ F \leqslant T \leqslant 500^\circ F$,

$$h_{fg} \; [\; BTU - lb^{-1} \;] = 1064.6 - 0.270T - 8.15 \times 10^{-4}T^2.$$

For $640^\circ F \leqslant T \leqslant 670^\circ F$,

$$h_{fg} \; [\; BTU - lb^{-1} \;] = 2505.67 - 0.32053T.$$

The fit of the first equation is plotted in Bell's work, and that of the second equation in Fig. (C.2).
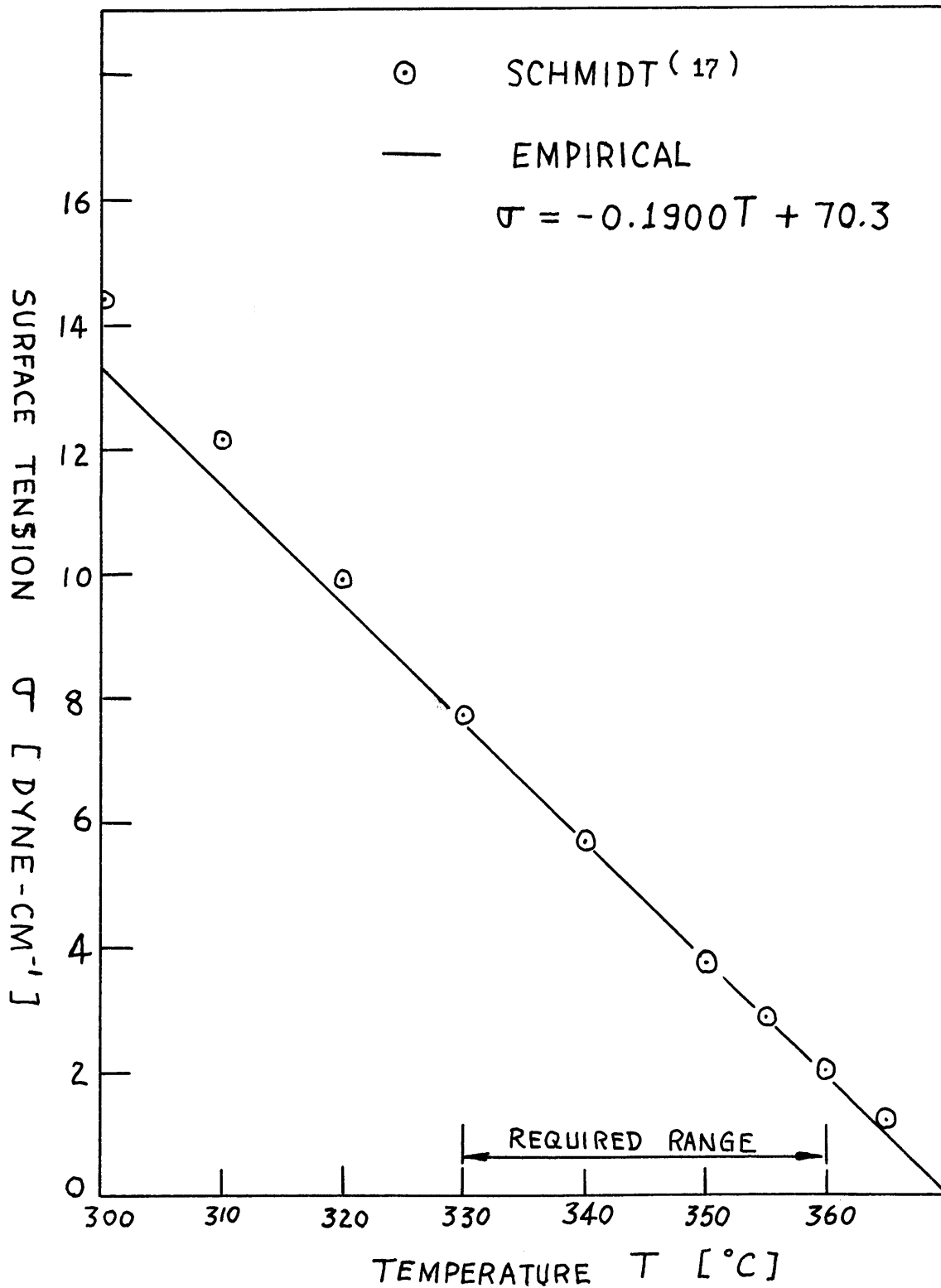
Fig. C.1 Surface tension of water vs. temperature.
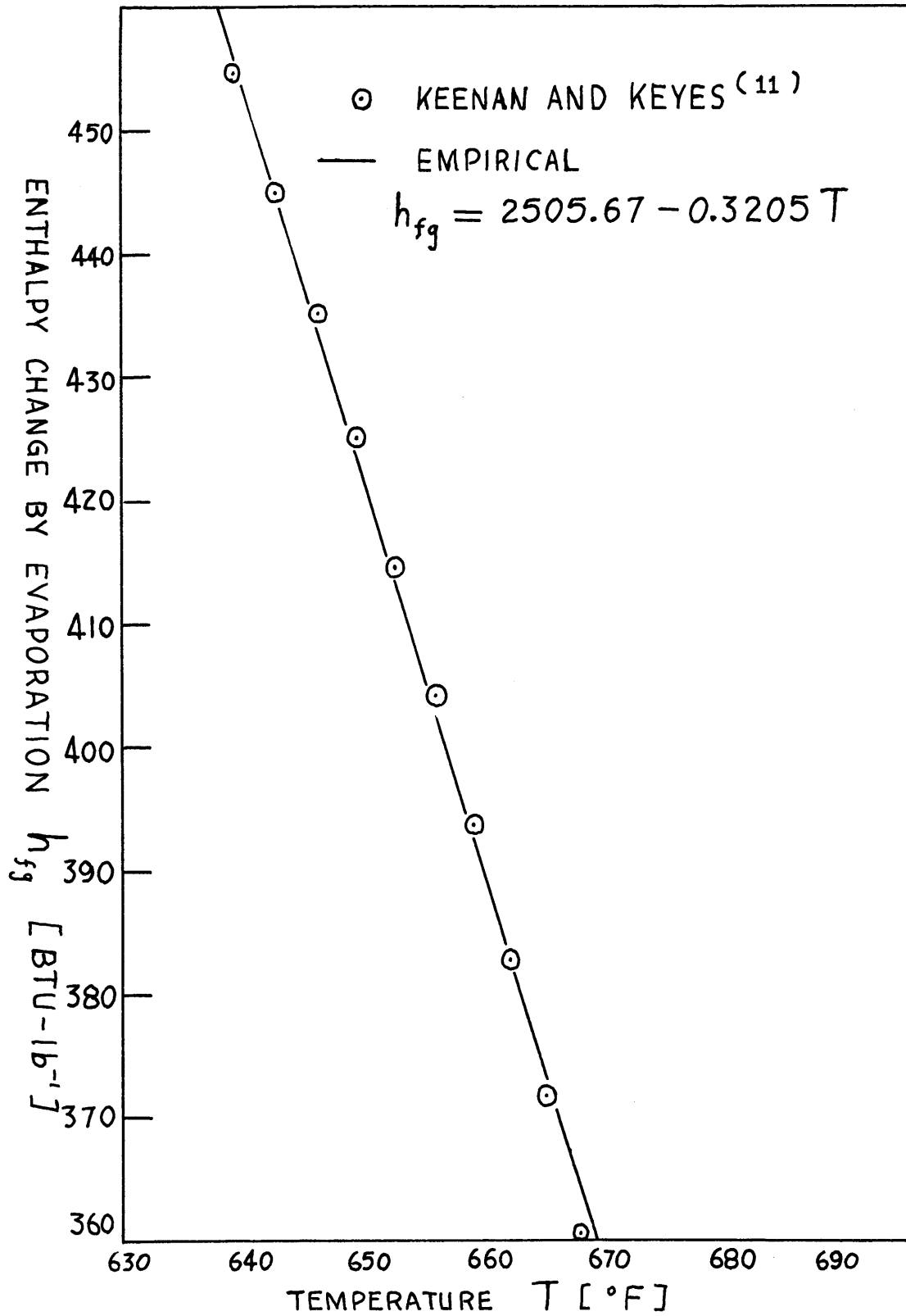
Fig. C.2 Enthalpy change of water vs. temperature.

Appendix D

Related Properties of Benzene

The five physical properties of benzene over the relevant temperature

range are described by empirical relationships as shown on Fig. D.1 to

D.5. they are obtained by using the polynomial regression computer

program[8] to generate polynomial series that fit tabulated data given

in references. The enthalpy change by evaporation, liquid density, vapor

density, and vapor pressure data are from Organick and Studhalter[13].

The surface tension data are from Timmermans[20].
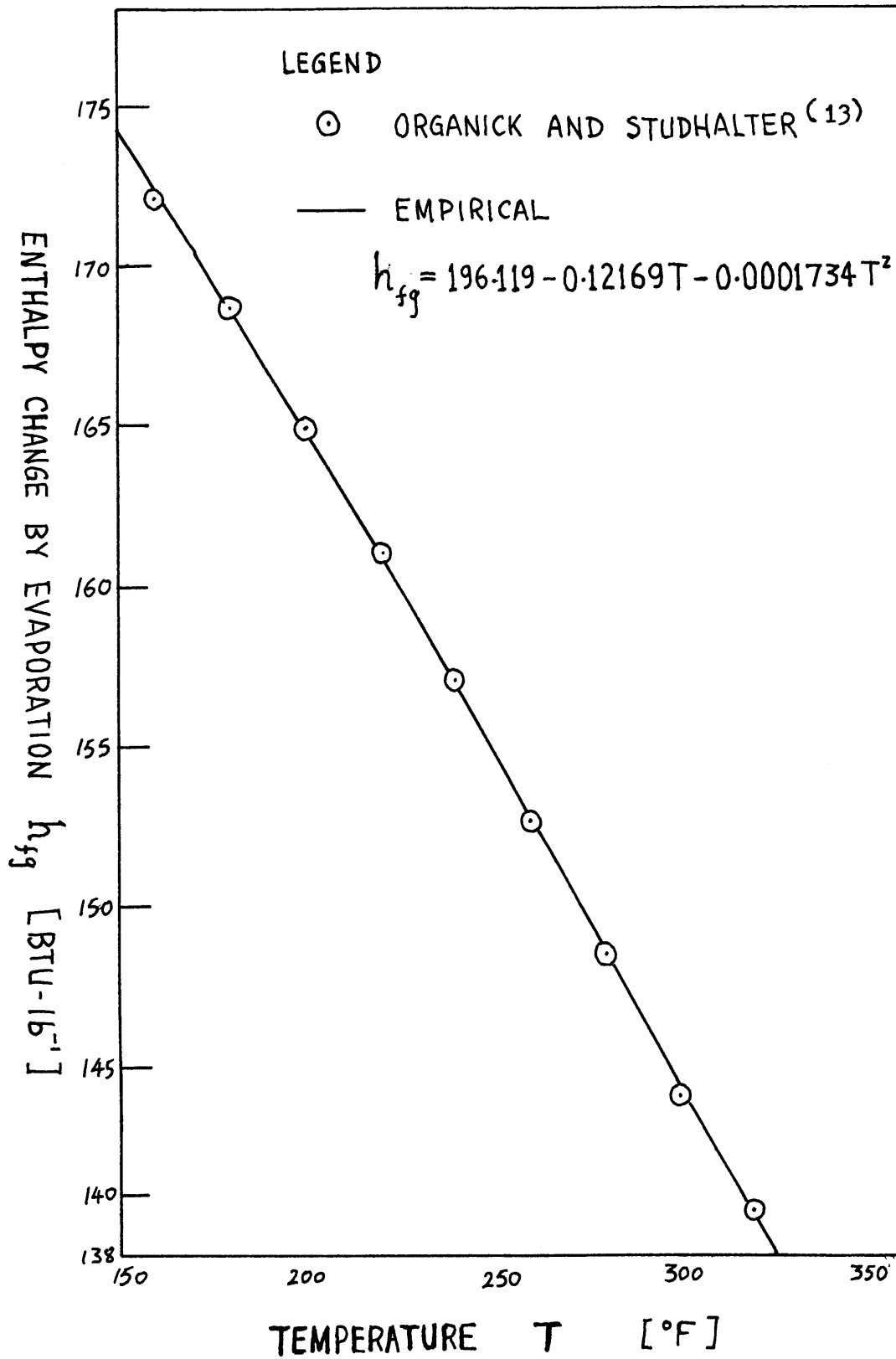
Fig. D.1 Enthalpy change by evaporation of benzene vs. temperature.
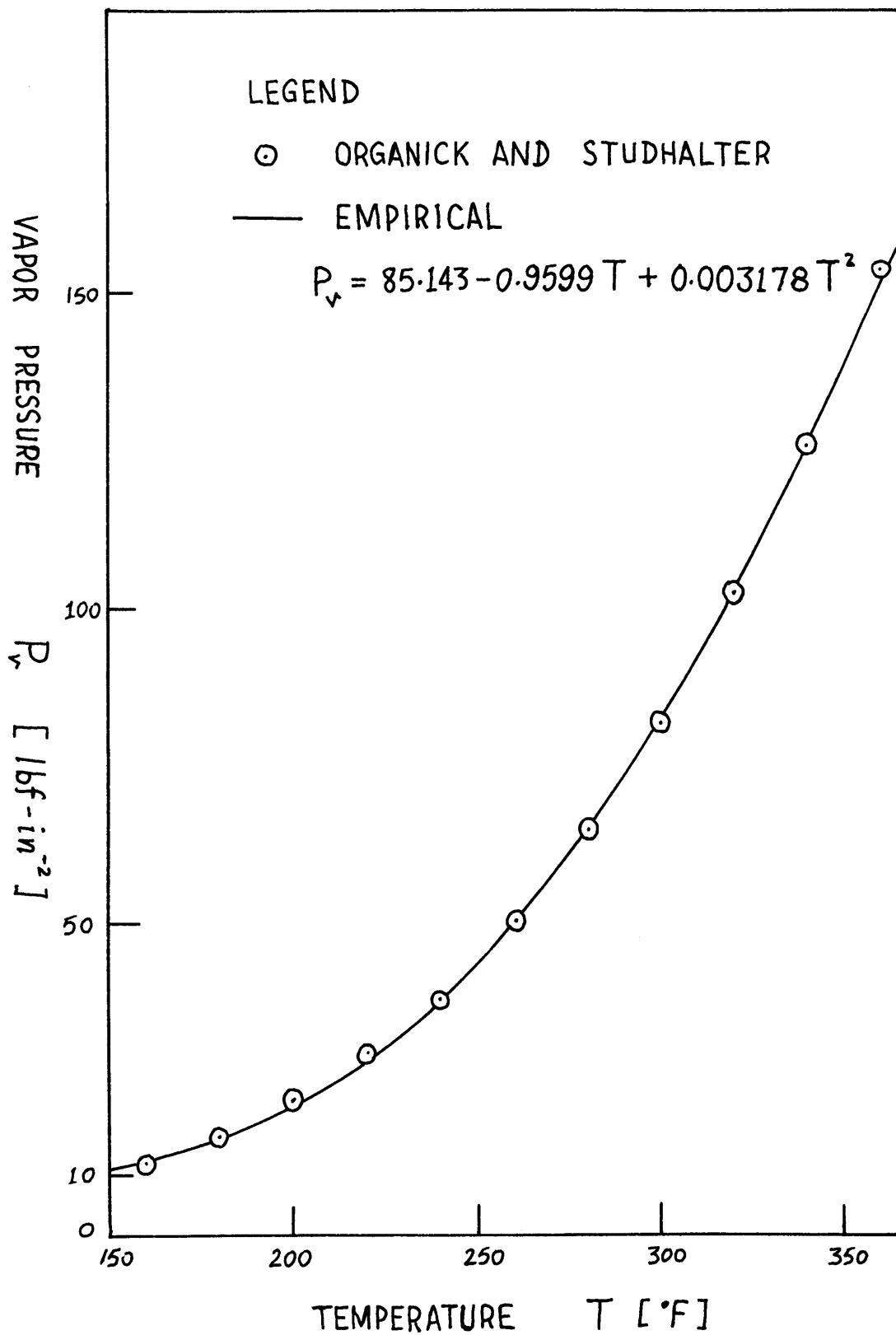
Fig. D.2 Vapor pressure of benzene vs. temperature.

LEGEND

⊙   TIMMERMANS [20]

——   EMPIRICAL

$\sigma = 30.9 - 0.121 \, T(°c)$

SURFACE TENSION σ [DYNES - CM^{-1}]
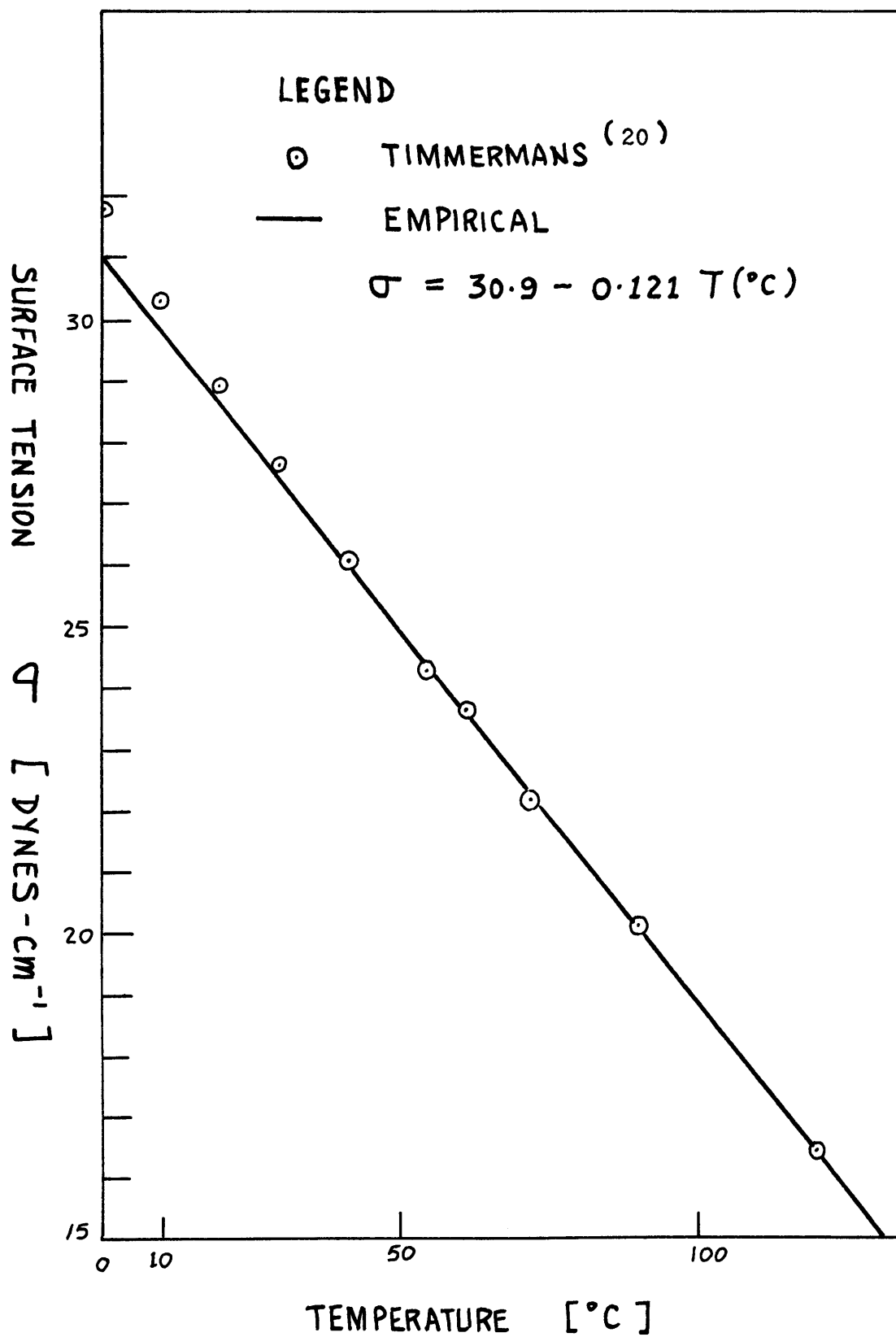
TEMPERATURE [°C]

Fig. D.3 Surface tension of benzene vs. temperature.
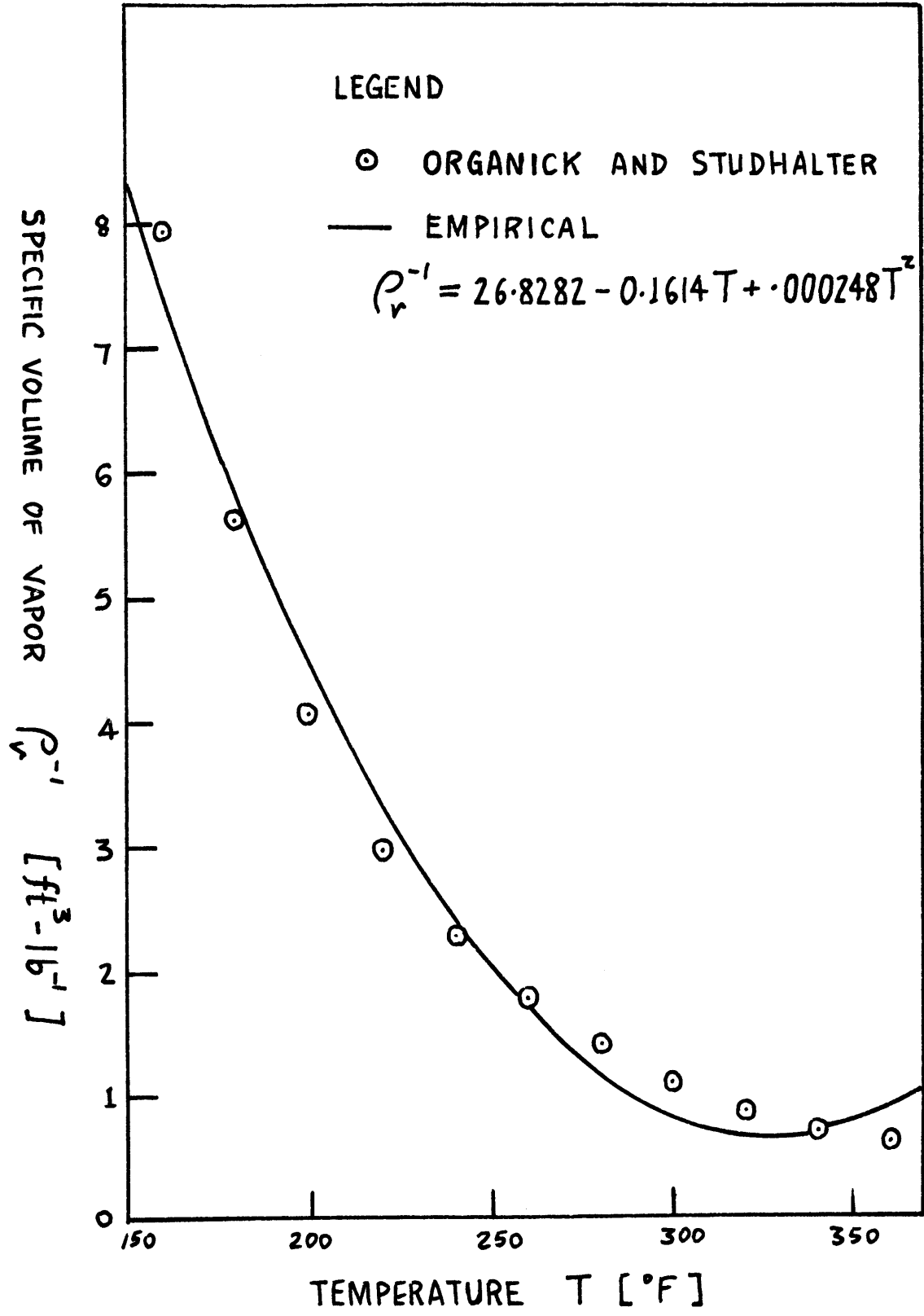
Fig. D.4 Specific volume of vapor benzene vs. temperature.
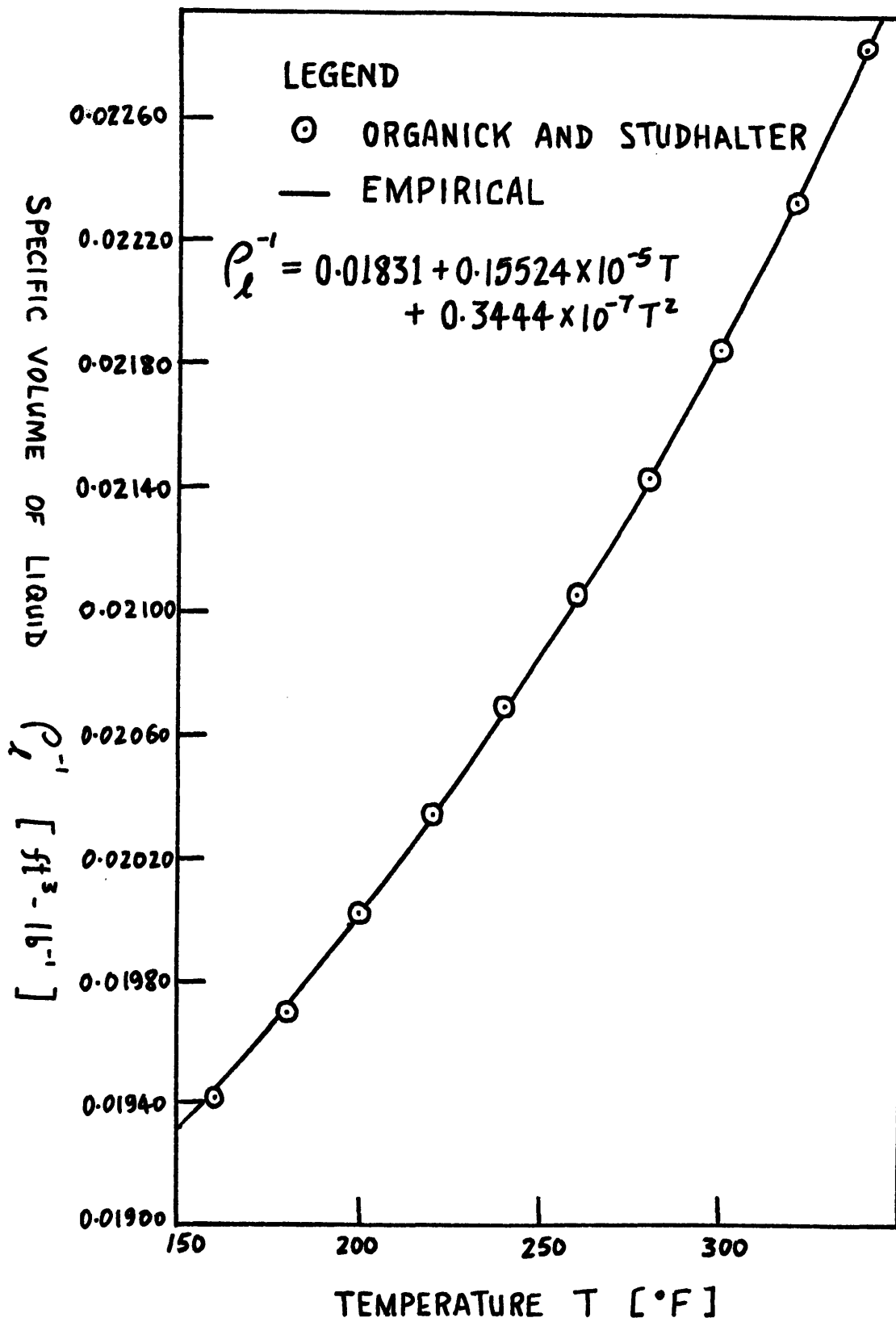
Fig. D.5 Specific volume of liquid benzene vs. temperature.

Appendix E

Sample Calculations for Energy Deposition Rate

Consider the case of section 3.4, that of fast neutrons in water at low pressure range, equations (3.14) and (3.15) will be derived here.

For oxygen, $Z_1 = 8$, $M_1 = 16$. The impact parameters are (from section 3.2),

$$a_H = \frac{0.52917 \times 10^{-8}}{(4+1)^{1/2}} = 2.3665 \times 10^{-9} \; cm$$

$$a_O = 1.8709 \times 10^{-9} \; cm$$

From equation (3.9)

$$\frac{1}{N}\frac{dE}{d\lambda} = \frac{4\pi \, 1.9732^2 \times 4 \times 10^{-22}}{0.511} \sum_{i=H,O} Z_i \, y_i \, \ell n \left[\frac{0.5488 \times 10^{-3} \, amu}{16 \, amu} \times \frac{2.246 \, E}{I_i \, 2} \right]$$

$$+ \frac{4\pi \, 2.818^2 \times 10^{-26} \times 0.511^2}{2E} \times 64 \sum_{i=H,O} \frac{M_i}{M_i} \, y_i \, Z_i^2 \, \ell n \left[\frac{M_i}{M_i + M_i} \times \frac{2 \, E \, a_i}{8 \times Z_i \, 2.818 \times 10^{-13} \times 0.511} \right]$$

$$= 3.8304 \times 10^{-20} \left\{ 1 \times 2 \, \ell n \left[\frac{3.85189 \times 10^{-5} E}{15.5 \times 10^{-6}} \right] + 8 \times 1 \, \ell n \left[\frac{3.85189 \times 10^{-5} E}{100 \times 10^{-6}} \right] \right.$$

$$+ \frac{8.3395 \times 10^{-24}}{E} \left\{ \frac{16}{1} \times 2 \times 1^2 \, \ell n \left[\frac{1}{16+1} \frac{E \times 3.520 \times 10^{-9}}{1 \times 5.760 \times 10^{-13}} \right] + \frac{16 \times 1 \times 8^2}{16} \ell n \left[\frac{16}{16+16} \times \right. \right.$$

$$\left. \left. \frac{E \times 2.30726 \times 10^{-9}}{8 \times 5.760 \times 10^{-13}} \right] \right\}$$

$$\therefore \quad \frac{1}{N}\frac{dE}{d\lambda} = 38.3040 \times 10^{-20} \ln(0.55906 E) + \frac{800.58 \times 10^{-24}}{E} \ln(282.47 E)$$

$$\therefore \quad \frac{dE}{d\lambda} = \rho_\ell \left\{ 1.28203 \times 10^4 \ln(0.55906 E) + \frac{26.7954}{E} \ln(282.47 E) \right\}$$

Ignoring energy loss from PKOA to protons, the above equation is precisely equation (3.14), i.e

$$\frac{dE}{d\lambda} = \rho_\ell \; 1.282 \times 10^4 \; \ln 0.5591 E$$

where $\frac{dE}{ds}$ is in E $[Mev\text{-}cm^{-1}]$, ρ_1 in $[gm\text{-}cm^{-3}]$ and E in $[Mev]$.

Putting equation (3.14) into equation (3.8) with $E(s_1) = J$,

$$\frac{[E(\lambda_2) - J]^2}{a r^*} = \int_J^{E(\lambda_2)} \rho_\ell \; 1.282 \times 10^4 \ln 0.5591 E \; dE$$

$$= \rho_\ell \; 1.282 \times 10^4 \left\{ -1.581 \left[E(\lambda_2) - J \right] + E(\lambda_2) \ln E(\lambda_2) - J \ln J \right\}$$

$$\therefore \quad \frac{[E(\lambda_2) - J]^2}{J \ln J - E(\lambda_2) \ln E(\lambda_2) - 1.581 [J - E(\lambda_2)]} = a r^* \rho_\ell \; 1.282 \times 10^4 \; .$$

Using equation (3.6), the right hand side of the above equation is

$$\frac{2\sigma a \, \rho_\ell}{P_v^* + P_g' - P_\ell} \times 1.282 \times 10^4$$

Or

$$\frac{a \sigma \, \rho_\ell}{P_v^* + P_g - P_\ell} \times 1.2516 \times 10^4$$

where σ is now in $[\text{lbf-ft}^{-1}]$, ρ_1 $[\text{lb-ft}^{-3}]$, and pressures in $[\text{lbf-ft}^{-2}]$. This is equation (3.15).

Appendix F

Computer Programs

```
      C
      C
      C    ......................................................................
      C
      C    SAMPLE MAIN PROGRAM FOR POLYNOMIAL REGRESSION - POLRG
      C
      C    PURPOSE
      C       (1) READ THE PROBLEM PARAMETER CARD FOR A POLYNOMIAL REGRES-
      C       SION, (2) CALL SUBROUTINES TO PERFORM THE ANALYSIS, (3)
      C       PRINT THE REGRESSION COEFFICIENTS AND ANALYSIS OF VARIANCE
      C       TABLE FOR POLYNOMIALS OF SUCCESSIVELY INCREASING DEGREES,
      C       AND (4) OPTIONALLY PRINT THE TABLE OF RESIDUALS AND A PLOT
      C       OF Y VALUES AND Y ESTIMATES.
      C
      C    REMARKS
      C       THE NUMBER OF OBSERVATIONS, N, MUST BE GREATER THAN M+1,
      C       WHERE M IS THE HIGHEST DEGREE POLYNOMIAL SPECIFIED.
      C       IF THERE IS NO REDUCTION IN THE RESIDUAL SUM OF SQUARES
      C       BETWEEN TWO SUCCESSIVE DEGREES OF THE POLYNOMIALS, THE
      C       PROGRAM TERMINATES THE PROBLEM BEFORE COMPLETING THE ANALY-
      C       SIS FOR THE HIGHEST DEGREE POLYNOMIAL SPECIFIED.
      C
      C    SUBROUTINES AND FUNCTION SUBPROGRAMS REQUIRED
      C       GDATA
      C       ORDER
      C       MINV
      C       MULTR
      C       PLOT  (A SPECIAL PLOT SUBROUTINE PROVIDED FOR THE SAMPLE
      C             PROGRAM.)
      C
      C    METHOD
      C       REFER TO B. OSTLE, 'STATISTICS IN RESEARCH', THE IOWA STATE
      C       COLLEGE PRESS', 1954, CHAPTER 6.
      C
      C    ...................................................................
      C
      C    THE FOLLOWING DIMENSION MUST BE GREATER THAN OR EQUAL TO THE
      C    PRODUCT OF N*(M+1), WHERE N IS THE NUMBER OF OBSERVATIONS AND M
      C    IS THE HIGHEST DEGREE POLYNOMIAL SPECIFIED..
0001
      C       DIMENSION X(1100)
      C
      C    THE FOLLOWING DIMENSION MUST BE GREATER THAN OR EQUAL TO THE
      C    PRODUCT OF M+M..
      C
0002
      C       DIMENSION D(1100)
      C
      C    THE FOLLOWING DIMENSION MUST BE GREATER THAN OR EQUAL TO
      C    (M+2)*(M+1)/2..
```

```
      C
0003  C       DIMENSION D(66)
      C
      C    THE FOLLOWING DIMENSIONS MUST BE GREATER THAN OR EQUAL TO M..
      C
0004  C       DIMENSION B(10),E(10),SB(10),T(10)
      C
      C    THE FOLLOWING DIMENSIONS MUST BE GREATER THAN OR EQUAL TO (M+1)..
      C
0005  C       DIMENSION XBAR(11),STD(11),COE(11),SUMSQ(11),ISAVE(11)
      C
      C    THE FOLLOWING DIMENSION MUST BE GREATER THAN OR EQUAL TO 10..
      C
0006  C       DIMENSION ANS(10)
      C
      C    THE FOLLOWING DIMENSION WILL BE USED IF THE PLOT OF OBSERVED DATA
      C    AND ESTIMATES IS DESIRED.  THE SIZE OF THE DIMENSION, IN THIS
      C    CASE, MUST BE GREATER THAN OR EQUAL TO N+3.  OTHERWISE, THE SIZE
      C    OF DIMENSION MAY BE SET TO 1.
0007  C       DIMENSION P(300)
      C
      C    ...................................................................
      C
      C    IF A DOUBLE PRECISION VERSION OF THIS ROUTINE IS DESIRED, THE
      C    C IN COLUMN 1 SHOULD BE REMOVED FROM THE DOUBLE PRECISION
      C    STATEMENT WHICH FOLLOWS.
      C
      C    DOUBLE PRECISION X,XBAR,STD,D,SUMSQ,DT,E,B,SB,T,ANS,DET,COE
      C
      C    THE C MUST ALSO BE REMOVED FROM DOUBLE PRECISION STATEMENTS
      C    APPEARING IN OTHER ROUTINES USED IN CONJUNCTION WITH THIS
      C    ROUTINE.
      C
      C    ...................................................................
0008  1 FORMAT(A4,A2,I5,I2,I1)
0009  2 FORMAT(2F10.0)
0010  3 FORMAT(27H1POLYNOMIAL REGRESSION......,A4,A2/)
0011  4 FORMAT(23H0NUMBER OF OBSERVATIONS,I6//)
0012  5 FORMAT(32H0POLYNOMIAL REGRESSION OF DEGREE,I3)
0013  6 FORMAT(12H0  INTERCEPT,E20.7)
0014  7 FORMAT(26H0  REGRESSION COEFFICIENTS/(6E20.7))
0015  8 FORMAT(1H0//24X,24HANALYSIS OF VARIANCE FOR,I4,19H  DEGREE POLYNOMI
      1AL/)
0016  9 FORMAT(1H0,5X,19HSOURCE OF VARIATION,7X,9HDEGREE OF,7X,6HSUM OF,9X
      1,4HMEAN,10X,1HF,9X,20HIMPROVEMENT IN TERMS/33X,7HFREEDOM,9X,7HSQUA
      2RES,7X,6HSQUARE,7X,5HVALUE,8X,17HOF SUM OF SQUARES)
```

```
0017    10 FORMAT(20H0  DUE TO REGRESSION,12X,I6,F17.5,F14.5,F13.5,F20.5)
0018    11 FORMAT(32H   DEVIATION ABOUT REGRESSION   ,I6,F17.5,F14.5)
0019    12 FORMAT(8X,5HTOTAL,19X,I6,F17.5///)
0020    13 FORMAT(17H0  NO IMPROVEMENT)
0021    14 FORMAT(1H0//27X,18HTABLE OF RESIDUALS//16H OBSERVATION NO.,5X,7HX
       1VALUE,7X,7HY VALUE,7X,10HY ESTIMATE,7X,8HRESIDUAL/)
0022    15 FORMAT(1H0,3X,I6,F18.5,F14.5,F17.5,F15.5)
       C
       C
       C    ...........................................................
       C
       C    READ PROBLEM PARAMETER CARD
0023        END=1000
       C
0024   100 READ (5,1) PR,PR1,N,M,NPLOT
       C
       C        PR....PROBLEM NUMBER (MAY BE ALPHAMERIC)
       C        PR1...PROBLEM NUMBER (CONTINUED)
       C        N.....NUMBER OF OBSERVATIONS
       C        M.....HIGHEST DEGREE POLYNOMIAL SPECIFIED
       C        NPLOT.OPTION CODE FOR PLOTTING
       C             0  IF PLOT IS NOT DESIRED.
       C             1  IF PLOT IS DESIRED.
       C
       C        PRINT PROBLEM NUMBER AND N.
       C
0025        WRITE (6,3) PR,PR1
0026        WRITE (6,4) N
       C
       C    READ INPUT DATA
       C
0027        L=N*M
0028        DO 110 I=1,N
0029        J=L+I
       C
       C        X(I) IS THE INDEPENDENT VARIABLE, AND X(J) IS THE DEPENDENT
       C        VARIABLE.
       C
0030   110 READ (5,2) X(I),X(J)
       C
0031        CALL GDATA (N,M,X,XBAR,STD,D,SUMSQ)
       C
0032        MM=M+1
0033        SUM=0.0
0034        NT=N-1
       C
0035        DO 200 I=1,M
0036        ISAVE(I)=I
       C
```

```
       C    FORM SUBSET OF CORRELATION COEFFICIENT MATRIX
       C
0037        CALL ORDER (MM,D,MM,I,ISAVE,DI,E)
       C
       C    INVERT THE SUBMATRIX OF CORRELATION COEFFICIENTS
       C
0038        CALL MINV (DI,I,DET,B,T)
       C
0039      . CALL MULTR (N,I,XBAR,STD,SUMSQ,DI,E,ISAVE,B,SB,T,ANS)
       C
       C    PRINT THE RESULT OF CALCULATION
       C
0040        WRITE (6,5) I
0041        IF(ANS(7)) 140,130,130
0042   130 SUMIP=ANS(4)-SUM
0043        IF(SUMIP) 140, 140, 150
0044   140 WRITE (6,13)
0045        GO TO 210
0046   150 WRITE (6,6) ANS(1)
0047        WRITE (6,7) (B(J),J=1,I)
0048        WRITE (6,8) I
0049        WRITE (6,9)
0050        SUM=ANS(4)
0051        WRITE (6,10) I,ANS(4),ANS(6),ANS(10),SUMIP
0052        NI=ANS(8)
0053        WRITE (6,11) NI,ANS(7),ANS(9)
0054        WRITE (6,12) NT,SUMSQ(MM)
       C
       C    SAVE COEFFICIENTS FOR CALCULATION OF Y ESTIMATES
       C
0055        COE(1)=ANS(1)
0056        DO 160 J=1,I
0057   160 COE(J+1)=B(J)
0058        LA=I
       C
0059   200 CONTINUE
       C
       C    TEST WHETHER PLOT IS DESIRED
       C
0060   210 IF(NPLOT) 100, 100, 220
       C
       C        CALCULATE ESTIMATES
       C
0061   220 NP3=N+N
0062        DO 230 I=1,N
0063        NP3=NP3+1
0064        P(NP3)=COE(1)
0065        L=I
```

```
FORTRAN IV G LEVEL 1, MOD 3              MAIN              DATE = 70117

0066                   DO 230 J=1,LA
0067                   P(NP3)=P(NP3)+X(L)*COE(J+1)
0068              230 L=L+N
         C
         C          COPY OBSERVED DATA
         C
0069                   N2=N
0070                   L=N*M
0071                   DO 240 I=1,N
0072                   P(I)=X(I)
0073                   N2=N2+1
0074                   L=L+1
0075              240 P(N2)=X(L)
         C
         C          PRINT TABLE OF RESIDUALS
         C
0076                   WRITE (6,3) PR,PR1
0077                   WRITE (6,5) LA
0078                   WRITE (6,14)
0079                   NP2=N
0080                   NP3=N+N
0081                   DO 250 I=1,N
0082                   NP2=NP2+1
0083                   NP3=NP3+1
0084                   RESID=P(NP2)-P(NP3)
0085              250 WRITE (6,15) I,P(I),P(NP2),P(NP3),RESID
         C
0086                   CALL PLOT (LA,P,N,3,0,1)
         C
0087                   STOP
0088             1000 CONTINUE
0089                   CALL EXIT
0090                   END
```

F.2 Sample Superheat Threshold Program, for PKOA in Water at PWR Conditions. (a=6.07)

```
44   26 PVPSF=PVA*14.6959*144.0
45   27 SIGMA=-7.275E-6*TF+5.081E-3
46   28 TR=TF+459.69
47   38 TC=TK-273.16
48   39 V2=TCRC-TC
49   46 ROWL =((1.0+B4**Y2**0.3333333+B5*Y2)/(VC+B1*Y2**0.3333333+B2*Y2+B3
          1*Y2**4))*62.428
50   50 BO=1.89-2641.62/TK*10.0**(8087C.0/(TK*TK))
51   51 G1=82.546/TK-1.6246E5/(TK*TK)
52   52 G2=0.21828-1.2697E5/(TK*TK)
53   53 G3=3.635E-4-6.7680F-8/(TK*10.0**(-3))**24
54   54 2*BO+BO*BO*G1*PVA/TK+BO*BO*BO*G2*PVA*PVA*PVA/(TK*TK*TK)-BO**13*
          1G3*PVA**12/TK**12
55   55 ROWV=(4.55504*TK/PVA+Z)**(-1)*62.428
56   56 HFG=2505.67-3.2059*TF
57   57 BA=(PVPSF-PLIQ(L))/PVPSF
58   58 E=1.79
59      ROWL =CCNST*RCWL
60 0158 COEF=1.2516E04*ROWL*A*SIGMA/(BA*PVPSF)
61 C258 CCC=EPKA*EPKA-COEF*EPKA*(ALOG(0.5592*EPKA)-1.0)
62 3258 DDD=1.5820*COEF*2.0*EPKA
63 0358 BBB=DDD-COEF*ALOG(E)
64 C458 EC=E-(E*E-BBB*E+CCC)/(2.0*E-BBB)
65 C558 IF(ABS(E-EC)-.0001)9858,0658,0658
66 0658 E=(E+EC)*0.5
67      IF(E.LT.1.0)E=1.0
68 0758 GO TO 0258
69 9858 IF(EC-1.79)96,0858,0858
70 C858 IF(EC-EPKA)C958,93,93
71 0958 DEDS=(EPKA-E)*BA*PVPSF/(60.96*A*SIGMA)
72      RCRIT=2.0*SIGMA/(BA*PVPSF)
73   62 GATE=3.700221F-19*A*TR*DEDS/SIGMA**2
74      ART=(2.0*GATE*(PVPSF-PLIQ(L))-1.0)**2-4.0*GATE**2*(PVPSF-PLIQ(L))*
          1*2
75      IF(ART.LT.0.0)GO TO 93
76   63 PGPSF=(1.0-2.0*GATE*(PVPSF-PLIQ(L))-SQRT(ART))/(2.0*GATE)
77   64 B=(PVPSF+PGPSF-PLIQ(L))/PVPSF
78 0164 IF(B-BA-.00001)464,0264,0264
79 C264 BA=B
80 0364 GO TO 0158
81  464 GO TO 103
82  103 EQA53=0.9010E-12*A*DEDS-RCRIT*RCRIT*ROWV*HFG*778.26-RCRIT*SIGMA
83  104 IF(EQA53-0.0)96,106,93
84   93 TF=TF-DELTF
85   94 DELTF=0.1*DELTF
86   95 IF(DELTF-00.0001)106,96,96
87   96 TF=TF+DELTF
88   97 GO TO 23
89  106 DELT3=TF-TSAT(L)
90      PKO2RT=C.0
91      XI=0.0
92      DELTI=0.0
93      ALPHA=0.0
94      J=0
95      XNI=0.0
96  107 WRITE(6,508)A,PKO2RT,DELTI,ALPHA,PLIQ(L),TSAT(L),E,DEDS,J,XN
          11,XI,PGPSF,PVPSF,DELT3,TF
97  109 CONTINUE
98      GO TO 1000
99      END
```

```
$JOB            JOB1,KP=20,TIME=1,PAGES=140,LINES=55,RUN=FREE
1       IMPLICIT REAL*8 (A-H,O-Z)
2       EXP(X)=DEXP(X)
3       ALOG(X)=DLOG(X)
4       SQRT(X)=DSQRT(X)
5       ABS(X)=DABS(X)
C       SUPERHEAT LIMIT FOR WATER EXPOSED TO FISSION NEUTRONS IN PWR
6       DIMENSION PLIQ(30),TSAT(30)
7  500 FORMAT(F10.4)
8  501 FORMAT(I3/(10X,2F10.2))
9  502 FORMAT(1H1,15X,78HTHE SUPERHEAT LIMIT FOR WATER EXPOSED TO FISSION
          1 NEUTRONS UNDER PWR CONDITIONS)
10 504 FORMAT(1H0,119H A PKO GT EPKA DELTI  ALPHA  PRESS   SAT    ENER A
          1VG ENER   J   XNI  REL SIZE  GAS     VAPOR   DEL T   DEL T   SUP
          1 )
11 505 FORMAT(1H ,119H      RATE      TIME           LIQUID  TEMP  LFVFL D
          1EP RATE          INIT ENRR  PRESS   PRESS   EQA48  E.R.M.  TEMP
          1 )
12 506 FORMAT(1H ,119H      NO/SEC     SEC          LRF/FT2 DEG F   MEV M
          1EV/CM           LRF/FT2 LRF/FT2  DEG F   DEG F   DFG F
          1 )
13 508 FORMAT(1H ,F3.1,D10.3,D8.1,F6.3,F8.1,F8.3,F6.3,D10.3,I5,F5.1,F10.8
          1,F7.1,F8.1,8X,F8.3,F8.3)
14 600 FORMAT(1H2,29HTHE VALUE OF THE CONSTANT IS ,F10.4//)
15      EPKA=3.74
16   16 TCRK=647.27
17   17 PCRA=218.167
18   18 AA=3.746313
19   19 BB=4.14113E-2
20   20 CC=7.515484F-9
21   21 DD=1.379449E-2
22   22 EE=6.56444E-11
23   37 TCRC=374.11
24   40 VC=3.1375
25   41 B1=-0.3151548
26   42 B2=-1.203374E-3
27   43 B3=7.48918E-13
28   44 B4=0.1342489
29   45 B5=-3.946263E-3
30    1 READ(5,501)N,(PLIQ(L),TSAT(L),L=1,N)
31 1000 READ(5,500)CCNST
32    3 WRITE(6,502)
33    4 WRITE(6,504)
34    5 WRITE(6,505)
35    6 WRITE(6,506)
36      WRITE(6,600)CCNST
C       THIS LOOP ALLOWS THE LIQUID PRESSURE TO TAKE DIFFERENT VALUES
37    8 DO 109 L=1,N,1
38      A=6.C7
39   10 DELTF=10.0
40   15 TF=TSAT(L)+DELTF
41   23 TK=5.0*(TF-32.0)/9.0+273.16
42   24 Y=TCRK-TK
43   25 PVA=PCRA  /EXP(+2.3*Y*(AA+BB*Y+CC*Y*Y*Y+EE*Y*Y*Y*Y*Y)/(TK*(1.0+DD*Y)
          1))
```

F.3 Sample Superheat Threshold Program, for 14.1 Mev Neutrons in Benzene. (a=2.00)

```
45    9858 IF(EC-2.00) 96,0858,C858
46    0858 IF(EC-EPKA) 0958,93,93
47    0958 DEDS=(EPKA-E)*BA*PVPSF/(60.96*A*SIGMA)
48         RCRIT=2.0*SIGMA/(BA*PVPSF)
49    62 GATE=3.700221E-19*A*(TF+459.69)*DEDS/SIGMA**2
50       ART=(2.0*GATE*(PVPSF-PLIQ(L))-1.0)**2-4.0*GATE**2*(PVPSF-PLIQ(L))*
       1*2
51       IF(ART.LT.0.0) GO TO 93
52    63 PGPSF =(1.0-2.0*GATE*(PVPSF -PLIQ(L))-SQRT(ART))/(2.0*GATE)
53    64 B=(PVPSF +PGPSF -PLIC(L))/PVPSF
54    0164 IF(B-BA-.00001)464,0264,0264
55    0264 BA=B
56    0364 GO TO 0158
57    464 GO TO 103
58    103 EQA53=0.8010E-12*A*DEDS-RCRIT*RCRIT*ROWV*HFG*778.26-RCRIT*SIGMA
59    104 IF(EQA53-0.0) 96,106,93
60    93 TF=TF-DELTF
61    94 DELTF=0.1*DELTF
62    95 IF(DELTF-00.009) 106,96,96
63    96 TF=TF+DELTF
64    97 GO TO 23
65    106 DELT3=TF-TSAT(L)
66       PKO2RT=0.0
67       XI=0.0
68       DELTI=0.0
69       ALPHA=0.0
70       J=C
71       XN1=0.0
72    107 WRITE(6,508)A,PKC2RT,DELTI,ALPHA,PLIQ(L),TSAT(L),E    ,DEDS  ,J,XN
       1I,XI,PGPSF ,PVPSF ,DELT3,TF
73    109 CONTINUE
74       GO TO 1000
75       END
```

```
*JOB         JOBI,KP=29,TIME=1,PAGES=140,LINES=55,RUN=FREE
1     IMPLICIT REAL*8 (A-H,O-Z)
2     EXP(X)=DEXP(X)
3     ALOG(X)=DLOG(X)
4     SORT(X)=DSORT(X)
5     ABS(X)=DABS(X)
C     SUPERHEAT LIMIT FOR BENZENE EXPOSED TO FAST NEUTRONS LP RANGE
6     DIMENSION PLIQ(30),TSAT(30)
7     500 FORMAT(E10.4)
8     501 FORMAT(I3/(10X,2F10.2))
9     503 FORMAT(1H1,30X,54HTHE SUPERHEAT LIMIT FOR BENZE EXPOSED TO FAST NE
       1UTRONS)
10    504 FORMAT(1H0,119H A PKO GT EPKA DELTI    ALPHA   PRESS    SAT    ENER  A
       1VG FNER  J    XNI   RFL SIZE    GAS    VAPOR   DEL T    DEL T    SUP
       1 )
11    505 FORMAT(1H ,119H         RATE       TIME          LIQUID  TEMP   LEVEL D
       1FP RATE              INIT EMBR  PRESS   PRESS    EQA48   F.BCM.  TEMP
       1 )
12    506 FORMAT(1H0,119H       NO/SEC       SEC            LBF/FT2 DEG F    MEV M
       1EV/CM                       LBF/FT2 LBF/FT2  DEG F    DEG F    DEG F
       1 )
13    508 FORMAT(1H ,F3.0,D10.3,D8.1,F6.3,F8.1,F8.3,F6.3,D10.3,I5,F5.1,F10.8
       1, F7.1,F9.1,8X,F8.3,F8.3)
14    600 FORMAT(1H0,29HTHE VALUE OF THE CONSTANT IS ,F10.4//)
        EPKA=4.00
16    1 READ(5,501)N,(PLIQ(L),TSAT(L),L=1,N)
17    1000 READ(5,500)CONST
18    3 WRITE(6,503)
19    4 WRITE(6,504)
20    5 WRITE(6,505)
21    6 WRITE(6,506)
22      WRITE(6,600)CONST
C     THIS LOOP ALLOWS THE LIQUID PRESSURE TO TAKE DIFFERENT VALUES
23    8 DO 109 L=1,N,1
24      A=2.00
25    10 DELTF=10.0
26    15 TF=TSAT(L)+DELTF
27    23 CONTINUE
28    25 PVA=85.143-0.0599*TF+0.003178*TF*TF
29    26 PVPSF=PVA*144.0
30    27 SIGMA=-4.610F-6*TF+2.268F-3
31    46 ROWL=1/(0.01831+0.15524E-5*TF+0.3444E-7*TF*TF)
32    55 ROWV=1.0/(26.8282-0.1614*TF+0.24878E-3*TF*TF)
33    56 HFG=196.119-0.12169*TF-0.1734E-3*TF*TF
34    57 BA=(PVPSF-PLIQ(L))/PVPSF
35    38 F=2.00
36      ROWL=CONST*ROWL
37    0158 COEF=1.00C0E04*ROWL*A*SIGMA/(BA*PVPSF)
38    0258 CCC=EPKA*EPKA-COEF*EPKA*(ALOG(0.9450*EPKA)-1.0)
39    3258 DDD=1.0565*COEF+2.0*EPKA
40    0358 BBP=DDD-COEF*ALOG(E)
41    0458 EC=F-(F*E-BBP*E+CCC)/(2.0*E-BBB)
42    0558 IF(ABS(E-EC)-.0001)9858,0658,0658
43    0658 F=(E+EC)*0.5
44    0758 GO TO 0358
```

Appendix G

References

1. Becker, A.G., "Effect of Nuclear Radiation on the Superheated Liquid State." Thesis. Wayne State University. Detroit, 1963.

2. Bell, C.R., "Radiation Induced Nucleation of the Vapor Phase." Ph.D. Thesis, Department of Nuclear Engineering, M.I.T. March, 1970.

3. Bergles A.E. and Rohsenow W.M., "The Determination of Forced-Convection Surface-Boiling Heat Transfer," Journal of Heat Transfer, 86, Series C, No. 3, 365-372 (Paper 63-HT-22) 1964.

4. Deitrich, L.W. "A Study of Fission-Fragment Induced Nucleation of Bubbles in Superheated Water." Technical Report No. SU-326-p13-4, Stanford University, 1969.

5. El-Nagdy, M.M., "An Experimental Study of the Influence of Nuclear Radiation on Boiling in Superheated Liquids." University of Manchester, England, Thesis. 1969.

6. Evans, R.D., "The Atomic Nucleus." McGraw-Hill, 1955.

7. Glasstone S. and Sesonske A., "Nuclear Reactor Engineering." D. Van Nostrand Inc., 1963.

8. IBM System/360 Scientific Subroutine Package H20-0205-3

9. Karaian, E., "Pu-Be Source Intercalibration." M.I.T. Reactor Memorandum, Aug. 21, 1961.

10. Kaplan I., "Nuclear Physics" Addison-Wesley Inc., 1964.

11. Keenan, J.H. and Keyes, F.G., "Thermodynamic Properties of Steam." John Wiley and Sons, 1962.

12. McAdams, W.H., "Heat Transmission." Third Edition, New York, McGraw-Hill, 1954.

13. Organick and Studhalter, "Thermodynamic Properties of Benzene." Chemical Engineering Progress, Vol. 44, 847, 1948.

14. Perry, Chilton, Kirkpatrick. "Perry's Chemical Engineer's Handbook." 4th Edition. McGraw-Hill, 1963.

15. Rohsenow, W.M. and H. Choi, "Heat Mass and Momentum Transfer." Prentice-Hall, 1961.

16. Rizika, J.W. and Rohsenow, W.M., "Thermocouple Thermal Error." Industrial and Engineering Chemistry, Vol. 44, No. 5, May 1952.

17. Schmidt, E., "Properties of Water and Steam in SI-Units." Springer-Verlag, N.Y. Inc., 1969.

18. Segre, E., "Experimental Nuclear Physics, Vol. II." John Wiley and Sons, 1953.

19. Seitz, F., "On the Theory of the Bubble Chamber." The Physics of Fluids, Vol. I, No. 1, Jan-Feb 1958.

20. Timmermans J., "Physico-Chemical Constants of Pure Organic Compounds." Elserier Publishing Co. Inc., 1950.

21. Tipton, C.R., "Reactor Handbook Vol. I--Materials." Interscience Publishers Ltd., 1960.

22. Todreas, N.E., Nuclear Engineering Department, Massachusetts Institute of Technology, Cambridge, Mass. 02139.

23. Todreas N.E. and Rohsenow W.M., "The effect of Non-uniform Axial Heat Flux Distribution." Department of Mechanical Engineering, M.I.T., Contract NsG-496, Report No. 9843-37, Sept. 1965.

24. WASH-1082, "Current Status & Future Technical & Economic Potential of Light Water Reactors." Division of Reactor Development & Technology, U.S.A.E.C., March 1968.